

https://dspace.org/

The Behaviour And Design Of Mineshaft Steelwork And Conveyances

Krige, Geoffrey Jack

2015-05-22
http://hdl.handle.net/10539/17835

Downloaded from a DSpace repository. https://dspace.org/

THE BEHAVIOUR AND DESIGN OF MINESHAFT STEELWORK AND CONVEYANCES

Geoffrey Jack Krige

A thesis submitted to the Faculty of Engineering, University of the Witwatersrand, Johannesburg in fulfillment of the requirements for the degree of Doctor of Philosophy.

JOHANNESBURG, MAY 1983

DECLARATION

I, Geoffry Jack Krige, declare that this thesis is my own unaided work, carried out while seconded to the University of the Witwatersrand, Johannesburg by my employer, Dorbyl Structural Engineering (Pty) Limited. No portion of this thesis has been submitted to any other university.

G J Krige

G J Krige

SYNOPSIS

An investigation into the dynamic forces between shaft steelwork and conveyance is described. The investigation involves both a computer model, which differs from other models in incorporating some flexibility into the conveyance, and field measurements. It is the first time to our knowledge that measurements of conveyance wheel loads and accelerations have been made in a wide range of different shafts. The results of the computer model and the measurements are analysed to give an assessment of the magnitude of the forces and of those variables which have a major influence on the forces.

An empirical formula is proposed for the determination of the magnitude of these forces and the problem of their possible dynamic magnification is addressed. Finally, recommendations are made regarding the shaft condition and the use of the empirical formula for the design of shaft guide steelwork and conveyances. This represents a significant advance on previous design practice, which has been based on assumed, rather than measured wheel loads.

ACKNOWLEDGEMENTS

Several acknowledgements must be made, before embarking on this thesis, for the generous assistance which I have had from many people and organisations.

Throughout this work Prof. A Kemp has offered most valuable criticism and advice, and has kept me at it.

The rest of the steering committee, Dr. Fritz, Dr. Adali and Steve van der Westhuizen of the CSIR, Mr. Hojem of the Chamber of Mines, and Mr. Geach of Dorbyl Structural Engineering, have ensured progress by enforcing regular reporting and keeping the goals in view.

Barry Alport and Mike Fotopoulos have given much practical and analytical assistance while completing their M.Sc theses.

Sandra Meyer spent many hours typing draft sections and Jean McClean most competently did the final typing of the thesis.

The technicians in the Civil Engineering Laboratories, and the staff of the Germiston Works of Dorbyl Structural Engineering have made many necessary pieces of equipment.

The engineering staff at the mines visited, senior staff of the mining houses and many professional colleagues have given time and assistance in discussing the problem and obtaining measurements.

This project would not have been possible without the financial contributions made by the CSIR in the form of an industrial scholarship, by the Chamber of Mines in the purchase of the measuring and analysis equipment, the University in the purchase of equipment, and most of all Dorbyl Structural Engineering in releasing me on a full-time basis for the duration of the project.

Finally, my sincere thanks to my family for their patience and constant encouragement and to my God for wisdom.

LIST OF CONTENTS

	PAGE
List of Figures	xii
List of Tables	xv
List of Equations	xvi
CHAPTER 1 Introduction	1
1.1 Historical development	1
1.2 The problem today	2
1.3 Scope of this research project ...	2
1.3.1 Imposed limitations	3
1.3.2 Major areas of investigation ...	4
CHAPTER 2 Computer Model	5
2.1 Description of the model	5
2.1.1 Modelling the guides	7
2.1.2 Modelling the conveyances ...	16
2.1.3 Natural frequencies of the conveyances ...	18
2.1.4 The Computer programmes	22
2.2 A consideration of other models ...	24
2.2.1 SKIP II	24
2.2.2 German model	25
2.2.3 Comparison with DISCS results ...	27
2.2.4 Conclusions	34

List of contents : continued

		PAGE
CHAPTER 3	Field Measurements	35
3.1	The equipment used	35
3.1.1	The transducers	36
3.1.2	Signal conditioning	41
3.1.3	Recording of data	41
3.1.4	Analogue to digital conversion ...	43
3.1.5	Cyclical force exciter	44
3.2	Types of measurements made	46
3.2.1	Measurements in the operating condition	46
3.2.2	Natural frequency measurements ...	51
3.2.3	Future measurements	51
3.3	Comments on assumptions in DISCS ...	52
CHAPTER 4	Analysis and Comparison of DISCS and Measured Results ...	54
4.1	Methods of analysis of data	54
4.1.1	A probability analysis	54
4.1.2	Spectral analysis	55
4.1.3	Fatigue analysis	56
4.1.4	Displacement analysis	56
4.2	Data Analysis	61
4.2.1	Maximum wheel load analysis ...	61

List of contents : continued

		Page
4.2.2	Fatigue cycle analysis	70
4.2.3	Expected value analysis	72
4.2.4	Frequency analysis	76
4.2.5	Accelerations	81
4.3	Comparison between DISCS and measurements	82
4.3.1	Wheel loads	85
4.3.2	Fatigue values	87
4.3.3	Frequencies	87
4.3.4	Accelerations	90
4.3.5	The practical usefullness of DISCS	90
4.4	Empirical derivation of maximum wheel loads	92
4.4.1	Effect of hoisting velocity ...	93
4.4.2	Effect of conveyance mass ...	95
4.4.3	Effect of conveyance length	95
4.4.4	Effect of misalignment	96
4.4.5	Effect of bunton spacing	100
4.4.6	Effect of guide and bunton stiffness	100
4.4.7	Effect of wheel preload	104
4.4.8	Effect of spring stiffness ...	104
4.4.9	Maximum wheel load equation ...	105
4.5	Relationship of wheel loads to accelerations	106

List of contents : continued

		PAGE
CHAPTER 5	Dynamic magnification	109
5.1	Literature survey	109
5.1.1	CSIR report	109
5.1.2	German approach	112
5.2	Prediction by DISCS of dynamic magnification	114
5.3	Measured dynamic magnification ...	118
5.4	Avoiding dynamic magnification ...	121
5.4.1	High frequency problems	121
5.4.2	Low frequency problems	126
5.5	Maximum wheel load with magnification	127
CHAPTER 6	Design load recommendations ...	131
6.1	Suggested basic operating limits ...	132
6.1.1	Misalignment of the guides ...	132
6.1.2	Lateral acceleration	135
6.2	Design rules	136
6.2.1	Assessment of wheel loads and their point of application ...	136
6.2.2	Guide and bunton stiffnesses ...	138
6.2.3	Basic permissable stresses ...	141
6.2.4	Fatigue life	141
6.2.5	Preventing dynamic magnification	141
6.3	Design method	142
6.3.1	Applying the rules	142
6.3.2	Example of design	142

List of contents : continued

PAGE

CHAPTER 7 Conclusions and further research needed 147

7.1 Conclusions 147

7.2 Further research needed 149

7.2.1 Geometric factors 149

7.2.2 Specific problem areas 151

7.2.3 Economic and maintenance aspects 152

7.4 Design recommendations 152

REFERENCES 153

MAJOR NOTATION 155

APPENDICES A1

A. Derivation of equations of motion A1

B. Derivation of guide stiffness equation A4

C. Calculation of guide displacement due to the other wheel load A6

D. Derivation of equation to calculate natural frequencies A14

E. Computer programmes A21

E1. DISDAT A21

E2. DISCS A29

E3. DATAPL A48

E4. SAMPLER A60

E5. CALIB A65

E6. INIT A70

E7. DYNMAG A75

List of contents : continued

PAGE

CHAPTER 7 Conclusions and further research needed 147

7.1 Conclusions 147

7.2 Further research needed 149

7.2.1 Geometric factors 149

7.2.2 Specific problem areas 151

7.2.3 Economic and maintenance aspects 152

7.4 Design recommendations 152

REFERENCES 153

MAJOR NOTATION 155

APPENDICES A1

A. Derivation of equations of motion A1

B. Derivation of guide stiffness equation A4

C. Calculation of guide displacement due to the other wheel load A6

D. Derivation of equation to calculate natural frequencies A14

E. Computer programmes A21

E1. DISDAT A21

E2. DISCS A29

E3. DATAPL A48

E4. SAMPLER A60

E5. CALIB A65

E6. INIT A70

E7. DYNMAG A75

List of contents : continued

		PAGE
	E8. TF	A80
	E9. INTEG	A84
	E10. Programme layout	A89
F.	Typical DISCS results and measurements	A90
G.	Mines at which measurements were conducted	A120

LIST OF FIGURES

		PAGE
2.1	Layout of model	8
2.2	Calculation of guide stiffness	11
2.3	Effective spring stiffness	11
2.4	Effective stiffness	13
2.5	Measurements showing damping	13
2.6	Guide misalignments	17
2.7	Effective guide position	17
2.8	Comparison of SKIP II and DISCS results	30
2.9	Wheel loads predicted by DISCS	33
3.1	Schematic of measuring and analysis equipment	37
3.2	Load cell bolts	39
3.3	Filter characteristics	42
3.4	Cyclical force exciter	45
3.5	Transducer layout on conveyance	49
3.6	Comparative accelerometer measurements	50
4.1	Typical results of double integration Hartebeestfontein No. 8 shaft	57
4.2	Average and one week maximum wheel loads	59
4.3	Areas under the power spectrum President Steyn No. 4 shaft	60
4.4	Significant frequencies at President Steyn 4	63

List of figures : continued

		PAGE
4.5	Blyvooruitsig guide wheels	71
4.6	Wheel load variation with hoisting speed	71
4.7	Traces subjected to expected value analysis	75
4.8	Comparison of measured and DISCS wheel loads	86
4.9	Accelerations - measured and DISCS predictions	89
4.10	Acceleration on Western Deep Levels top wheel	91
4.11	Expected acceleration values	93
4.12	Wheel loads with preload subtracted	94
4.13	Hartebeestfontein No. 8 shaft layout	102
4.14	Wheel load variation with bunton stiffness ratio	103
5.1	Dynamic magnification according to CSIR report	111
5.2	Areas of high dynamic magnification	111
5.3	Guide misalignment	115
5.4	Dynamic magnification predicted by DISCS	117
5.5	Decreasing dynamic magnification with increasing misalignment	117
5.6	Flexural vibration made of Deelkraal No. 2 shaft cage	122

List of figures : continued PAGE

5.7 Wheel loads at President Steyn No. 4 shaft 123

5.8 Wheel loads in bad section of the Deelkraal No. 1 shaft 124

5.9 Dynamic magnification on Deelkraal No. 1 shaft 21 tonne skip 125

5.10 Conveyance movement in a shaft 125

5.11 Dynamic magnification hump 128

5.12 Magnification factor 128

6.1 Misalignment of guides 134

6.2 Design wheel loads 139

6.3 Deflection limits 140

6.4 Layout of Free State Geduld No. 5 shaft 144

6.5 DYNMAG dynamic predictions for F S G No. 5 shaft 144

7.1 Other guide layouts 150

LIST OF TABLES

		PAGE
2.1	Important frequencies	31
2.2	Predicted maximum wheel loads	32
3.1	Measured natural frequencies Hartebeestfontein No. 8 shaft	51
4.1	Summary of maximum measured wheel loads (in kN)	64
4.2	Expected maximum values of wheel loads and accelerations	76
4.3	Hartebeestfontein frequencies	78
4.4	Frequency comparisons	79
4.5	Natural frequencies with varying load conditions	80
4.6	Peak acceleration values	82
4.7	Frequency comparison	88
4.8(a)	Maximum wheel load ratios-skips	97
4.8(b)	Maximum wheel load ratios-cages	98
4.9	R values	107
6.1	Basic operating limits	135
6.2	Design, measured and DISCS wheel loads at 15 m/sec	137
6.3	Design comparisons	143

LIST OF EQUATIONS

	PAGE
2.1	7
2.2	19
2.3	20
2.4	20
2.5	21
2.6	21
2.7	21
6.1	136

CHAPTER 1 : INTRODUCTION

1. INTRODUCTION

1.1 Historical Developments

The historical development of mineshafts has been amply described by Penning[1], Wayman[2], van Wyk[3], and many others. An integral part of this development has been the trend to larger conveyances, higher hoisting speeds and more flexible guide systems. These are all variables which have a significant effect on the dynamic behaviour of the conveyance, so that over the years the magnitude of dynamic loads and movements have increased and become a serious problem in shafts. Improvements have been made by trial-and-error means, such as fitting guide wheels to replace hard slippers, and later adding spring suspension to the wheels. It has, however, often been necessary to reduce hoisting speed or revert to previously proven guide layouts when dynamic behaviour has become excessive[4]. It is unfortunate that very little of the empirical knowledge gained in this way has been published, but much useful information is available from what has been published by Krok[5], Calver[6], and McKechnie[7] relating to specific shaft problems and experience.

Some other research work has been done in this field by Penning[1] at Colorado in the USA, Reinke[8] at Tremonia in Germany, and at the CSIR[9] in Pretoria. The findings of these research projects are discussed and, where applicable, incorporated in the relevant chapters below.

1.2 The Problem Today

The primary cause of the dynamic behaviour of conveyances is probably guide misalignment. It is physically impossible to eliminate this misalignment, which is thus kept within specified limits, typically of the order of ± 6 mms, from some vertical reference line.

Every conveyance in every shaft is thus subjected to dynamic behaviour to some degree, horizontal accelerations in some shafts having been measured at two or three times gravity, with associated high dynamic loads.

This causes fatigue damage, plastic deformation of conveyance or guides, and there can also be magnification of dynamic effects if excitation coincides with natural frequencies, leading to unsafe operation.

In order to limit the extent of these problems, a fuller understanding of the dynamic behaviour of conveyances is necessary. This needs to be formulated in such a way that the conveyance or shaft designer can predict the consequences, in terms of increased or decreased dynamic loading, of decisions regarding parameters such as shaft geometry, bunton spacing and stiffness, guide stiffness, wheel preload and spring constants, hoisting speed, conveyance size and mass, and magnitude of misalignment.

1.3 Scope of the Research Project

This research project encompasses a theoretical and experimental study of the problem of dynamic behaviour of conveyances, and some design recommendations are made, based on the findings. The problem is a complex one, and it was necessary to limit the scope of the study to reduce the complexity.

1.3.1 Imposed limitations

(a) Types of shaft. In this study only vertical, steel-equipped shafts are considered. This includes all the newer main shafts on the South African gold mines, where for some years the practice has been to use circular, concrete-lined, steel-equipped shafts.

Some of the older rectangular shafts are also included. Timber-equipped shafts, shafts with rope guided conveyances, and inclined shafts have not been considered.

(b) Types of conveyance. The only limitation on types of conveyance is that only conveyances running between two guides are considered. Small cages running on three or four guides are excluded, except for one set of measurements.

All skips, and many cages have this assumed configuration, so the majority of conveyances are covered.

(c) Dynamic forces. As a conveyance moves through a hoisting cycle it is subjected to several different dynamic forces. There are vertical effects due to winder acceleration and braking. Loading and tipping or unloading cause vertical and horizontal dynamic forces. There are also aerodynamic forces, due to a velocity differential, between downcast air and a conveyance moving up, which may be as high as 30 m/sec.

Attention is however focussed primarily on the excitation due to guide misalignment which is

constantly present, and the resulting forces and movements of the conveyance. For further simplification, the dynamic behaviour in the plane between the guides is, apart from a few measurements, the only one considered.

1.3.2 Major areas of investigation

The two major areas of the investigation, described in full detail in separate chapters below, are a computer model and field measurements. The computer model and instrumentation for measurements both produce values of the same accelerations and wheel loads, which are then analysed in the same way. The two methods are then used for carrying out a parametric study of the variables involved, from which empirical design rules are derived. In a separate chapter, the magnification of dynamic behaviour, due to possible adverse interaction between natural frequencies and exciting frequencies, is considered.

CHAPTER 2 : COMPUTER MODEL

The aim here, in setting up a computer model, is not to achieve a highly sophisticated mathematical solution. Rather, emphasis is placed on configuring the model to accommodate the variables, and describe the behaviour, which practical experience has found to be important, while at the same time keeping it simple.

2.1 Description of the Model.

Most of the engineers consulted felt that the dynamic behaviour was more pronounced in the plane between the guides, than perpendicular to this plane. In general the centre of gravity of conveyances is in, or very close to this plane, so it is assumed that coupling of the motions in the two planes is insignificant, and the conveyance is modelled in one plane only - the plane between the two guides. The validity of these assumptions is discussed with reference to measurements in the next chapter. From experience it appears[4] that the most important variables are the following:-

(i) guide and bunton stiffness

(ii) plumb and gauge misalignments

(iii) joint mismatch

(iv) winding speed

(v) conveyance mass

(vi) bridle stiffness

(vii) wheel spring stiffness

(viii) preload on wheels

(ix) height of the centre of gravity of the conveyance

(x) ratio between overall conveyance length and bunton spacing

(xi) rope twist (but this does not have any significant effect on behaviour in the plane of the guides, so it is not included).

(xii) damping.

Most of the measurements showed that wheel irregularity was important, so this was also included. Several assumptions have been made in setting up this model, and are listed below:-

(i) aerodynamics have no effect on the dynamic behaviour,

(ii) rope whip has a damping, rather than an exciting, contribution to dynamic behaviour and can thus be neglected,

(iii) the dynamic responses of the shaft steelwork are not significant,

(iv) there is no basic difference between upward or downward motion, and

(v) higher order dynamic modes and natural frequencies of local components such as the wheel sets are neglected.

Some of these assumptions are discussed in the light of the measurements in the next chapter.

In order to include these variables, the model is configured as shown in figure 2.1.

The equations of motion for this model can be written as:-

$$I_R\ddot{\phi}+(F_1-F_2+F_3)d_1/2+F_3d_3+F_4d_4+(-F_5+F_6+F_4)d_6/2=0$$
$$M_1\ddot{v}_1+F_3-F_4=0$$
$$M_2\ddot{v}_2+F_1-F_2-F_3=0$$
$$M_3\ddot{v}_3+F_5-F_6+F_4=0 \qquad \text{..... 2-1}$$

where:

$$F_1=(v_2-w_{01})K_{e1}+(\dot{v}_2-\dot{w}_{01})C_{S1}$$
$$F_2=(-v_2-w_{02})K_{e2}-(\dot{v}_2+\dot{w}_{02})C_{S2}$$
$$F_3=(v_1+d_3\phi-v_2)K_{C3}+(\dot{v}_1+d_3\dot{\phi}-\dot{v}_2)C_{B3}$$
$$F_4=(-v_1+d_4\phi+v_3)K_{C4}+(-\dot{v}_1+d_4\dot{\phi}+\dot{v}_3)C_{B4}$$
$$F_5=(v_3-w_{03})K_{e5}+(\dot{v}_3-\dot{w}_{03})C_{S5}$$
$$F_6=(-v_3-w_{04})K_{e6}-(\dot{v}_3+\dot{w}_{04})C_{S6}$$

and other values are as defined in figure 2.1 and in the notation. The derivation of these equations is given in Appendix A.

2.1.1 Modelling the Guides

The inclusion of the guides as semi-continuous elastically supported beams makes the solution of the equations a very complex mathematical problem, but they cannot be neglected. The approach followed here is thus to include the guide stiffness with the wheel stiffness to give an "effective spring stiffness" at each wheel, and to alter the displacement across the springs, w, to show the effects of the guide misalignment, mismatch, wheel irregularity and preload.

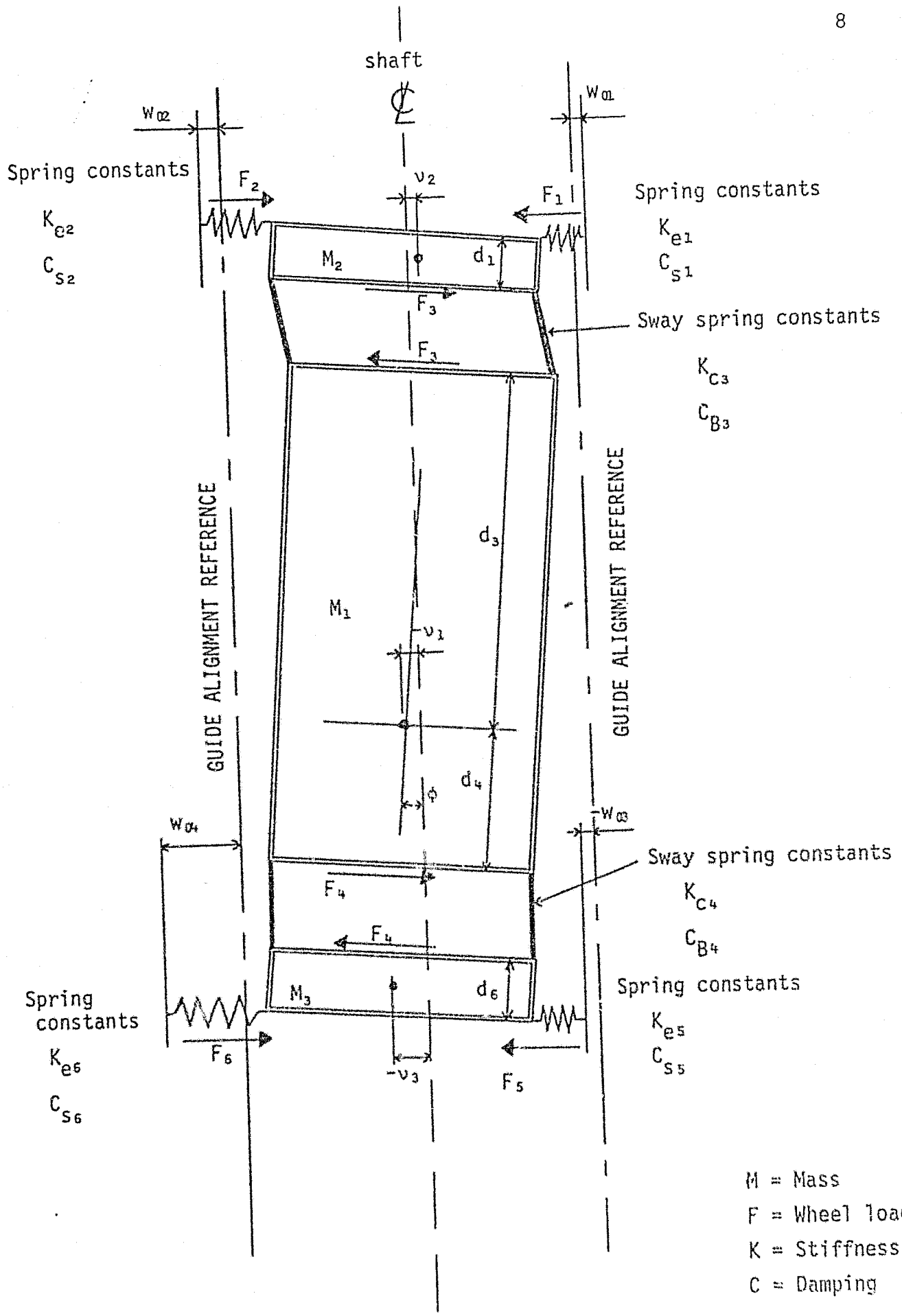


FIGURE 2.1 LAYOUT OF MODEL

The guide stiffness under each wheel varies cyclically with a period equal to the time taken for the wheel to move from one bunton to the next. This varying stiffness is calculated by considering the guide to be continuous over a three span beam, span length equal to bunton spacing, where the outside supports are considered fixed in the aligned position and the internal supports are springs with stiffness equal to the bunton stiffness, as shown in figure 2.2. The guide stiffness is then a repetition of the varying stiffness as the wheel traverses the centre span only, i.e. for $L/3 \leq x \leq 2L/3$:
the stiffness of the guide, modelled as above is:-

$$K_g = b_3 / [(-b_1-b_2) + (38b_1+22b_2)a + (54-479b_1-175b_2)a^2 - (108-1044b_1-630b_2)a^3 + (54-927b_1-1125b_2)a^4 + (486b_1+972b_2)a^5 - (162b_1+324b_2)a^6]$$

where:

$a = x/L$

$b_3 = 162EI/L^3$

$b_1 = 1/(b_3/K_b+5)$

$b_2 = b_1\left(\frac{7/3}{b_3/K_b+1/3}\right)$

The derivation of this equation is shown in appendix B. Combining this stiffness with the wheel stiffness, as shown in figure 2.3 gives the effective stiffness as:-

$$K_e = \frac{K_g K_w}{K_g+K_w}$$

where K_w = wheel stiffness

providing the assumption is made that both stiffnesses are linear.

This gives the normal effective stiffness for the wheel at any position on the guide. There are however two other cases which may apply.

(a) The wheels may move out of contact with the guides. When this happens, the effective stiffness is zero.

$$K_e = 0$$

(b) The wheel spring travel, or the clearance between the guide and the slippers on the conveyances, may be exceeded by the relative displacement between the guide and the conveyance, i.e. "hard contact" may occur. In this case the only remaining deflection possible is deflection of the guides, so that the effective stiffness becomes equal to the guide stiffness only.

$$K_e = K_g$$

In this latter case the load-displacement curve is no longer linear, but linearity of the equations can be maintained by adjusting the relative displacement between conveyance and guide, by the preload distance, w_{xx}, to ensure compatability of wheel loads. This adjustment is described under the guide positioning below.

The full "effective spring stiffness" is thus as shown in figure 2.4.

The damping of the guides is also included with the wheel damping to give one constant. Here again there are two cases.

(a) For the wheels in contact with the guides,

$$C_s = C_s$$

(b) For the wheels not in contact with the guides,

$$C_s = 0$$

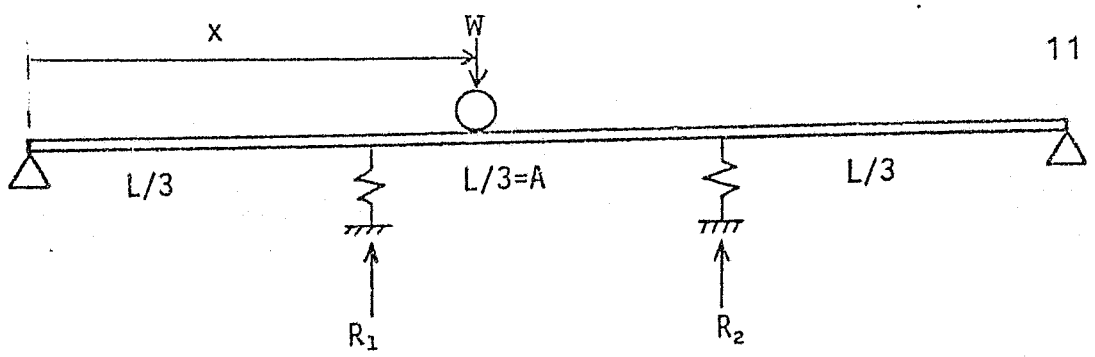
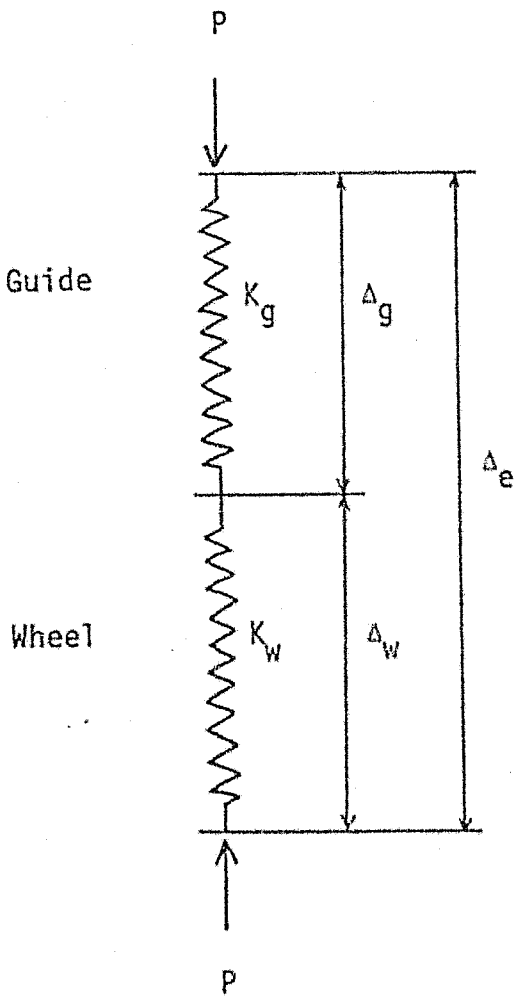


FIGURE 2.2 Calculation of guide stiffness



For applied load P:-

$$\Delta_e = \frac{P}{K_e}$$

$$\Delta_g = \frac{P}{K_g}$$

$$\Delta_w = \frac{P}{K_w}$$

but:-

$$\Delta_e = \Delta_g + \Delta_w$$

$$\text{ie } \frac{P}{K_e} = \frac{P}{K_g} + \frac{P}{K_w}$$

$$\text{ie } \frac{1}{K_e} = \frac{K_a + K_w}{K_g K_w}$$

$$\text{ie } K_e = \frac{K_g K_w}{K_g + K_w}$$

FIGURE 2.3 Effective spring stiffness.

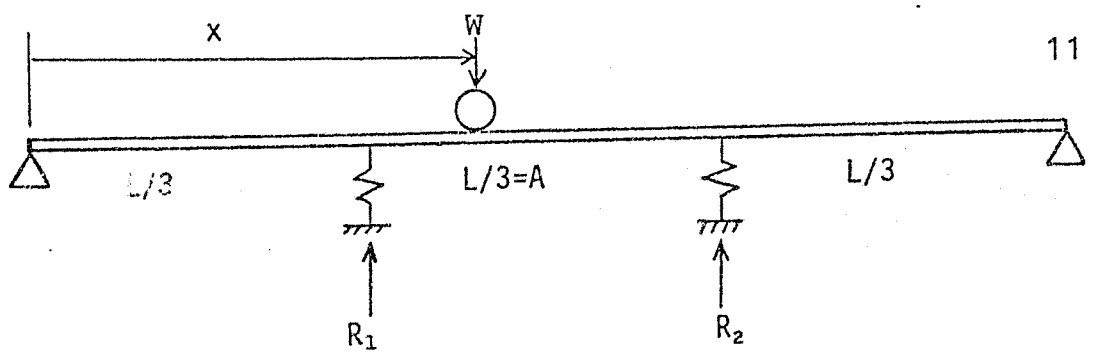
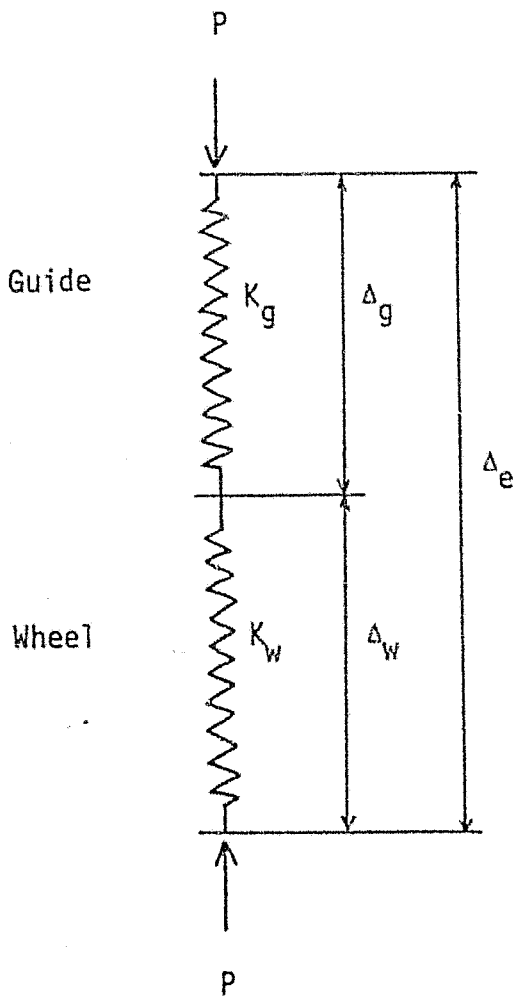


FIGURE 2.2 Calculation of guide stiffness



For applied load P:-

$$\Delta_e = \frac{P}{K_e}$$

$$\Delta_g = \frac{P}{K_g}$$

$$\Delta_w = \frac{P}{K_w}$$

but:-

$$\Delta_e = \Delta_g + \Delta_w$$

$$\text{ie } \frac{P}{K_e} = \frac{P}{K_g} + \frac{P}{K_w}$$

$$\text{ie } \frac{1}{K_e} = \frac{K_a + K_w}{K_g K_w}$$

$$\text{ie } K_e = \frac{K_g K_w}{K_g + K_w}$$

FIGURE 2.3 Effective spring stiffness.

The type of damping to use is difficult to assess. The components of the overall damping are listed by Reinke[8] as:-

- rubber buffers and wheels
- ropes and rope connections
- friction at connections in conveyances and shaft steelwork.
- air turbulence

These components show structural, frictional and viscous damping. A visual assessment of several typical sections of acceleration measurements, illustrated in figure 2.5, shows an exponential decrease of peaks. The assumption is thus made that the overall damping can be approximated by viscous damping.

Measurements made by Reinke[8] have shown that for most shafts the damping falls in the region of 4% to 10% of critical. The actual damping constant is then:

$$C_{s_1} = C_{s_2} = C_s \times \sqrt{M_2 \times K_{e_1}}$$

for the top wheels, and

$$C_{s_5} = C_{s_6} = C_s \times 2 \times \sqrt{M_3 \times K_{e_5}}$$

for the bottom wheels, where K_e is the effective stiffness value at a bunton. This is not strictly mathematically correct for more than 1 degree of freedom, but the damping is not well known anyway, so this will give a reasonable working value.

The guide position is the final variable relating to modelling the guides. The guide misalignment is the primary cause of the dynamic behaviour considered in

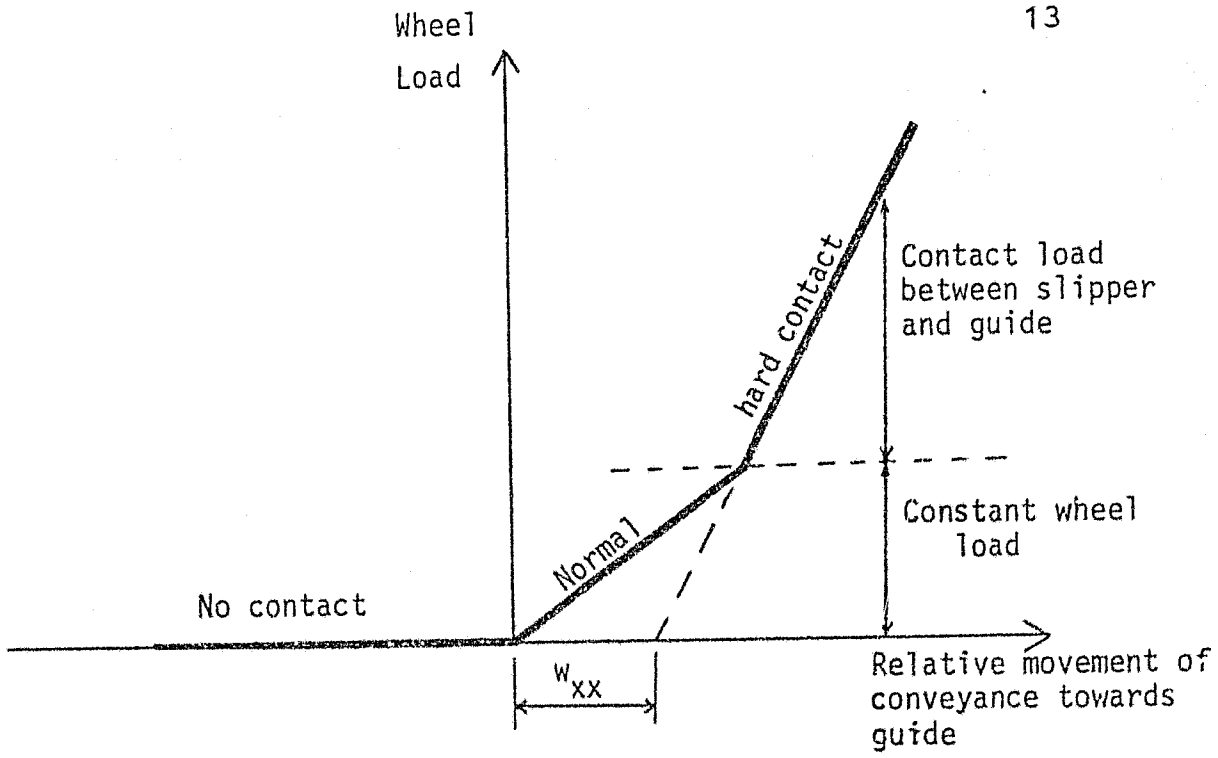


FIGURE 2.4 Effective stiffness

ln (Ratio between peaks) is:

ln (30/19,5) = 0,43
ln (19,5/13,0) = 0,41
ln (13,0/8,0) = 0,49

Average = 0,44, damping $= \frac{0,44}{2\pi} = 0,07$

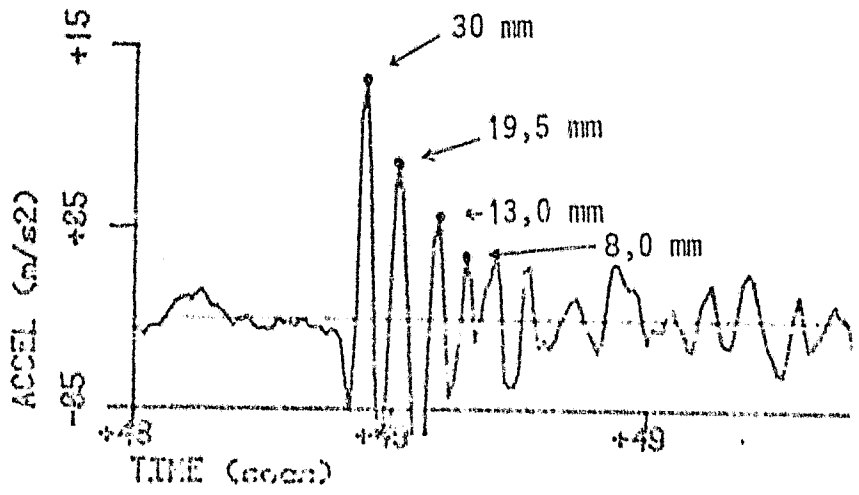


FIGURE 2.5 Measurements showing damping

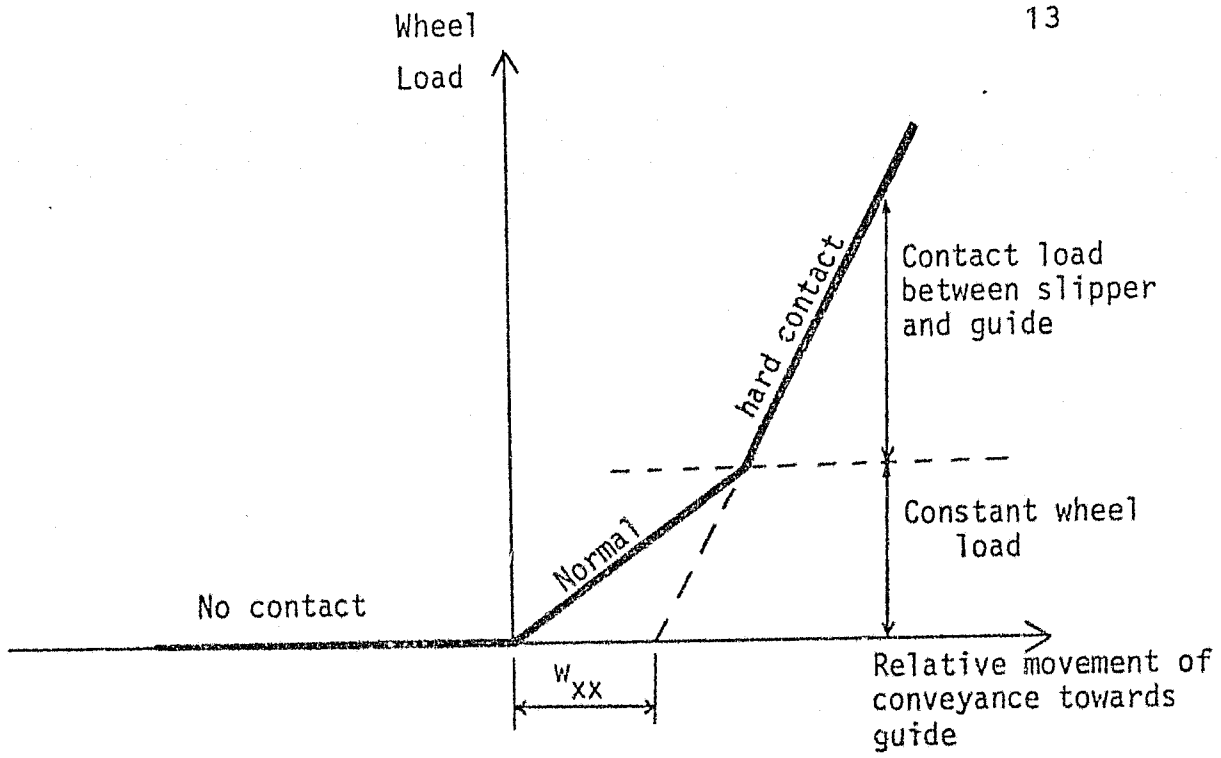


FIGURE 2.4 Effective stiffness

ln (Ratio between peaks) is:

ln (30/19,5) = 0,43
ln (19,5/13,0) = 0,41
ln (13,0/8,0) = 0,49

Average = 0,44, damping $= \frac{0,44}{2\pi} = 0,07$

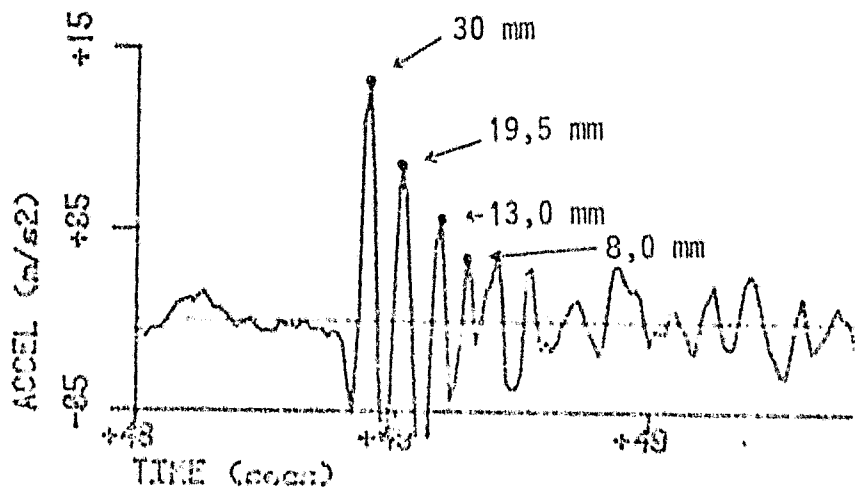


FIGURE 2.5 Measurements showing damping

this report. It is considered as being made up of three parts, relating to the physical installation.

(a) Mismatch is due to the guides being joined in such a way that the back of the guides are aligned at splices. By virtue of the rolling process, adjacent guides may, however, not be exactly the same depth, so that there may be a step between the faces of adjacent guides. It is assumed that the magnitude of mismatch is a normally distributed variable with zero mean. Measurement of the depth of 30 guides taken at random, showed a standard deviation of the mismatch of 0,59 mm.

(b) One guide is aligned by surveyors according to some vertical line, and within specified tolerances. It is assumed that the alignment process will lead to off-vertical distances which vary, with approximately a uniform distribution, from one bunton to the next, always remaining within greater overall limits. This is reflected in DISDAT by calculating one guide position at a bunton as the guide position at the previous bunton plus an increment which is generated randomly between specified limits. There is then a check to ensure that the guide position is within the greater overall limit.

(c) The other guide is then aligned with templates, giving a fairly accurate gauge, but with an error which is again assumed to be uniformly distributed within specified limits. This is reflected in DISDAT by adding a randomly generated gauge error to the other guide position.

These misalignments, which are shown diagrammatically in figure 2.6 combine to form the basic guide position.

In a similar way to the stiffness, several other significant factors are included with the guide position to give an effective position, used in the subsequent model.

First, the guide wheels may be set clear of the guides or with a certain preload. Where they are set clear of the guides,

$$w_o = w_o + \text{clearance}$$

Where there is a preload, p_r;

$$w_o = w_p - p_r/K_e$$

where K_e is the effective guide stiffness at a bunton. In effect, the guide position is moved out for wheel clearance or in for wheel preload.

Secondly, each wheel load effects the deflection of the guide at the other wheel on the same guide. This displacement of the guide, OWE, is calculated as shown in appendix C. Then;

$$w_o = w_o + OWE$$

Thirdly, when hard contact occurs, the guide position is moved out a distance, h, to maintain linearity of the equations as described above. For compatability, the wheel load immediately before hard contact, W_b, must equal that immediately afterwards, W_a.

$$W_b = W_a$$

The wheel loads are equal to the stiffness times the spring compression, ie. from figure 2.3

$$W_b = K_g \Delta_g = W_a$$

When K_e becomes K_g, Δ_e must be altered to Δ_g, ie.

$$h = \Delta_e - \Delta_g = \Delta_w$$

at hard contact;

$$\Delta_w = w_{xx}$$

where w_{xx} is the spring travel or guide/slipper clearance.
Thus;

$$h = w_{xx}$$

So that;

$$w_o = w_o + w_{xx}$$

Finally, it was found very early in analysing measurements of conveyance behaviour that the frequency of revolution of the wheels played a very important part (see chapter 4). A wheel irregularity was thus also added to the effective guide position. This irregularity is assumed to be a sine wave, with a specified amplitude and a frequency of :-

$$f = \frac{\pi D}{V}$$

where f is the frequency
D is the wheel diameter
V is the hoisting speed

Thus:

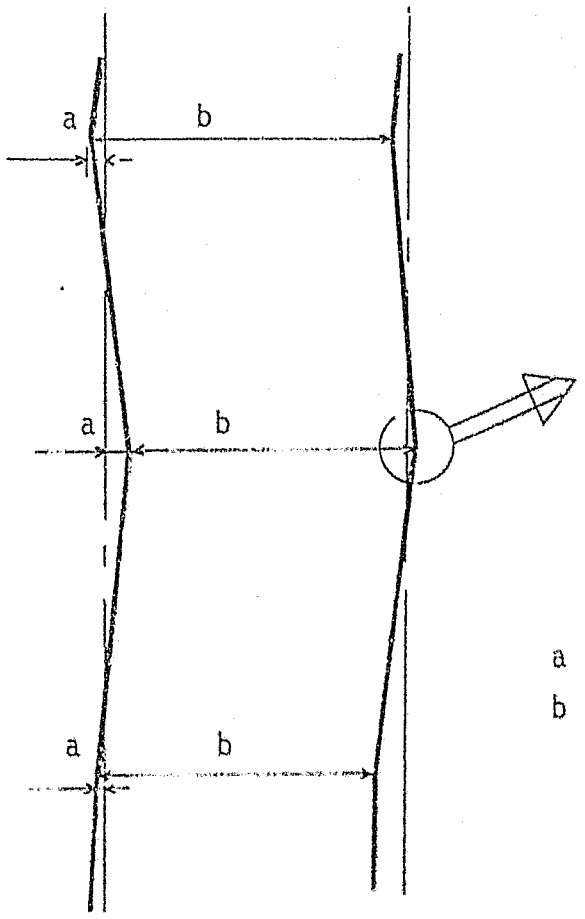
$$w_o = w_o + A \sin \left(\frac{t}{360f} + PH\right)$$

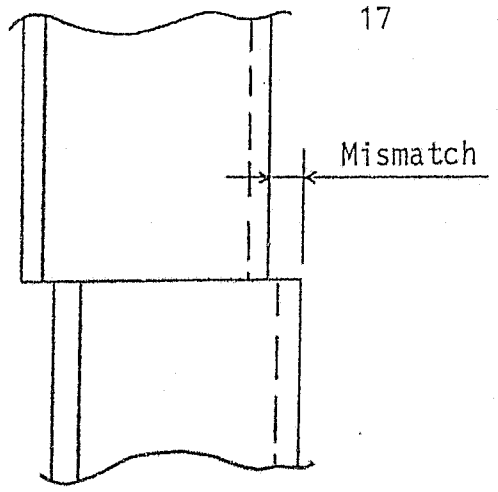
where A is the amplitude
t is the time
PH is a specified phase angle.

Figure 2.7 shows schematically how the effective guide position is made up of these factors.

2.1.2 Modelling the conveyances

As shown in figure 2.1, the conveyance is modelled in





a - off vertical misalignment

b - gauge error

FIGURE 2.6 Guide Misalignments

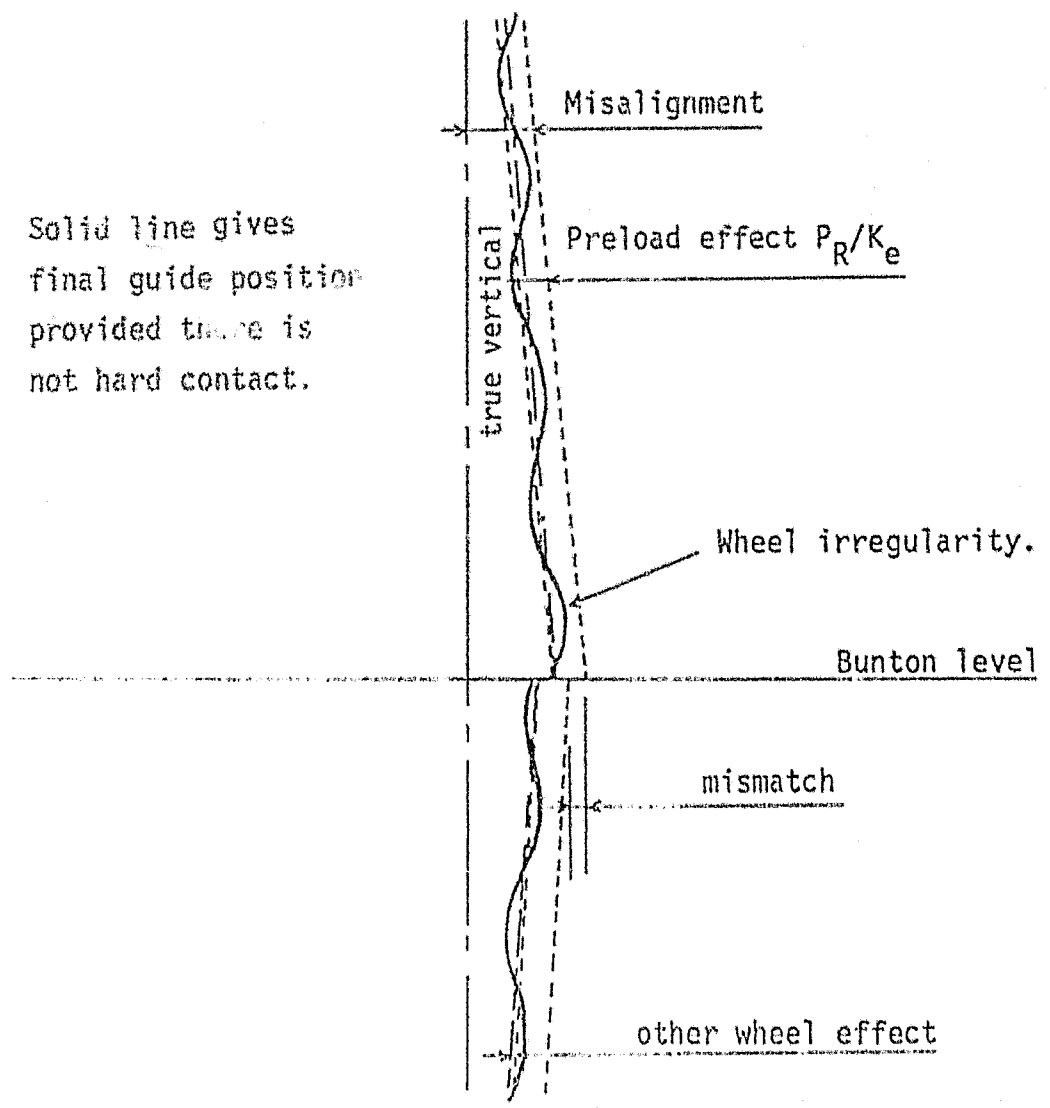


FIGURE 2.7 Effective Guide Position

one plane, as three rigid bodies. The bodies are connected by the bridle, which has sway stiffnesses K_{e_3} and K_{e_4} and related damping constants C_{b_3} and C_{b_4} connecting the top and bottom transoms to the body of the conveyance. Each rigid body thus has its own independent translational degree of freedom. The bridle is however considered to be inextensible, so that there is only one rotational degree of freedom, the rotation of all three rigid bodies being the same. All vertical motion and distortions are neglected. The conveyance is thus modelled as a four degree of freedom system, with equations as shown above.

The stiffnesses K_{e_3} and K_{e_4} are calculated according to the structure of the conveyance, and remain constant.

The damping constants are derived from the critical damping ratios as:

$$C_{b_3} = C_b \times \sqrt{(M_1+M_2)\tfrac{1}{2} \times K_{e_3}}$$

and

$$C_{b_4} = C_b \times \sqrt{(M_3+M_1)\tfrac{1}{2} \times K_{e^4}}$$

Again these are not strictly mathematically correct, but provide an acceptable measure of damping. Also viscous damping is again assumed.

2.1.3 Natural Frequencies of the Conveyance

Having set up the full equations of motion, it is possible to calculate the natural, undamped frequences of the conveyances.

Expanding the equations of motion, equations 2-1, we have:

$$I_r\ddot{\phi}+A_1\dot{\nu}_1+A_2\dot{\nu}_2+A_3\dot{\nu}_3+A_4\dot{\phi}+A_5\nu_1+A_6\nu_2+A_7\nu_3+A_8\phi+A_9 = 0$$

$$M_1\ddot{\nu}_1+A_{10}\dot{\nu}_1-C_{b_3}\dot{\nu}_2-C_{b_4}\dot{\nu}_3+A_{11}\dot{\phi}+A_{12}\nu_1-K_{c_3}\nu_2-K_{c_4}\nu_3+A_{13}\phi = 0$$

$$M_2\ddot{\nu}_2-C_{b_3}\dot{\nu}_1+A_{14}\dot{\nu}_2+A_{15}\dot{\phi}-K_{c_3}\nu_1+A_{16}\nu_2+A_{17}\phi+A_{18}=0$$

$$M_3\ddot{\nu}_3-C_{b_4}\dot{\nu}_1+A_{23}\dot{\nu}_3+A_{19}\dot{\phi}-K_{c_4}\nu_1+A_{20}\nu_3+A_{21}\phi+A_{22} = 0 \quad \ldots 2\text{-}2$$

where:

$$A_1 = C_{b_3}\frac{d_1}{2} + C_{b_3}d_3 - C_{b_4}d_4 - C_{b_4}\frac{d_6}{2}$$

$$A_2 = C_{s_1}\frac{d_1}{2} + C_{s_2}\frac{d_1}{2} - C_{b_3}\frac{d}{2} - C_{b_3}d_3$$

$$A_3 = C_{b_4}d + C_{b_4}\frac{d_6}{2} - C_{s_5}\frac{d_6}{2} - C_{s_6}\frac{d_6}{2}$$

$$A_4 = C_{b_3}d_3\frac{d_1}{2} + C_{b_3}d_3^2 + C_{b_4}d_4^2 + C_{b_4}d_4\frac{d_6}{2}$$

$$A_5 = K_{c_3}\frac{d_1}{2} + K_{c_3}d_3 - K_{c_4}d_4 - K_{c_4}\frac{d_6}{2}$$

$$A_6 = K_{e_1}\frac{d_1}{2} + K_{e_2}\frac{d_1}{2} - K_{c_3}\frac{d_1}{2} - K_{c_3}d_3$$

$$A_7 = K_{c_4}d_4 + K_{c_4}\frac{d_6}{2} - K_{e_5}\frac{d_6}{2} - K_{e_6}\frac{d_6}{2}$$

$$A_8 = K_{c_3}d_3\frac{d_1}{2} + K_{c_3}d_3^2 + K_{c_4}d_4^2 + K_{c_4}d_4\frac{d_6}{2}$$

$$A_9 = K_{e_2}\frac{d_1}{2}w_{02} - K_{e_1}\frac{d_1}{2}w_{01} + K_{e_5}\frac{d_6}{2}w_{03} - K_{e_6}\frac{d_6}{2}w_{04} + C_{s_1}\frac{d_1}{2}\dot{w}_{01}$$
$$- C_{s_2}\frac{d_1}{2}\dot{w}_{02} + C_{s_5}\frac{d_6}{2}\dot{w}_{03} - C_{s_6}\frac{d_6}{2}\dot{w}_{04}$$

$$A10 = C_{b_3} + C_{b_4}$$

$$A_{11} = C_{b_3}d_3 - C_{b_4}d_4$$

$$A_{12} = K_{c_3} + K_{c_4}$$

$$A_{13} = K_{c_3}d_3 - K_{c_4}d_4$$

$$A_{14} = C_{s_1} + C_{s_2} + C_{b_3}$$

$$A_{15} = C_{b_3}d_3$$

$$A_{16} = K_{e1} + K_{e2} + K_{c3}$$

$$A_{17} = K_{c3}\, d_3$$

$$A_{18} = K_{e2}\, w_{02} - K_{e1}\, w_{01} + C_{s2}\, \dot{w}_{02} - C_{s1}\dot{w}_{01}$$

$$A_{19} = C_{b4}\, d_4$$

$$A_{20} = K_{c4} + K_{e5} + K_{e6}$$

$$A_{21} = K_{c4}\, d_4$$

$$A_{22} = K_{e6}\, w_{04} - K_{e5}\, w_{03} + C_{s6}\dot{w}_{04} - C_{s5}\, \dot{w}_{03}$$

$$A_{23} = C_{s5} + C_{s6} + C_{b4}$$

In calculating the natural, undamped frequencies, the damping terms and the values A_9, A_{18} and A_{22} which are externally applied forces are neglected. The equations of motion thus simplify to:

$$\begin{aligned}
&M_1\ddot{\nu}_1 + A_{12}\,\nu_1 - K_{C_3}\,\nu_2 - K_{C_4}\nu_3 + A_{13}\,\phi = 0\\
&M_2\ddot{\nu}_2 - K_{C_3}\,\nu_1 + A_{16}\,\nu_2 + 0 + A_{17}\,\phi = 0\\
&M_3\ddot{\nu}_1 - K_{C_4}\,\nu_1 + 0 + A_{20}\,\nu_3 + A_{21}\,\phi = 0\\
&I_r\ddot{\phi} + A_5\nu_1 + A_6\,\nu_2 + A_7\nu_3 + A_8\,\phi = 0
\end{aligned} \qquad \ldots\ldots\ldots\ldots \; 2.3$$

In matrix form this can be written as:

$$\begin{bmatrix} M_1 & 0 & 0 & 0\\ 0 & M_2 & 0 & 0\\ 0 & 0 & M_3 & 0\\ 0 & 0 & 0 & I_R \end{bmatrix}\begin{bmatrix} \ddot{\nu}_1\\ \ddot{\nu}_2\\ \ddot{\nu}_3\\ \ddot{\phi} \end{bmatrix} + \begin{bmatrix} A_{12} & -K_{C_3} & -K_{C_4} & A_{13}\\ -K_{C_3} & A_{16} & 0 & A_{17}\\ -K_{C_4} & 0 & A_{20} & A_{21}\\ A_5 & A_6 & A_7 & A_8 \end{bmatrix}\begin{bmatrix} \nu_1\\ \nu_2\\ \nu_3\\ \phi \end{bmatrix} = 0 \qquad \ldots\ldots\ldots\ldots \; 2\text{-}4$$

The stiffness matrix here is not exactly symmetrical, the small differences being due to some of the initial simplifying assumptions. This should not have a significant effect on the results unless the equations are ill-conditioned, in which case no proper solution would be achieved. In order to calculate the natural cyclical frequencies, ω, we write equation 2-4 in the form:

$$\left[K - M\,\omega^2\right]\left[\nu\right] = 0$$

ie.

$$\begin{bmatrix} A_{12} - M_1\omega^2 & -K_{C_3} & -K_{C_4} & A_{13} \\ -K_{C_3} & A_{16} - M_2\omega^2 & 0 & A_{17} \\ -K_{C_4} & 0 & A_{20} - M_3\omega^2 & A_{21} \\ A_5 & A_6 & A_7 & A_8 - I_R\omega^2 \end{bmatrix} \begin{bmatrix} \nu_1 \\ \nu_2 \\ \nu_3 \\ \phi \end{bmatrix} = 0 \qquad \text{..... 2-5}$$

In order to obtain a non-trivial solution to this equation, and hence obtain ω, the determinant must be zero, ie:

$$\begin{vmatrix} A_{12} - M_1\omega^2 & -K_{C_3} & -K_{C_4} & A_{13} \\ -K_{C_3} & A_{16} - M_2\omega^2 & 0 & A_{17} \\ -K_{C_4} & 0 & A_{20} - M_3\omega^2 & A_{21} \\ A_5 & A_6 & A_7 & A_8 - I_R\omega^2 \end{vmatrix} = 0$$

..... 2-6

Expanding this determinant, the following equation is obtained:

$$\omega^8 - b_1\omega^6 + b_2\omega^4 + b_3\omega^2 + b_4 = 0 \qquad \text{..... 2-7}$$

where b_1, b_2, b_3 and b_4 are as defined in appendix D.

Solving this equation yields four values for ω^2, from which the natural frequencies are:

$$f_n = \frac{\sqrt{\omega_n}}{2\pi} \qquad n = 1, 2, 3, 4$$

The derivation of equations 2-2 and the expansion of the determinant to obtain equation 2-7 are shown in appendix D.

2.1.4 The Computer programmes

Two programmes comprise the computer model : DISCS (for Dynamic Interaction of Shaft Conveyance Systems) and DISDAT 'for DIScs DATa generation).

DISDAT is a simple programme to interactively generate all the input data, including guide misalignments and mismatch, for DISCS. The units for all input are kN and m. DISCS constitutes the full computer model.

It initially reads the input and calculates certain constants. The wheel positions on the guide are calculated, and every time a new bunton is reached its misalignment values are read then typed out. The guide stiffness is then calculated, followed by the guide position, w_0, as described in section 2.1.1 above.

The natural frequencies of the conveyance are then calculated, at several positions over one guide span

to reflect the differences due to the varying guide stiffness, by solving equation 2-7 for ω.

The main section of DISCS performs a step-by-step solution to the equations of motion. Equations 2-2 are rewritten as eight first order differential equations, ie:

$$x_1 = \dot{\nu}_1$$

$$x_2 = \dot{\nu}_2$$

$$x_3 = \dot{\nu}_3$$

$$\theta = \dot{\phi}$$

$$I_r\dot{\theta}+A_1x_1+A_2x_2+A_3x_3+A_4\theta+A_5\nu_1+A_6\nu_2+A_7\nu_3+A_8\phi+A_9 = 0$$

$$M_1\dot{x}_1+A_{10}x_1-C_{b_3}x_2-C_{b_4}x_3+A_{11}\theta+A_{12}\nu_1-K_{c_3}\nu_2-K_{c_4}\nu_3+A_{13}\phi = 0$$

$$M_2\dot{x}_2-C_{b_3}x_1+A_{14}x_2+A_{15}\theta-K_{c_3}\nu_1+A_{16}\nu_2+A_{17}\phi+A_{18} = 0$$

$$M_3\dot{x}_3-C_{b_4}x_1+A_{23}x_3+A_{19}\theta-K_{c_4}\nu_1+A_{20}\nu_3+A_{21}\phi+A_{22} = 0$$

..... 2-8

The Adams-Moulton Predictor-Corrector method[10,11] is used for the step-by-step solution. This method, however requires that the first four values are known. The Runge-Kutta method [10,11] is thus used to give the solution at the first four time steps.

Early trial runs of DISCS showed very high initial accelerations and wheel loads, which were not repeated, even when calculating over 500 bunton spaces. This was found to be due to the conveyance being initially at rest at the zero position whereas the first buntons had some misalignment. DISCS was thus altered to reset

the time at zero after the conveyance has traversed one guide span and only record predictions of wheel loads and accelerations from this point onwards.

A listing of DISDAT and DISCS, as well as flowcharts and a description of the input and output is given in Appendix E.

2.2 A Consideration of Other Models

Two other computer models are described by Penning[1] and Reinke[8]. Some comments on these, and comparisons with DISCS results follow.

2.2.1 SKIP II

SKIP II is a computer model set up at the Colorado School of Mines, and described by Penning[12] and Robertson[13]. Their basic approach to setting up the model was similar to that used for DISCS, but with several important differences, which are listed below.

(a) The guides are modelled as being simply supported between rigid buntons. This does not allow for any investigation of the important relationship between guide and bunton stiffness.

(b) The conveyance is modelled as a single rigid body. This excludes the higher frequency vibrations, which have been measured by Calver[6] for example, and are thought to be due to relative motion between skip and transom.

(c) The model is in three dimensions, so that behaviour can be predicted in more than just the plane between the guides.

(d) Other smaller differences are that SKIP II makes no allowance for guide mismatch or wheel irregularity.

The solution procedure used by SKIP II is also a time step-by-step solution.

2.2.2 German Model

Reinke[8] takes a rather different approach, which consists of four steps.

(a) From measurements of misalignment in the shaft, and allowing a 3 mm deflection of the guide between buntons, to allow for guide flexibility between buntons, the correlation function and the power spectrum for the guide misalignment are calculated, using the equations:

$$R_{ww}(m.\Delta t) = \frac{1}{N-m} \sum_{k=1}^{N-m} |w(k.\Delta t)-\bar{w}|\,|w(k.\Delta t+m.\Delta t)-\bar{w}|$$

In comparing this to DISCS, the mean off-vertical displacement is zero.

i.e. $\bar{w} = 0$

Thus:

$$R_{ww}(m.\Delta t) = \frac{1}{N-m} \sum_{k=1}^{N-m} w(k.\Delta t).w(k.\Delta t+m.\Delta t)$$

$$S_{ww}(\omega_\ell) = 2 \sum_{k=0}^{N} R_{ww}(k.\Delta t).\cos(\omega_\ell.k.\Delta t).\Delta t$$

$\ell = 0, 1, 2, \ldots\ldots\ldots\ldots$

(b) The transfer function between guide misalignment and conveyance displacement is calculated, assuming a single rigid body and considering only the plane between the guides. The guide wheel spring stiffness is assumed to be one equivalent constant value, K_e. These transfer functions are:-

$$H_{11}(i\Omega) = \frac{\alpha_1}{\Delta}\left(\omega_{22}^2 - \Omega^2 + \frac{C_s(\ell_1+\ell_2)}{100}\,\omega_{22}\, i\Omega\right)$$

$$H_{12}(i\Omega) = \frac{\alpha_2}{\Delta}\omega_{11}^2 \qquad H_{21}(i\Omega) = \frac{\alpha_1}{\Delta}\,\omega_{22}^2$$

$$H_{22}(i\Omega) = \frac{\alpha_2}{\Delta}\left(\omega_{11}^2 - \Omega^2 + 2\,\frac{C_s}{100}\,\omega_{11}\, i\Omega\right)$$

where:

$$\omega_{11}^2 = \frac{4Ke}{M} \qquad \omega_{22}^2 = \frac{2Ke}{I_R}(\ell_1^2+\ell_2^2)$$

$$\omega_{12}^2 = \frac{4Ke}{M}(\ell_2-\ell_1) \qquad \omega_{21}^2 = \frac{2Ke}{I_R}(\ell_2-\ell_1)$$

$$\alpha_1 = \frac{Ke}{M} \qquad \alpha_2 = \frac{Ke}{I_R}$$

$$\Delta = \left(\omega_{11}^2 - \Omega^2 + 2\,\frac{C_s}{100}\,\omega_{11}\, i\Omega\right)\left(\omega_{22}^2-\Omega^2 + \frac{C_s(\ell_2+\ell_1)}{100}\,\omega_{22}\, i\Omega\right)$$

$$-\omega_{12}^2 \cdot \omega_{21}^2$$

(c) From these functions, the power spectrum of conveyance displacements can be calculated as:

$$S_{vv}(\Omega) = |H_{11}(i\Omega)|^2 2S_{ww}(\Omega) + |H_{12}(i\Omega)|^2(\ell_1^2+\ell_2^2)S_{ww}(\Omega)$$

$$S_{\phi\phi}(\Omega) = |H_{21}(i\Omega)|^2 2S_{ww}(\Omega) + |H_{22}(i\Omega)|^2(\ell_1^2+\ell_2^2)S_{ww}(\Omega)$$

for translational and rotational displacements.

(d) The final step is to calculate the expected square value of the displacements and hence the probability distribution function of the maximum wheel loads. The expected square displacements are given by:

$$E\{\nu^2\} = \frac{1}{\pi} \int_0^\infty S_{\nu\nu}(\Omega)\, d\Omega$$

$$E\{\phi^2\} = \frac{1}{\pi} \int_0^\infty S_{\phi\phi}(\Omega)\, d\Omega$$

Where the mean values of ν and of ϕ are zero, which is always very nearly true in mineshafts, the standard deviations of these displacements are:-

$$\sigma_\nu = \sqrt{E\{\nu^2\}}$$

$$\sigma_\phi = \sqrt{E\{\phi^2\}}$$

The standard deviation of the wheel load, from a mean value equal to the preload on the wheels, is then given by:

$$\sigma_w = \sigma_\nu K_e + \sigma_\phi K_e \ell_2 + \sigma_w K_e$$

Assuming a normal distribution the probability of the wheel load having a particular value, above the preload, of W_0 is thus:

$$P(W_0) = \frac{1}{\sigma_w \sqrt{2\pi}} . e^{\frac{-W_0^2}{2\sigma_w^2}}$$

2.2.3 Comparison with DISCS results

(a) The results given by Robertson[13] for a SKIP II run, are compared to the DISCS results for each of four

different cases, in Figure 2.8. From visual comparison of the two results, the following comments may be made:-

(i) The guide inertia was the same for both models, so that the simply supported guides in SKIP II were more flexible than the continuous guides in DISCS. The effect of this can be seen clearly at the beginning of the curves, where with zero misalignment, the wheel load reduction below preload is substantially more for SKIP II than for DISCS. It is not clear why, for SKIP II, the wheel load does not return to the preload value at the second bunton, for cases 2 and 4, as would be expected for zero misalignment.

(ii) in cases 2 and 3, the SKIP II and DISCS predictions are very similar, except that SKIP II has a higher frequency superimposed on the lower one. This higher frequency is the frequency of passing buntons, i.e. 4,2 hz at 15,24 m/sec for case 2, and 2,1 hz at 7,62 m/sec for case 3.

(iii) The natural frequencies of the conveyance predicted by DISCS are:

	Empty	Full
Translation	1,6 hz	1,0 hz
Rotation	2,4 hz	2,2 hz

The frequencies present in the SKIP II predictions, simply calculated as the inverse of the periods most clearly present are:-

	Empty	Full
7,62 m/sec	1,2 hz	0,8 hz
15,24 m/sec	1,2 hz	0,8 hz

Clearly in all cases of the SKIP II model the translational mode is excited at a lower frequency than predicted by DISCS because of the greater guide flexibility. In the DISCS model, dynamic motion is damped out very quickly in case 1, in cases 2 and 3 the translational mode is excited, while in case 4 the rotational mode is excited, the frequency being very close to the frequency of passing 2 buntons.

(iv) The predicted magnitude of wheel loads is similar in all but case 1, where no dynamic behaviour is excited in the DISCS model.

(b) In order to compare the DISCS results with the predictions given by Reinke[8], it is necessary to run DISCS with the same input and then calculate a power spectrum of the wheel loads and hence estimate the expected wheel load values. This can also be compared to the expected wheel load given by a probability analysis of the wheel loads. (The computer programmes which calculate the power spectrum and probability functions are described in section 4.1).

The significant frequencies predicted by Reinke[8] and by DISCS are shown in Table 2.1.

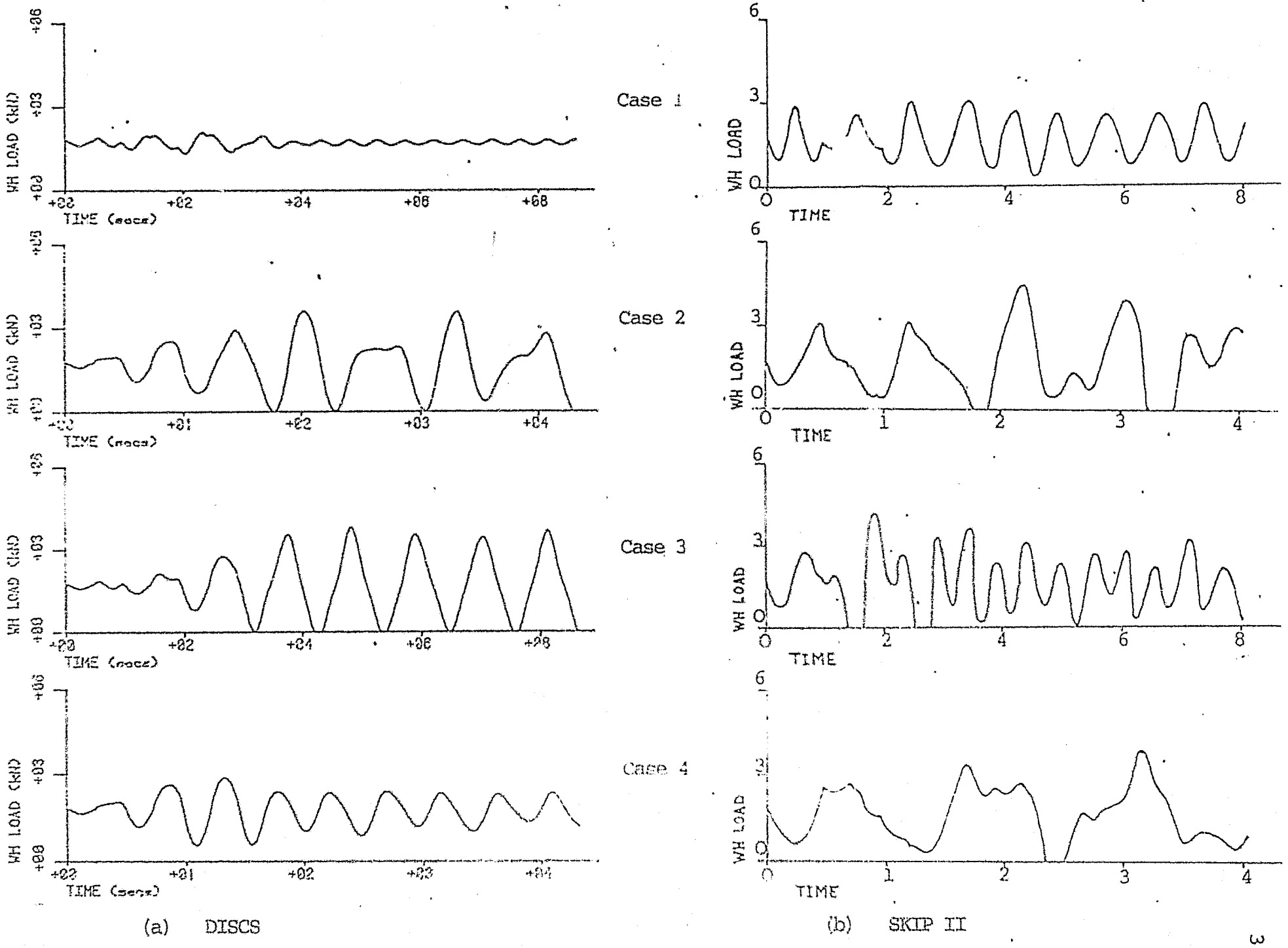


FIGURE 2.8 : Comparison of SKIP II and DISCS results

Two comments should be made here.

(i) The DISCS natural frequencies are somewhat higher than Reinke's. The higher frequencies predicted by DISCS probably reflect the fact that DISCS assumes continuous guides, whereas the 3 mm central guide deflection assumed by Reinke[8] gives a situation which is closer to simply supported guides, which are more flexible than continuous guides. The frequency of passing buntons is however much the same, as it should be. The frequency of passing two buntons, or of passing guide joints is reflected by DISCS, but as an insignificant peak.

TABLE 2.1 : IMPORTANT FREQUENCIES

	REINKE[8] EMPTY	DISCS EMPTY	
		Calculated	Spectral Analysis
Frequency of passing 2 buntons	1,1 hz	1,17 hz	1,16 hz
Frequency of passing buntons	2,2 hz	2,34 hz	2,31 hz
Natural frequency of translation	1,98 hz	2,26 hz	2,31 hz
Natural Frequency of rotation	2,42 hz	3,49 hz	3,40 hz

(ii) In the DISCS predictions the natural frequency of translation very nearly coincided with the frequency of passing buntons. This did not produce dynamic magnification but there was a high peak at 2,31 hz. This translation mode behaviour can be seen to some extent in the wheel loads shown in Figure 2.9. At the positions marked A, a maximum wheel load on the top wheel coincides with a maximum wheel load at the bottom. The wheel loads shown, exhibit to a much greater extent, maximum load peaks at the buntons. The top and bottom peaks occur out-of-phase because the conveyance length is very nearly 1,5 times the bunton spacing.

The wheel loads predicted by Reinke[8] are stated to fall into the range:

$$\text{PRELOAD (or mean load)} \pm 3\sigma$$

where σ is the standard deviation of the wheel loads. He used a preload of 8 kN and gives a standard deviation of 1,93 kN for the empty cage and 2,25 kN for the fully loaded cage. The maximum predicted loads are then as given in Table 2.2 below.

TABLE 2.2 : PREDICTED MAXIMUM WHEEL LOADS

	REINKE[8]	DISCS (maximum in 500 buntons)
Empty cage	13,8 kN	13,4 kN
Full cage	14,8 kN	18,3 kN

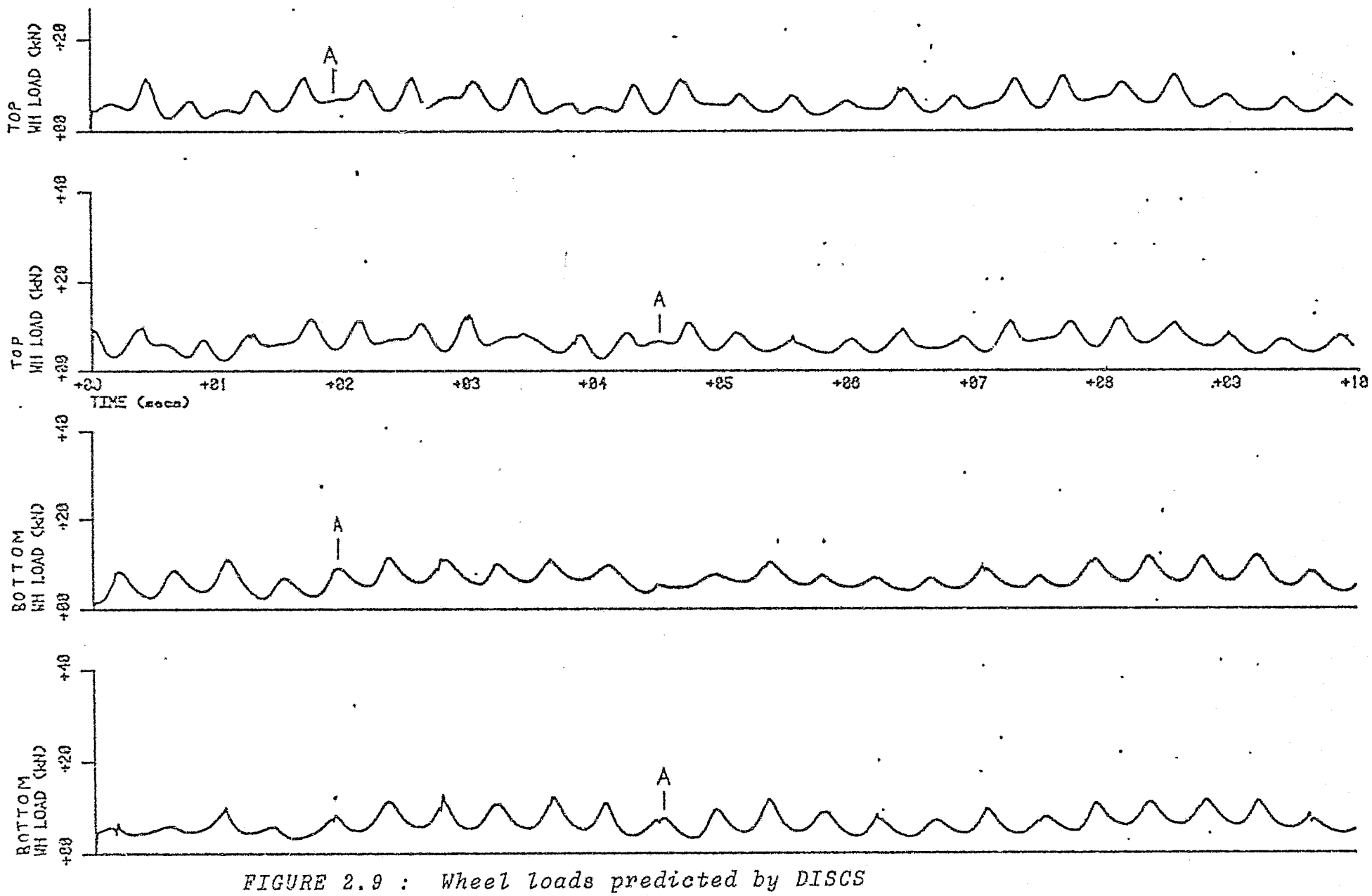


FIGURE 2.9 : Wheel loads predicted by DISCS

These predicted wheel loads are in good agreement. The load given for DISCS for the empty cage is the average of all four wheels, whereas for the full cage it is the average of the top two wheels only. DISCS appeared to show some dynamic magnification for this case, probably because the natural frequency of rotation was about 2,6 hz, which is not very different from the frequency of passing buntons. Due to this, the loads predicted by DISCS for the bottom wheels were very high and have been ignored for this comparison. This probably also explains why the DISCS loads are higher than the Reinke[8] prediction in this case.

2.2.4 Conclusions

It is clear from the above comparisons that the results from the three models considered are not directly comparable because of different assumptions, but the similarity of the results does indicate predictions which are not obviously wrong and which can be reasonably well explained.

CHAPTER 3 : FIELD MEASUREMENTS

Field measurements form a necessary part of this research for two reasons.

a) DISCS and other theoretical models must be checked against measurements.

b) The measurements may be used in identifying empirical relationships for use in design.

3.1 The Equipment Used.

In setting out to obtain field measurements, several points had to be borne in mind:

a) In order to check DISCS comprehensively a wide range of measurements, necessitating work in many different shafts would have to be obtained. The equipment to obtain the measurements would thus have to be portable, and set up as quickly as possible, to ensure the least interference with the production of the mines concerned.

b) Measurements of guide and bunton behaviour, apart from being very difficult and time consuming to instrument, would not reflect anything predicted by DISCS, so they are omitted. The misalignment also varies down the shaft, so that in the absence of measured misalignment data from which a good representative length of shaft could be selected, there would be no means of establishing any relationship between measured behaviour in the test section and the behaviour elsewhere in the shaft.

c) Accelerations on the conveyance are the easiest of the dynamic behaviour parameters of conveyances to measure, and several mines already measure top transom lateral acceleration as an indication of shaft condition. However, for structural design it is preferable to work from a knowledge of loads. The tests done should thus include both acceleration and wheel load measurements.

d) The hostile environment in the shaft and the limited time available for measurements, mean that the equipment must be self contained in all respects, it must be as robust as possible and should incorporate as large a data storage capacity as possible.

e) All results had to be in a form in which they could be analysed electronically.

Bearing these considerations in mind, a set of measuring and analysis equipment as shown in figure 3.1 was obtained.

3.1.1 The transducers

Two types of transducers were used, i.e. accelerometers and load cells. This is fundamentally the same instrumentation used by Reinke[8], but he also recorded the loading on guide slippers and measured the relative displacement between guides and the conveyance. Load recording guide slippers would have been useful, but making measurements at different shafts would have required new tailor-made guide slippers for each set of measurements and it would not have been possible to fit them in the time available in each shaft. The wheels are however adjusted to avoid guide-slipper contact as far as possible so it is believed that neglecting this contact force will not seriously affect the results.

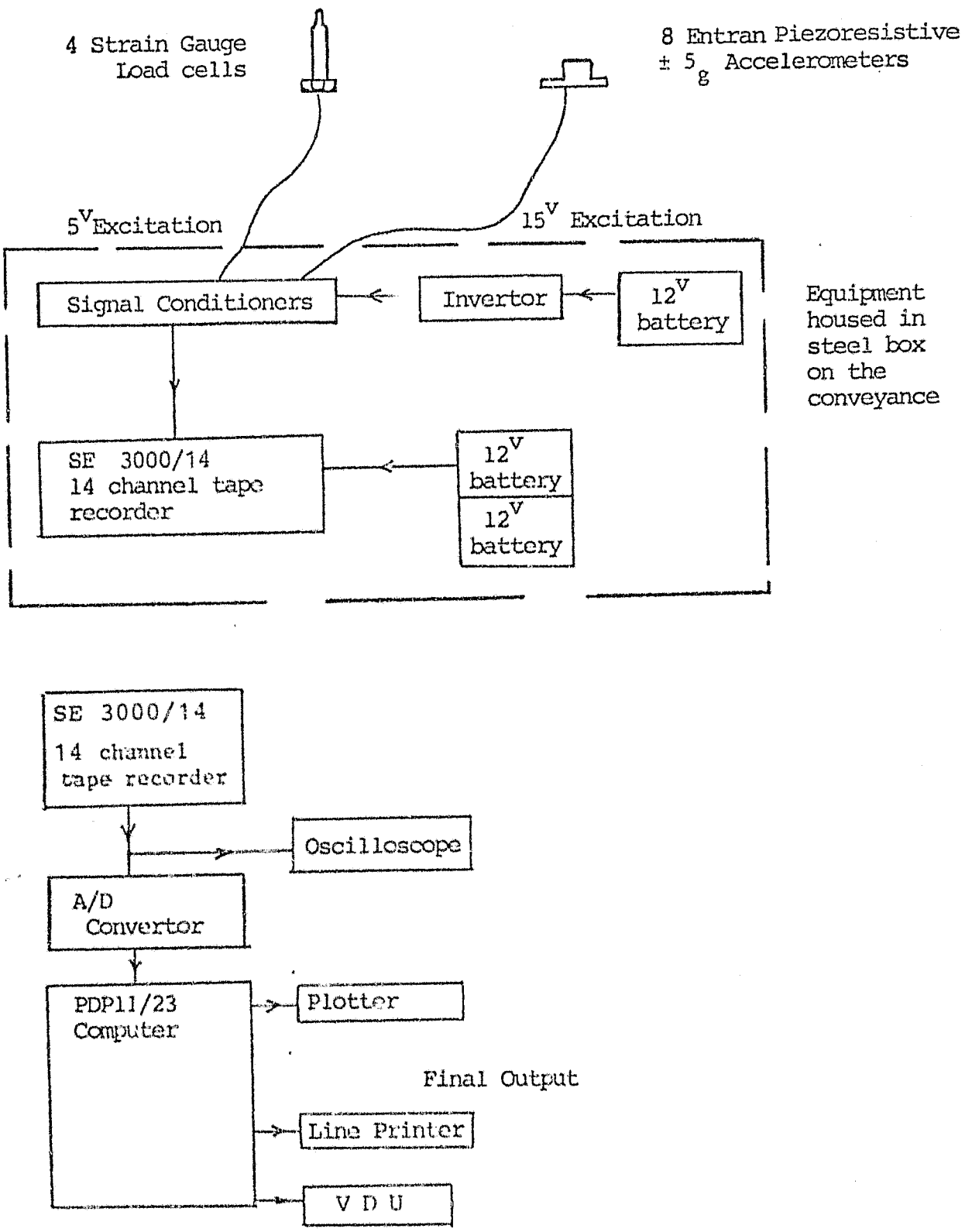


FIGURE 3.1 Schematic of Measuring and Analysis Equipment

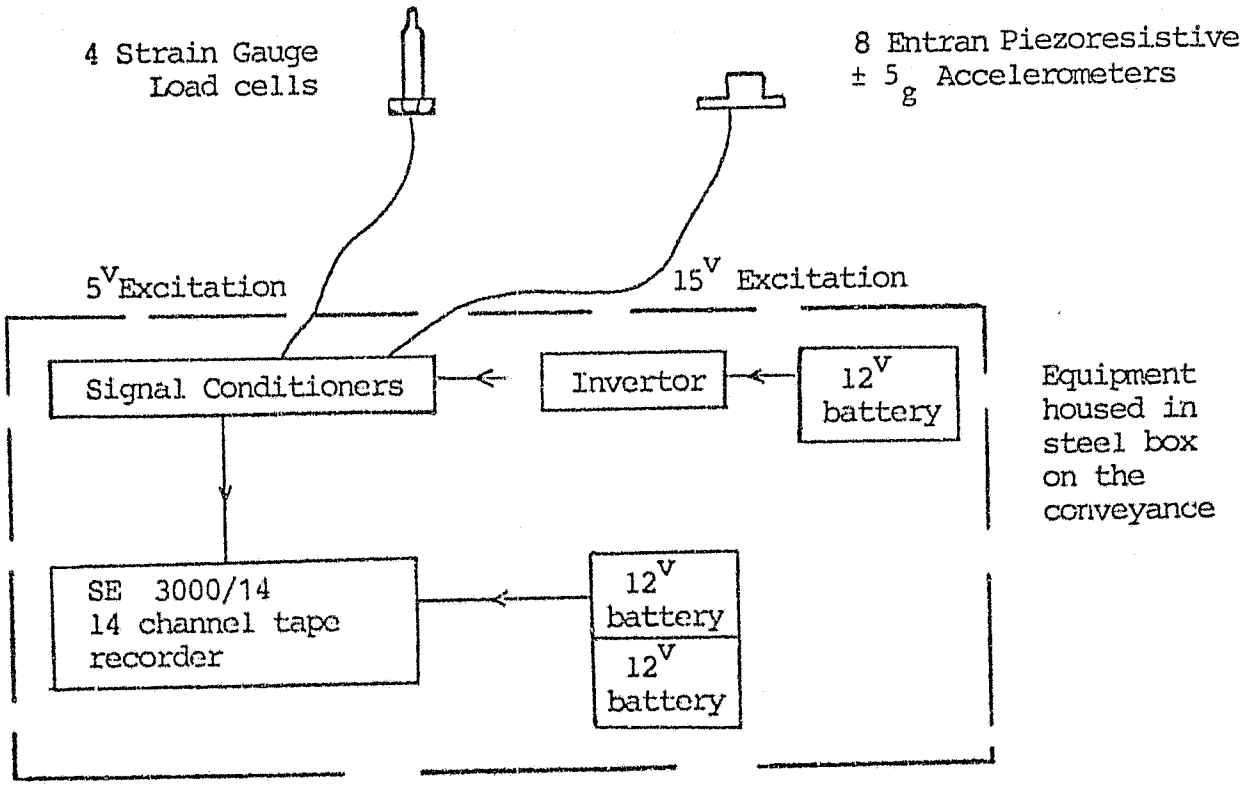


FIGURE 3.1 Schematic of Measuring and Analysis Equipment

a) For the accelerometers, it was necessary to have small units which could easily be fixed to conveyances, which were fairly sensitive, and which had a constant response from 0hz to at least 50hz. To meet these requirements it was decided to use ENTRAN ECG accelerometers, which have the following specifications:

Range ± 5g
Excitation 15V D C
Output 25mV/g

Response constant 0hz - 100hz

b) In order to measure wheel loads, bolts which fitted into the guide wheel sets were made up, with necked sections to which strain gauges were fitted in a form of a 4-arm bridge, as shown in figure 3.2. Three different types of load cell were required to fit the different types of wheel sets. Calibration procedures and other details are described by Fotopoulos[15]. Of particular note is his finding that the calibrations of load cells fitted on new and very old wheel sets is very similar, so that the state of the wheel set has little effect on the calibration.

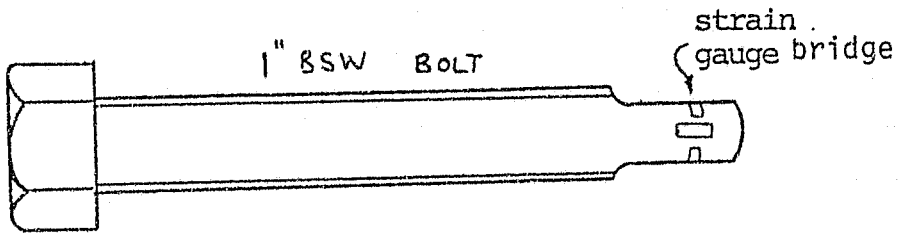
The calibration for these load cells is:-

Excitation 5V D C

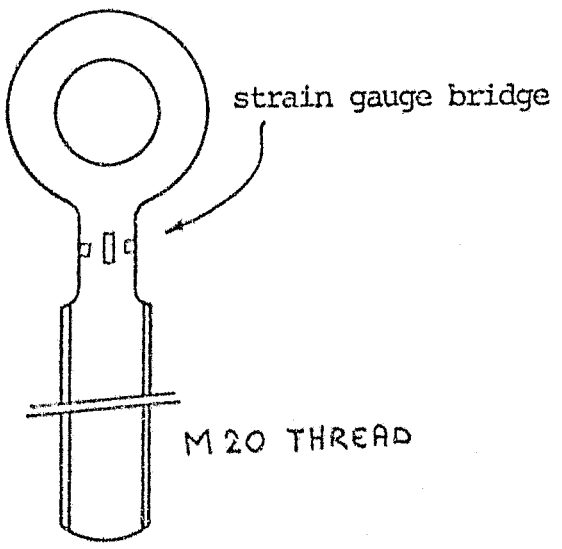
Output:-

Type A	26mV/kN
Type B	21mV/kN
Type C	22mV/kN

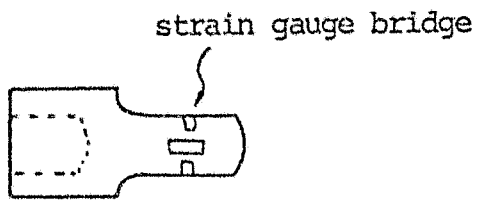
(All with gain of 100 on signal conditioners)



Type A - compression



Type B - tension



Type C - compression

FIGURE 3.2 Load Cell Bolts

c) A transducer producing a pulse to locate the bunton positions on the tape was desired, but could not be achieved. Magnetic transducers had too short a range to operate properly. Mechanical sensors had too low a frequency response. The noise level in the shaft meant that sonic proximity sensors would not give successful results. A light sensor with co-axial fibre optic source and reflection sensing cables was tested, but did not give useful results, probably because of very poor reflection from the buntons. An attempt to locate the buntons by means of a double integration of lateral accelerations to give lateral displacement is described in section 4.1.4. This was also not successful. Omitting the bunton sensor had several disadvantages.

(i) the hoisting speed could not be calculated exactly by dividing bunton spacing by time taken between buntons. An accelerometer measuring vertical accelerations which could be integrated to give hoisting speed did not give useful results because of the low level of winder acceleration relative to dynamic behaviour accelerations. It was thus necessary to rely on the hoisting speed indicated on the winder, which engineers estimated to be accurate only within 10% or 15%, although the ratio between different speeds on one winder is accurate to within very small margins. This presents some difficulties in comparing one shaft with another.

(ii) much greater use could be made of the measurements by the mines themselves, for maintenance purposes, if the measurements were located exactly in the shaft. Exact location in the shaft is however of no benefit to the research project because the guide misalignment is not known.

d) Some method of determing guide misalignment was initially also considered, but would have been far too time consuming. Reinke[8] describes in detail tests on various guide alignment measuring devices. He concludes that they are only effective over short distances, and need much improvement before they are of practical use. The South African mining industry is at present constructing a frame of bending and torsion bars with displacement tranducers, to measure the guide alignment as it runs down the shaft. There may thus soon be simple, quick methods of measuring guide misalignment, but it was not possible at the time of making measurements. It was thus necessary to base all misalignment on a random distribution within the engineer's assessment of the limits.

3.1.2 Signal conditioning was achieved by means of converted SE994 signal condition units. These produced the regulated excitation for the transducers, as well as amplification of the output. Amplification used was 10 or 100 for the accelerometers and 100 or 1000 for the load cells. A 40hz low pass filter was built into these signal conditioners, so that 50hz noise from the high voltage electricity supply in the shafts would be eliminated. Figure 3.3 shows the filter characteristics. All cabling was also shielded to reduce this noise.

3.1.3 Recording of Data was done by means of an SE3000/14, 14 channel portable tape recorder. Data was recorded in analogue form for two reasons. Firstly, less equipment was required on the conveyance itself. A

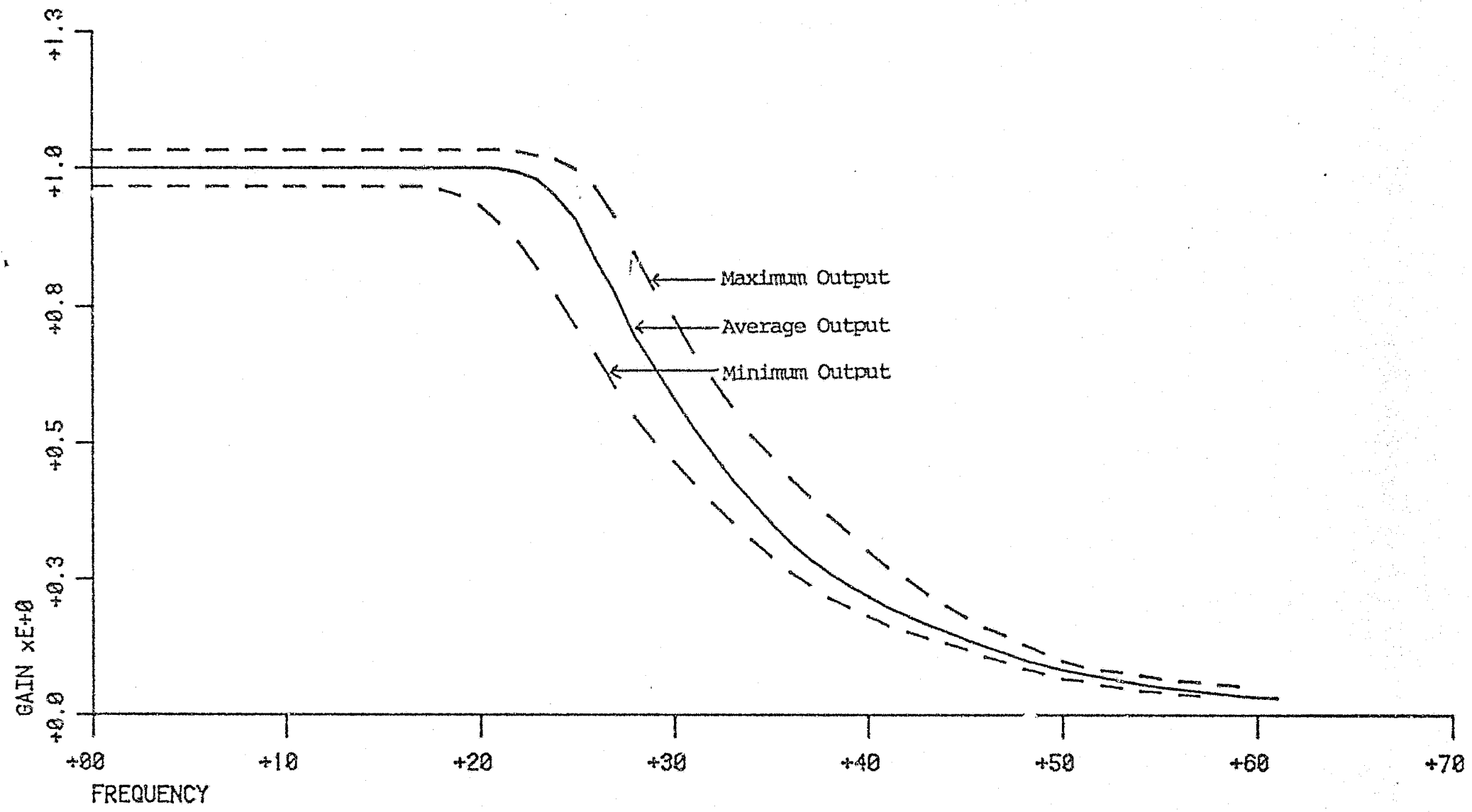


FIGURE 3.3 Filter Characteristics.

sufficiently fast analogue to digital converter handling 14 channels was bulky and had fairly high power requirements, so that it could not easily be included with the equipment on the conveyance. Secondly, the quantity of data stored in analogue form on a tape was very much greater than that in digital form.

Tape speeds of 15/16 and $1\frac{7}{8}$ inches per second were used to give recording time of 8 and 4 hours respectively and specified signal to noise ratio of 46 and 47 dB respectively. The input levels on the tape recorder were set to accept peak to peak levels of 3,0 V or 30 V for the accelerometer channels amplified 10 times and 100 times respectively. This represented acceleration values between ±6 g.

3.1.4 Analogue to Digital conversion was accomplished by means of a DEC KWV11-A 16 channel analogue-to-digital converter. A programme called SAMPLER was written to sample from the tape recorder and store the record on disk in the computer. In order to sample and store the data fast enough (i.e. at a maximum rate of 14 channels at 200 hz each) it was necessary to do no manipulation of the data, and to store it in an unformatted form. A programme called CALIB was then written to retrieve this unformatted data, adjust it for zero value and the correct scale, and then store it again, in the same format as the DISCS output.

A third programme, called INIT was written to sample slowly and display the values on the VDU, so that the transducer calibrations, which were recorded on the tape could be viewed, and the zero and scaling factor used in CALIB could be found.

sufficiently fast analogue to digital converter handling 14 channels was bulky and had fairly high power requirements, so that it could not easily be included with the equipment on the conveyance. Secondly, the quantity of data stored in analogue form on a tape was very much greater than that in digital form.

Tape speeds of 15/16 and $1\frac{7}{8}$ inches per second were used to give recording time of 8 and 4 hours respectively and specified signal to noise ratio of 46 and 47 dB respectively. The input levels on the tape recorder were set to accept peak to peak levels of 3,0 V or 30 V for the accelerometer channels amplified 10 times and 100 times respectively. This represented acceleration values between ±6 g.

3.1.4 Analogue to Digital conversion was accomplished by means of a DEC KWV11-A 16 channel analogue-to-digital converter. A programme called SAMPLER was written to sample from the tape recorder and store the record on disk in the computer. In order to sample and store the data fast enough (i.e. at a maximum rate of 14 channels at 200 hz each) it was necessary to do no manipulation of the data, and to store it in an unformatted form. A programme called CALIB was then written to retrieve this unformatted data, adjust it for zero value and the correct scale, and then store it again, in the same format as the DISCS output.

A third programme, called INIT was written to sample slowly and display the values on the VDU, so that the transducer calibrations, which were recorded on the tape could be viewed, and the zero and scaling factor used in CALIB could be found.

These three programmes are listed and described in more detail in appendix E.

The channels were not sampled exactly simultaneously, but consecutively, the analogue-to-digital converter reading channel 1, then 2, 3, 4 etc. up to however many channels were being sampled. It was considered whether some form of interpolation should be used to convert the samples from channels 2, 3, 4, etc to a simultaneous time with channel 1. The sampling time was approximately 40 microseconds, so that even sampling all fourteen channels would take only 560 microseconds or 0,6 milliseconds. The time between samples was five milliseconds or longer, i.e. eight or more times the sampling time. The samples on different channels were thus considered to be sufficiently close together in time to be taken as simultaneous. The time between samples on any one channel is exactly the specified sampling interval, so that the only analyses which may be slightly affected are cross correlations.

Initially sampling was carried out at 200 hz, but it was found that all significant frequencies were below 25 hz, and amplitudes were uncertain above this because of the filter. All further sampling was thus done at 100 hz to give better resolution of the lower frequencies. The position of sampling was determined using an oscilloscope. The positions where the conveyance was stationary could clearly be seen by very low amplitude signals. Sampling was then done, usually over 6000 or 10000 points, i.e. 60 or 100 secs, well inside these stationary positions, to avoid areas where the conveyance was accelerating or decelerating.

3.1.5 Cyclical force exciter

Some method of measuring the natural frequencies of

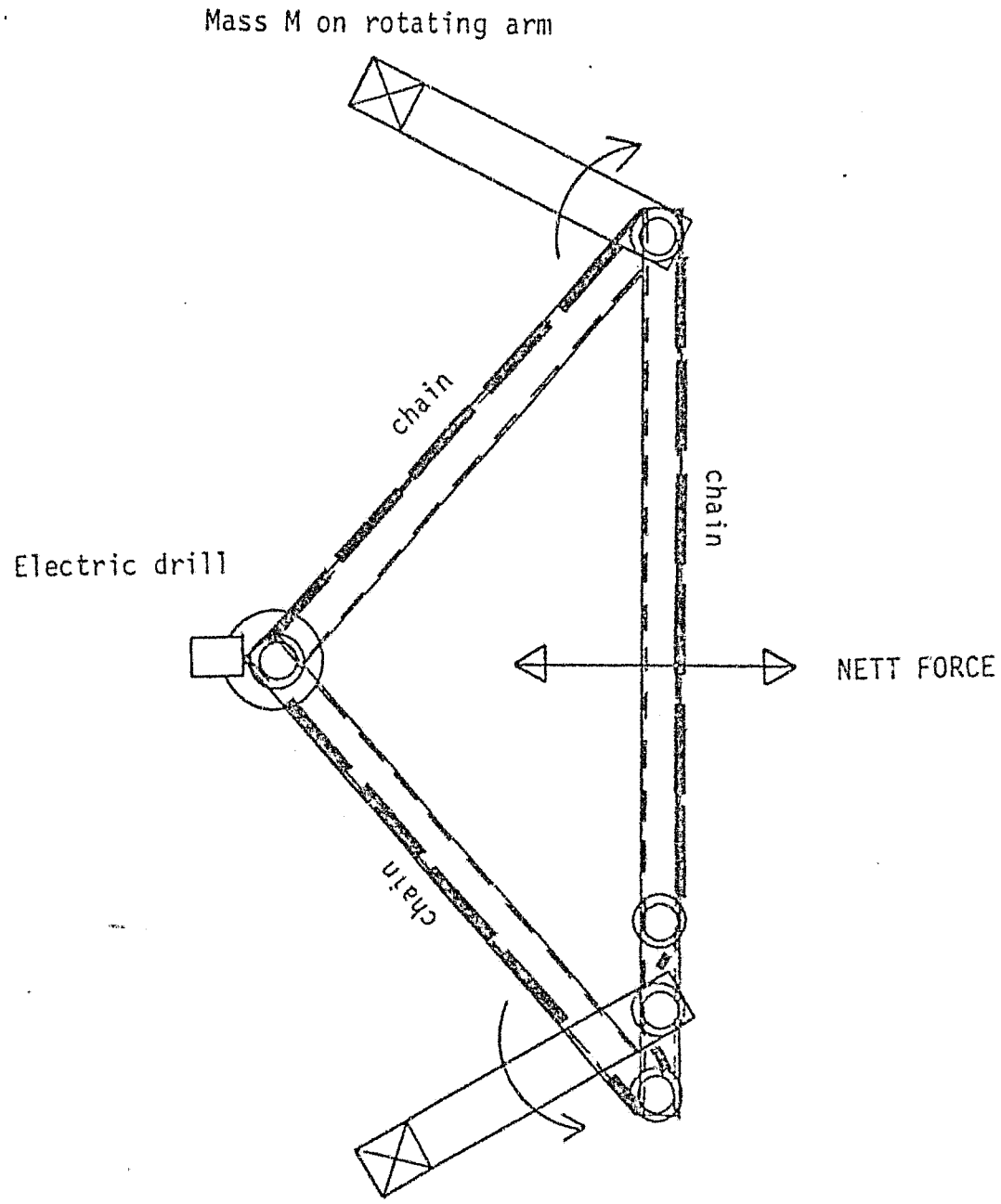


FIGURE 3.4: Cyclical force exciter

conveyances was desired, to confirm the frequencies shown by the power spectra. An exciter, shown schematically in figure 3.4 was thus built, giving a net force output in one direction varying sinusoidally, with variable frequency.

The total mass of this exciter was 80 kg, which was considered negligible in comparison with the conveyance mass of several tons. This exciter was thus clamped in the conveyance, orientated so as to give a force in the desired direction. It was placed as near as possible to the centre of gravity in order to measure the translational mode frequency, and at the top or bottom of the conveyance to measure the rotational mode frequency.

The exciter was powered by a hand electric drill, with a maximum frequency of 17hz which could be stepped down by a factor of 2,6. A variable speed control varied the frequency from zero to the maximum, so that the frequency range was either 0 -17 hz or alternatively 0 -6,7hz. The mass M, could be varied up to 5 kg by placing masses on the end of the rotating arms.

3.2 Types of Measurements made

3.2.1 Measurements in the Operating Condition

Most of the measurements were made with the conveyances operating normally, and at reduced speeds and payloads, but otherwise normal operation. In each shaft, it was desired, if possible, to carry out the following set of tests:

2 runs at maximum speed, empty
2 runs at maximum speed, half full
2 runs at maximum speed, full
2 runs at 3/4 speed, empty
2 runs at 3/4 speed, half full
2 runs at 3/4 speed, full
1 run at half speed, empty
1 run at half speed, full

In most tests, this full series was not possible because of one or more of the following factors:-

(i) the full set of tests occupied some 1½ to 2 hours, which length of time was not always available after fitting the transducers to the conveyance,

(ii) winder limitations, e.g. in one shaft winder overload would have occurred hoisting full load at half speed.

(iii) rope coiling problems or severe rope whip ruled out certain hoisting speeds in some cases, or

(iv) the position in which the equipment was fixed in some instances prevented tipping or loading of skips, so that only empty tests could be conducted.

The transducers were placed so as to measure in the plane between the guides, (in plane) but in some cases a few tranducers were placed so as to measure at right angles to this plane (out of plane) as close as possible to the side wheels. This gave a simple and useful comparison between the relative behaviour in the two directions.

The layout of the transducers in the plane of the guides is shown in figure 3.5. Up to four accelerometer

measurements were made. These were on the top and bottom transoms, and where possible at one or more positions on the cage body. Acceleration measurements on skip bodies were usually not possible because of the difficulty of fixing accelerometers in the plane between the guides in order to eliminate the out of plane component of acceleration. In one instance, as a check on the performance of the accelerometers, two were placed near each other measuring in the same direction. The two measurements, portions of which are shown in figure 3.6 slightly offset from each other, showed only very slight differences apart from a constant difference in magnitude of approximately 11%. This gives a reasonable assessment of the expected accuracy of the measurements.

The intention was to place load cells on all four face guide wheels, but this was not achieved in any shaft because of one or more of the following factors:-

(i) load cells took longer to fit than accelerometers, so that time limitations in the shaft meant that the load cells could not all be fitted in some cases,

(ii) the load cells required a certain minimum clearance on the adjusting bolts to which they were fitted, to avoid either applying too great a preload to the wheels or reducing the clearance between guide face and slipper to an unacceptably small amount. In most cases this meant one or two load cells had to be omitted,

(iii) in one case the skip had other instrumentation fitted which meant omitting one load cell.

In one set of measurements one load cell was fitted to a side wheel, to measure the out-of-plane load.

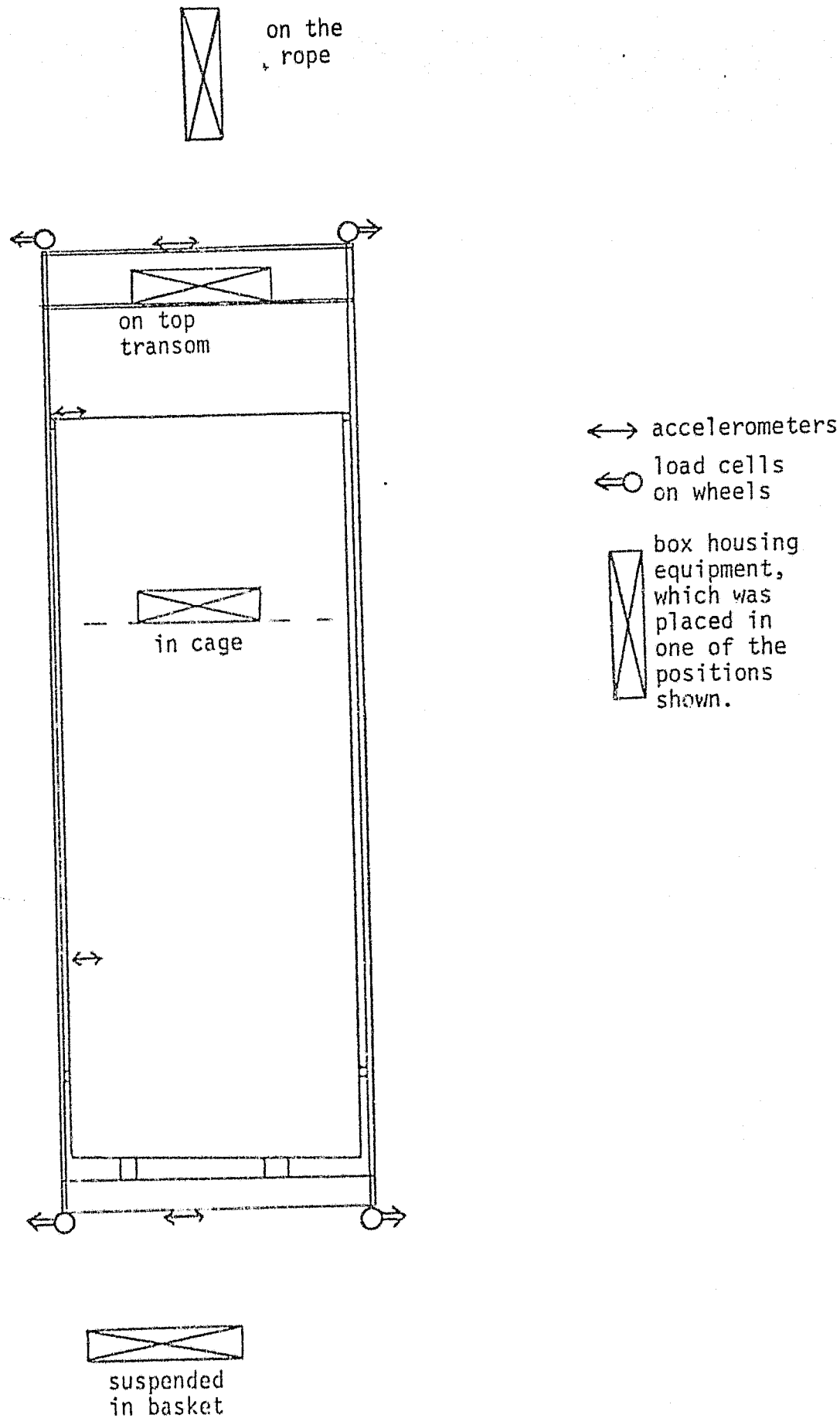
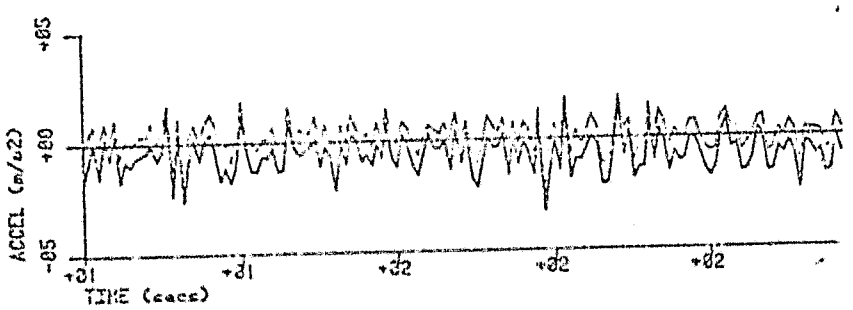


FIGURE 3.5 Transducer Layout on conveyance.



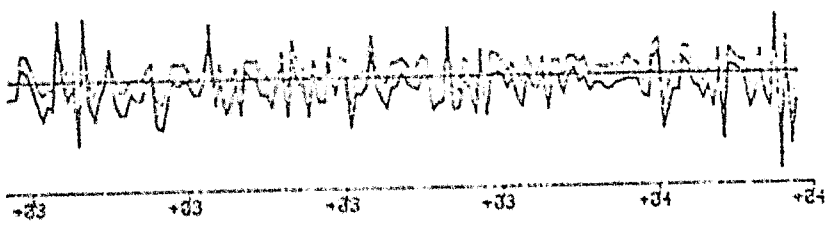


FIGURE 3.6: Comparative Accelerometer Measurements

3.2.2 Natural frequency measurements

In order to confirm the natural frequencies shown by the power spectra of the measurements, the natural frequencies of one cage were measured. Two accelerometers were fixed to the cage, one at the top and one at the bottom. The cyclical exciter was fixed in the cage and its frequency was increased until resonance was achieved. This was clearly indicated both visually and by the accelerometer output.

The position of the variable speed control was noted and then the frequency checked in the laboratory using a strobe light. Analysis of the accelerometer readings gave the frequency as well as an indication of the overall vibration mode. The results, for the Hartebeestfontein No. 8 shaft mancage are given in table 3.1 below.

Table 3.1 Measured natural frequencies Hartebeestfontein No. 8 Shaft

	Exciter frequency	Accelerometer measured frequency
Fundamental mode (translation)	3,0 hz	3,09 hz
Second mode (rotation)	5,0 hz	- hz

3.2.3 Future measurements

As mentioned above, an instrument which records guide alignment will soon be available, at least for some gold mine shafts. Such a record, made shortly before or after a set of test measurements would be most valuable

in relating guide misalignment to the magnitude of dynamic behaviour.

Together with this, a specific location of the conveyance in the shaft should be recorded. The methods which are most likely to give this location are either using the light sensor described above together with proper reflectors fixed to buntons at the top and bottom of the shaft and at two or three intermediate locations, by using a transducer which gives a pulse for each rotation of the sheave wheel or winder drum and transmitting this signal down the rope to the recorder, or the use of a light source and light sensor placed one each side of a guide, which will record a pulse at the gap between guides.

Were there to be more time made available in a few shafts, slipper contact forces, using a load recording guide slipper as described by Reinke[8] could be made. This would provide a more complete record of the overall forces between guides and conveyances.

A constant record, measured over several months or even years, as envisaged at President Steyn number 4 shaft, would form a very valuable contribution. An analysis of the data at, say, monthly intervals would provide information on which basis other measurements could be extrapolated to provide long term predictions.

More out-of-plane measurements of accelerations and wheel loads would also be valuable, as would strain gauge measurements at strategic positions on the bridle.

3.3 Comments on Assumptions in DISCS

It was perhaps unfortunate that the field measurements were only available after DISCS had been set up. The measurements highlighted some problems with these assumptions, which should be corrected as future alterations to DISCS.

Measurements with accelerometers measuring out-of-plane at the wheels typically showed acceleration values 1,5 to 2 times those in the plane of the guides. This differs from what the engineers had found because their accelerometer traces were done with the out-of-plane accelerometer as close as possible to the centre of the top transom, hence eliminating the effects of rotation in the horizontal plane. This indicates the importance of extending the model to three dimensions. The one out-of-plane wheel load was however significantly smaller than other face wheel loads, because the mass moment of inertia in the horizontal plane is less than in other planes, (by a factor of about three to ten, depending on the skip configuration) so that higher accelerations do not lead to higher forces in this plane. The present DISCS model does thus model the plane in which the higher wheel loads can be expected.

The power spectra of out-of-plane accelerations also included low frequency peaks at the natural frequencies in the in-plane direction. These peaks were not of great significance, but do indicate some coupling between motion in the different planes, again highlighting the need for a three dimensional model.

Measurements in at least one shaft showed resonance between the wheel rotation frequency and the fundamental frequency of the wheelset itself. Thus these local effects cannot be ruled out, and the wheelsets should perhaps be modelled in more detail in DISCS. Once this is seen from measurements to be a problem, it can be accommodated by DISCS by specifying a high value of wheel irregularity, but it cannot be predicted.

The assumption that there is no basic difference between upward or downward motion was confirmed by the measurements. Although there were some small differences in the results of up and down runs on a few sets of measurements, in general up and down runs gave the same results.

CHAPTER 4

ANALYSIS AND COMPARISON OF DISCS AND MEASURED RESULTS

In order to assess the measured results and the DISCS predictions properly, and to draw comparisons between them or establish empirical relationships, it was necessary to perform various types of analysis on the data. These are described briefly below, followed by a detailed assessment of what can be learnt from this analysis. The analysis of the data, which is performed both on the measured data and on the DISCS results includes a probability analysis on peak wheel loads, spectral analysis to establish the frequency characteristics, fatigue loading cycle counting and an analysis of the displacements. The measurements and DISCS predictions are compared on the basis of these analyses and are found to show satisfactory agreement, and conclusions are drawn regarding the maximum wheel loads, the level of fatigue loading and the important frequencies.

4.1 Methods of Analysis of Data

4.1.1 A probability analysis of the maximum wheel loads was developed and is described by Alport[16]. A computer programme, POWER, establishes the maximum wheel load during a time interval equivalent to travelling between two adjacent buntons, and then carries out a probability analysis on this data. The results are in the form of the maximum expected wheel loads for any specified number of buntons passed.

CHAPTER 4

ANALYSIS AND COMPARISON OF DISCS AND MEASURED RESULTS

In order to assess the measured results and the DISCS predictions properly, and to draw comparisons between them or establish empirical relationships, it was necessary to perform various types of analysis on the data. These are described briefly below, followed by a detailed assessment of what can be learnt from this analysis. The analysis of the data, which is performed both on the measured data and on the DISCS results includes a probability analysis on peak wheel loads, spectral analysis to establish the frequency characteristics, fatigue loading cycle counting and an analysis of the displacements. The measurements and DISCS predictions are compared on the basis of these analyses and are found to show satisfactory agreement, and conclusions are drawn regarding the maximum wheel loads, the level of fatigue loading and the important frequencies.

4.1 Methods of Analysis of Data

4.1.1 A probability analysis of the maximum wheel loads was developed and is described by Alport[16]. A computer programme, POWER, establishes the maximum wheel load during a time interval equivalent to travelling between two adjacent buntons, and then carries out a probability analysis on this data. The results are in the form of the maximum expected wheel loads for a ·ified number of buntons passed.

4.1.2 Spectral analysis computer programmes, FFT and CMP, also developed and described by Alport[16], give frequency and phase information about the data.

The programme FFT calculates the power spectrum of the data by using a fast fourier transform method.

The power spectrum can also be calculated by CMP, which also gives auto-or cross-correlation functions or auto-or cross-covariance functions.

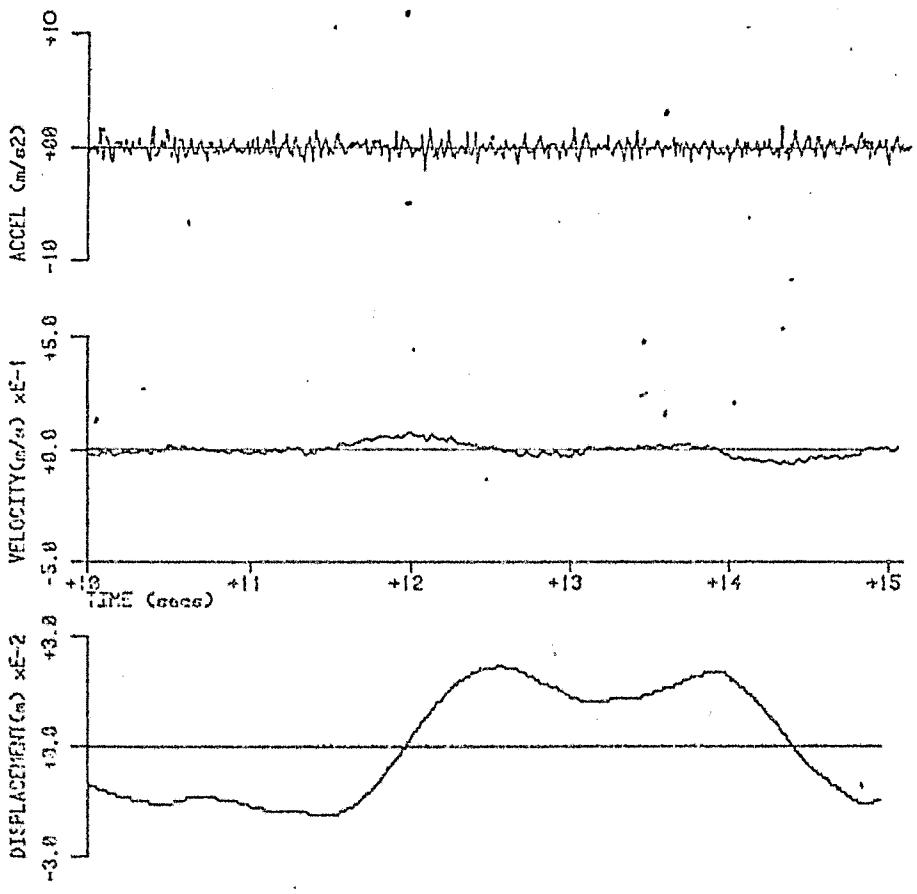
The power spectrum calculated by the programme FFT can be averaged over any number of consecutive data blocks, and plotted to a li ar and a logarithmic scale by the progr e FFTPL.

The programme CMP was also used to calculate the cross covariance function between specified records, usually near the beginning, middle and end of the test.

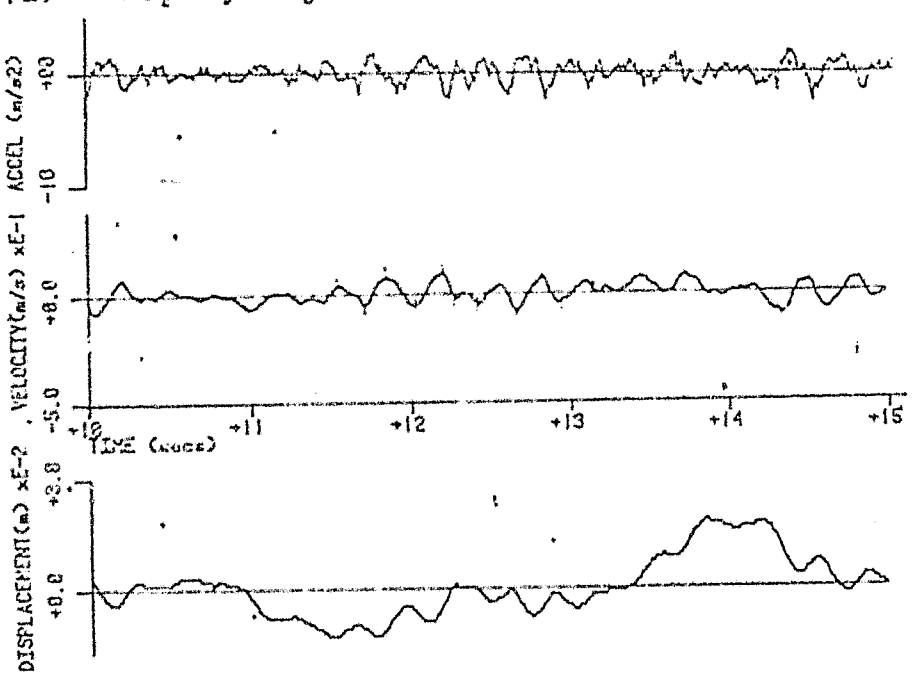
A programme TF was developed, and is described in appendix E, to calculate the transfer function between any two channels.

4.1.3 Fatigue analysis was also carried out. This was developed by Fotopoulos[15] and is calculated by his programme FAG. The wheel load data is scanned and the number of load reversals, at various magnitude levels, are recorded giving a curve relating the force range to the number of cycles. (An F-N curve). On a given conveyance this can be altered to the normal S-N curve by carrying out a stress analysis of the conveyance with a unit wheel load. In most cases the stress at the point of concern can then simply be multiplied by the F-N curve to give the S-N curve, because the frequency of the exciting force (i.e. the wheel load) is usually lower than the fundamental natural frequency of the conveyance itself, and in the frequency range below the fundamental natrual frequency the transfer function is equal or nearly equal to one.

4.1.4 Displacement Analysis. It was thought that a double integration of top and bottom accelerations, giving velocity and displacement, may be a means of locating buntons and indicating to some extent the magnitude of misalignment. Two computer programmes were written, INTEG to carry out the integration, after first adjusting the data for zero mean and removing any general slope, and VELPL to plot the results. These two programmes are described in appendix E.



(a) Top of cage



(b) Bottom of cage

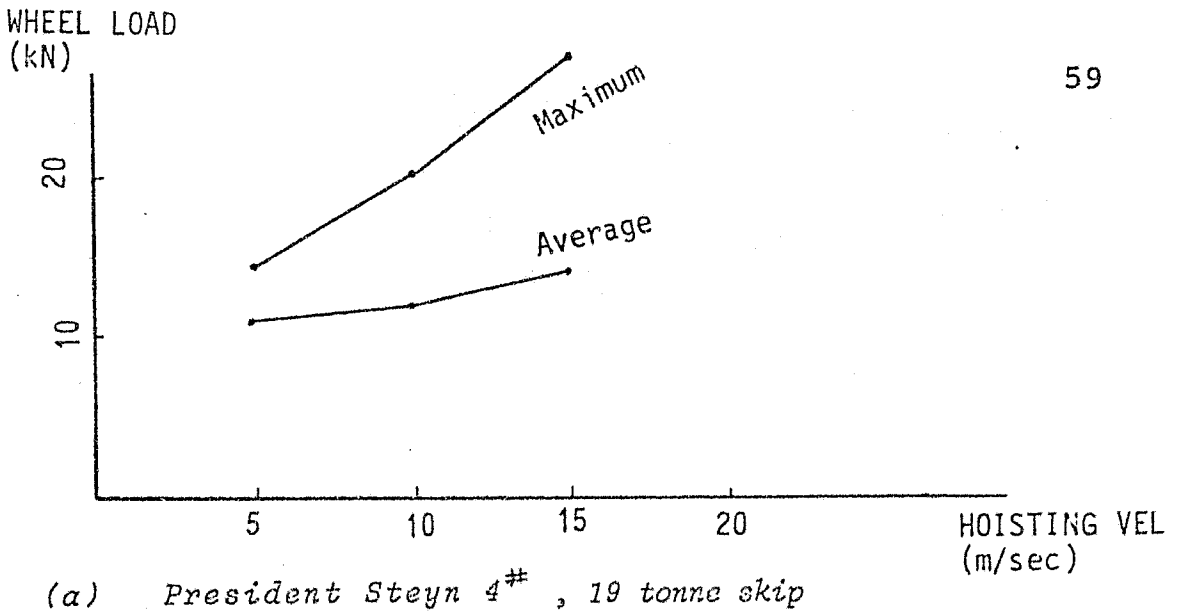
FIGURE 4.1 : Typical results of double integration Hartebeestfontein No. 8 Shaft.

In carrying out this analysis on several measurements it was clear that it was not reliable for locating buntons or for assessing misalignment. This was because in most cases the displacement was more a function of conveyance behaviour than of guide position. With reference to figure 4.1 which shows a typical result, it can be seen that:-

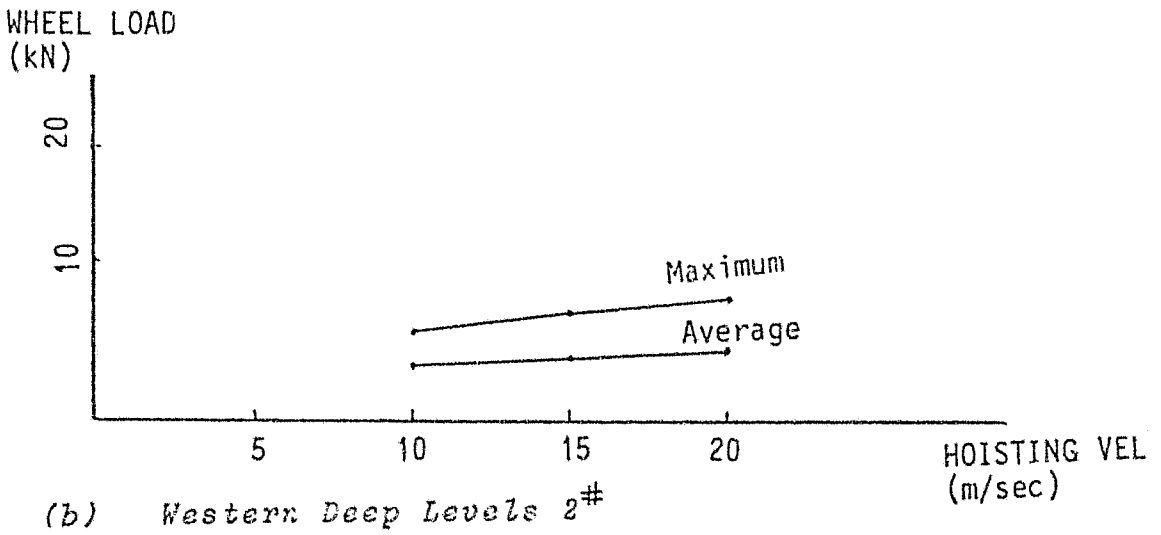
(i) The major displacement is a low frequency one. Comparing the top and bottom values shows in this instance that the top and bottom of the cage are being displaced in the same direction, i.e. translation of the conveyance is indicated. Other cases showed rotation.

(ii) The higher frequency displacement does not have a regular wavelength, probably due to interaction between the rotational natural frequency and the bunton positions. A very similar displacement frequency was maintained at half the hoisting speed, indicating that it is basically a natural frequency and not a bunton passing frequency.

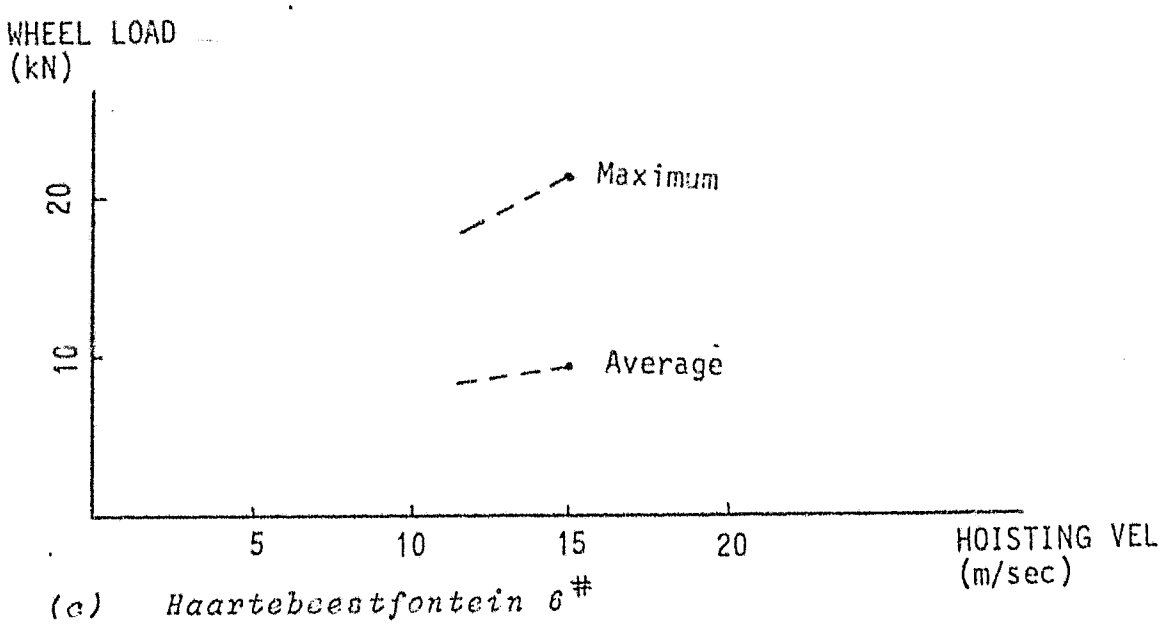
Thus, although this double integration has no value for bunton location or misalignment assessment, by effectively removing the higher frequency accelerations it does give a much clearer picture of behaviour in the two basic natural frequency modes, i.e. translation and rotation. It can thus form a useful part of the frequency analysis.



(a) President Steyn 4# , 19 tonne skip

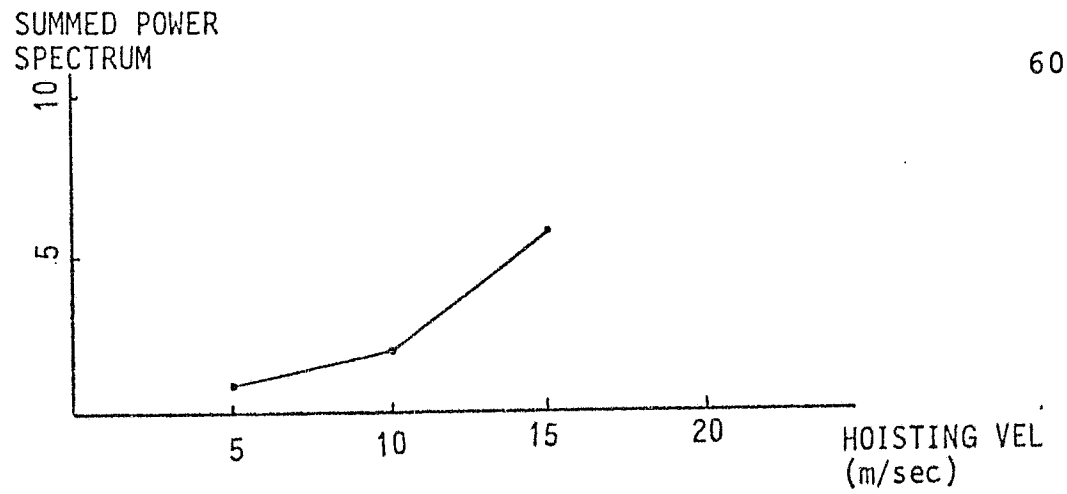


(b) Western Deep Levels 2#

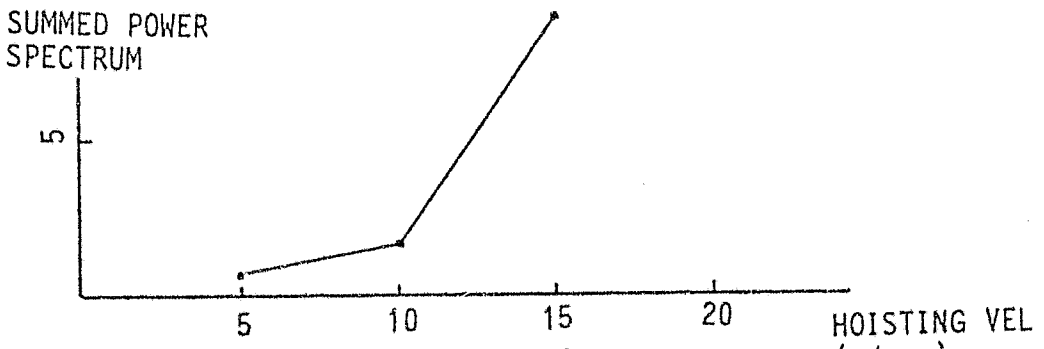


(c) Haartebeestfontein 6#

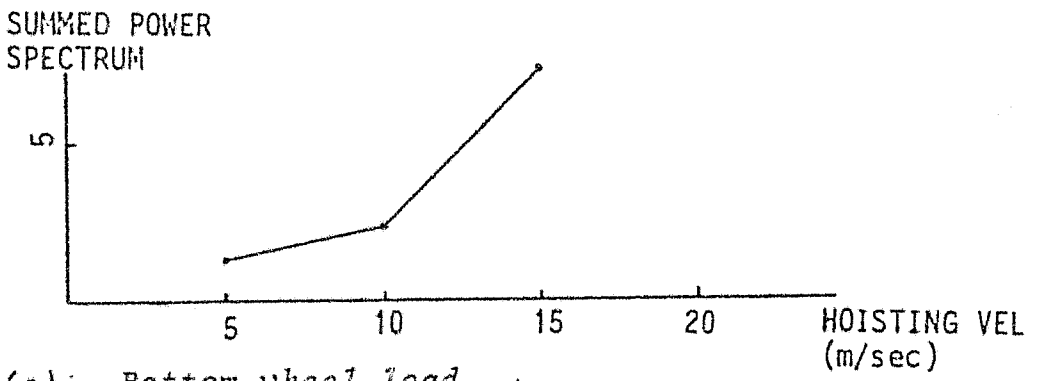
FIGURE 4.2 : Average and one week maximum wheel loads



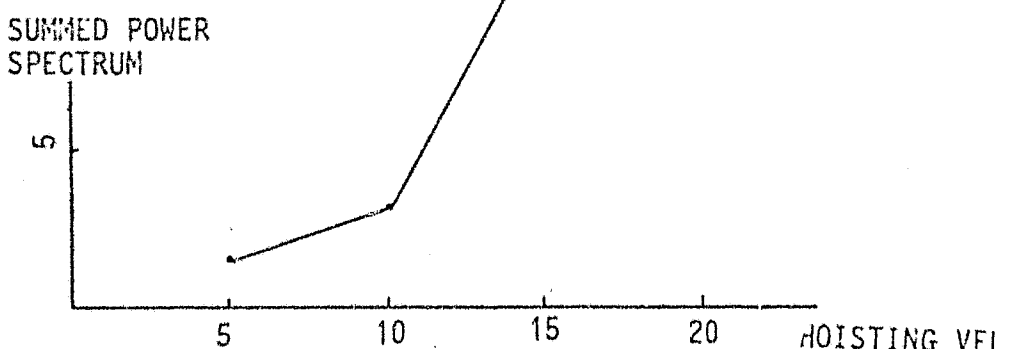
(a) Top wheel load



(b) Top transom acceleration



(c) Bottom wheel load



(d) Bottom transom acceleration

FIGURE 4.3: Areas under the power spectrum, President Steyn No. 4 shaft, 10 tonne skip

4.2 DATA ANALYSIS

The programmes listed above are set up in such a way that they all read the same basic input file, whether data from measurements or predictions from DISCS, as shown in appendix E.10.

For the purpose of analysing and comparing different data sets, the primary analyses done were a probability analysis using the programme POWER, and a calculation of the power spectrum using the programme FFT. The maximum wheel load in a one week period as well as the average maximum wheel load between buntons could then be plotted for different cases, as shown in Figure 4.2, and the total area under the power spectrum of a variable gives some measure of the expected level of vibration as shown in section 4.2.3. See Figure 4.3. The height of peaks on the power spectrum gives an indication of the relative importance of the significant frequencies. An example of significant frequencies is shown in Figure 4.4.

4.2.1 Maximum wheel load analysis

The maximum wheel load for which conveyances or shaft steelwork must be designed is the primary concern of shaft equipment designer. . In analysing measurements or predictions of wheel loads, the aim is thus to provide guidelines as to what the design load should be. As described

by Alport[16], the approach is to locate the maximum load in each time unit equal to the time between passing buntons i.e.

$$\text{time unit} = \frac{\text{bunton spacing}}{\text{velocity}}$$

Once these maximum loads have been obtained, a mean and standard deviation is calculated, as well as predictions of the maximum expected load for any specified return periods (in terms of the basic time unit). Alport's SMEMAX and POWER transformations give similar values, so all comments and conclusions made here are based on the SMEMAX transformation analysis.

It would be desirable to extend these predictions to the expected life of a shaft but there is little validity in a prediction to, say, 30 years, based on 60 seconds of measurements. There exists the possibility of drawing generalised conclusions by combining all the measurements obtained from various mines. This can however only be expected to provide general overall guidelines, because of the many altered variables in different measurements, and the indication that in different shafts high wheel loads are attributable to different variables. The results of all the wheel load measurements are summarised in Table 4.1 below, which gives the average and standard deviation of maximum loads and the expected maximum wheel load in a return period of one million time units (which is typically approximately one week of operation) and the average plus 3,8 standard deviations, which gives a probability of exceedance of 0,01% for a normal distribution.

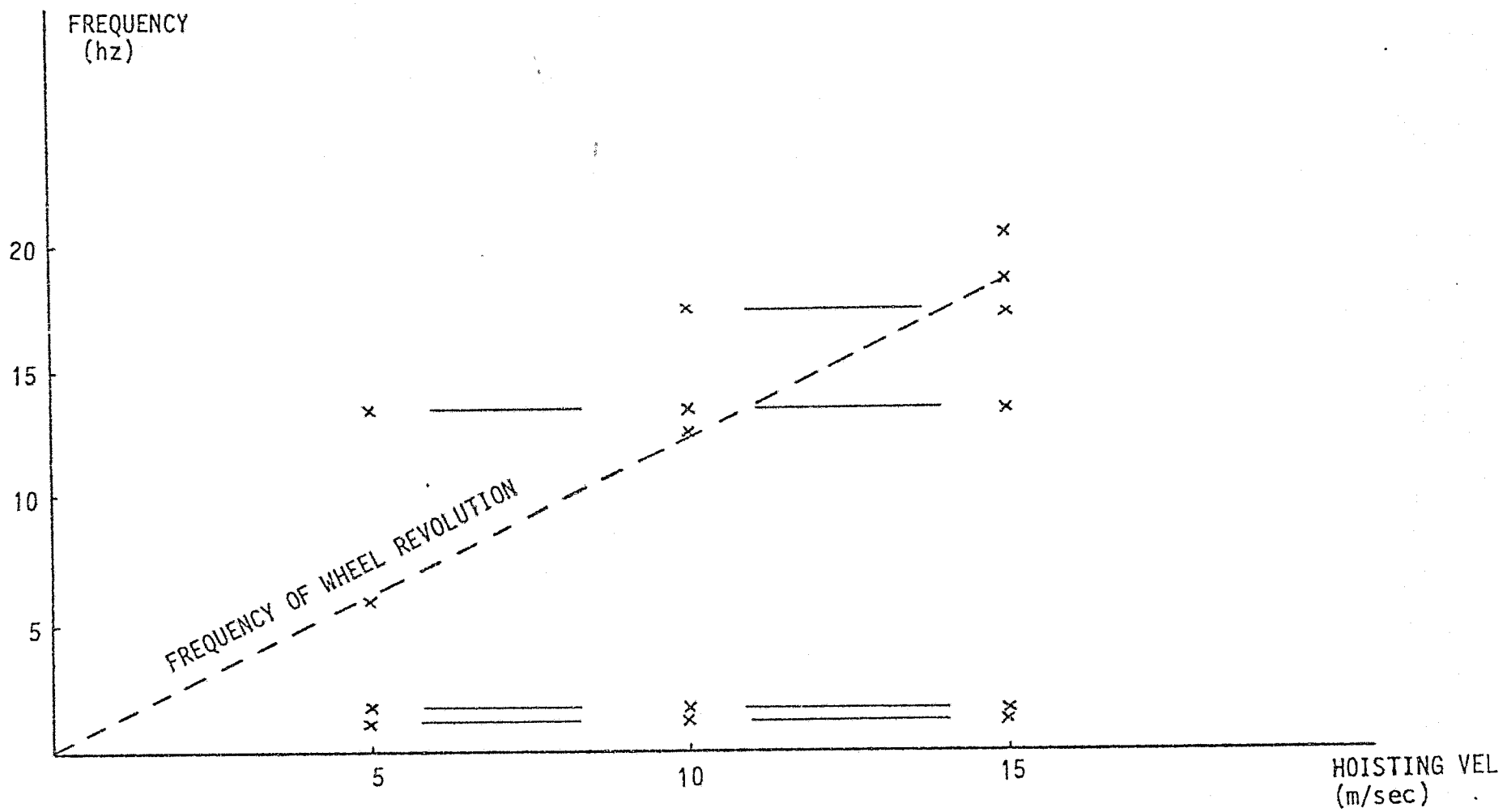


FIGURE 4.4 : Significant frequencies at President Steyn 4#, 19 tonne skip

TABLE 4.1 : SUMMARY OF MAXIMUM MEASURED WHEEL LOADS (in kN)

SHAFT	Ave. Load	Std. dev σ	Ave + 3.8σ	1 week max	W/10
Western Deep Levels 2# (top wheel)					
Full skip	4,0	0,45	5,7	7,3	28,0
½ full skip	4,0	0,41	5,6	6,4	19,0
Empty skip	3,7	0,39	5,2	6,2	10,0
Empty skip increased preload	4,1	0,49	6,0	7,6	10,0
President Steyn 4# (top wheel)					
Empty 19^t skip	9,2	0,84	12,4	14,9	12,0
Full 19^t skip (bottom wheel)	9,7	1,00	13,5	16,8	31,0
Empty 19^t skip	13,2	1,85	20,2	24,7	12,0
Full 19^t skip (top wheel)	14,3	2,36	23,3	27,6	31,0
Down full 10^t skip	8,6	1,4	13,9	21,6	16,7
Up full 10^t skip (bottom wheel)	8,2	1,7	14,7	20,0	16,7
Down full 10^t skip	10,2	1,3	15,2	20,6	16,7
Up full 10^t skip	10,5	1,8	17,3	24,4	16,7
Western Holdings 1# (top wheel)					
Empty skip	1,6	0,56	3,7	5,7	3,8
8,0^t payload	1,9	0,68	4,5	6,8	11,8
Full skip (bottom wheel)	2,6	0,80	5,6	7,8	13,6
Empty skip	1,3	0,85	4,5	8,5	3,8
8,0^t payload	0,9	0,38	2,3	4,0	11,8
Full skip	1,5	0,46	3,2	4,0	13,6

TABLE 4.1 : continued

SHAFT	Ave. Load	Std. dev σ	Ave + 3.8σ	1 week max	W/10
Haartebeesfontein 8# Mancage (top wheel)					
Empty cage	4,0	0,58	6,2	7,3	6,1
64 men	4,6	0,65	7,1	8,5	10,5
106 men	2,9	0,47	4,7	5,5	13,4
(bottom wheels)					
Empty cage	5,4	0,59	7,6	8,9	6,1
	7,2	1,27	12,0	14,5	6,1
64 men	5,5	0,57	7,7	8,7	10,5
	7,9	1,25	12,7	14,9	10,5
106 men	5,3	0,58	7,5	8,6	13,4
	8,2	1,35	13,3	17,3	13,4
Skip (bottom wheels)					
Empty skip	6,1	0,48	7,9	8,5	8,0
	12,2	1,78	19,0	23,8	8,0
Full skip	6,1	0,61	8,4	9,3	18,0
	12,9	1,81	19,8	25,5	18,0
Haartebeestfontein 6# Mancage (top wheel)					
Down Empty	8,1	1,45	13,6	16,8	6,1
Up full	8,0	1,64	14,2	17,9	13,4
(Bottom wheels)					
Down empty	9,9	2,00	17,5	21,6	6,1
	7,6	1,90	14,8	19,1	6,1
Up full	9,6	1,90	16,8	20,3	13,4
	7,1	1,86	14,2	18,5	13,4

TABLE 4.1 : continued

Shaft	Ave. load	Std. dev σ	Ave + 3,8σ	1 week max	W/10
Blyvooruitsig 4 * (top wheel)					
Full skip	3,2	0,56	5,3	6,2	16,0
Empty skip	3,8	0,30	5,0	6,7	5,9
(bottom wheel)					
Full skip	1,9	0,25	2,8	4,0	16,0
Empty skip	1,8	0,19	2,5	3,2	5,9
F.S.G. 5 * (bottom, out-of-plane wheel)					
Full skip up	9,2	1,16	13,6	17,1	23,1
Empty skip up	10,7	1,42	16,1	18,2	9,1
Full skip down	9,1	1,65	15,4	21,3	23,1
Empty skip down	10,3	1,64	16,5	20,9	9,1
Deelkraal 1 * (top wheel)					
Empty skip	4,7	1,48	10,3	19,7	13,6
Full skip	4,3	1,34	9,4	14,8	29,3
(bottom wheel)					
Empty skip	7,0	2,15	15,2	24,6	13,6
Full skip	6,7	1,19	11,2	14,4	29,3

In each case the conveyance weight W, divided by ten is also given, because this is the design load typically used at present. The wheel loads given are all at a hoisting speed of 15 m/s, and are in kN.

From a study of the loads shown in Table 4.1, the following conclusions may be drawn.

(i) The current design load of W/10 should be maintained. In all cases except the Hartebeestfontein No. 8 shaft skip, and the Hartebeestfontein No. 6 shaft man cage the load given by the average plus 3,8 standard deviations is less than the value of W/10 for a fully loaded conveyance. The measured average maximum load is always at least 35% below the value of W/10. In several cases Alport's[16] programme predicts a maximum load in a one week return period which is in excess of W/10, but this may be due to a certain amount of unreliability in a prediction to one million events from about two hundred measured events, as this excess only occurs where the standard deviation is high.

(ii) For fatigue life calculation it would be more appropriate to use a value closer to the average maximum load, as this is the value which is repeated continuously. Where there is a significant pre-load, i.e. at President Steyn and Hartebeestfontein, the average load is approximately W/15 to W/18. In these cases however, the load does not become zero very often, it varies from a positive value up to W/15, so that the actual load variation is not more than about W/20. In the other cases the average load is W/20 or less. A wheel load variation of W/20 should thus be considered as a reasonable fatigue design value, applied twice per trip over the life of the shaft for shaft steelwork, and once per bunton passed for the life of the conveyance.

This aspect is dealt with more fully by Fotopoulos,[15] whose findings are summarised in section 4.2.2 below.

(iii) In general there was not a significant difference between the wheel loads on conveyances travelling up or down. The differences shown in Table 4.1 for the Free State Geduld No. 5 shaft wheel loads are typical of the differences noted. This to some extent confirms the assumption made in DISCS that gravity loads can be neglected, because they effectively act in opposite directions when the conveyance travels up or down.

(iv) There was also no very significant difference recorded between wheel loads on empty or fully loaded conveyances.

This indicates the actual conveyance mass is not an important factor in determining the wheel loads. It does, however, seem clear that there is a general increase in wheel loads on larger conveyances. At this stage it thus seems reasonable that the full or empty weight of the conveyance be used as a measure of the size of the conveyance and hence of the magnitude of the wheel loads.

(v) In general on skips, the bottom wheel loads are higher than the top wheel loads. The ratio of top wheel loads to bottom wheel loads is of the same order as the ratio between the distances from the centre of gravity of the skip to the bottom wheels and to the top wheels, and the difference may relate to this in some cases. In other cases the relative magnitude of the wheel loads is probably more a function of transom mass and stiffness of its connection to the body of the skip.

(vi) Three conveyances had considerably lower wheel loads than the others. These were:- Western Deep Levels No. 2 shaft skip, which was the only koepe winder on which tests were carried out, and where the heavy tailropes probably assist in reducing dynamic behaviour; (This has in fact proved to be a good shaft, requiring little maintenance) Blyvooruitsig No. 4 shaft, where the wheels could not be properly adjusted with the load cells fitted, as shown in Figure 4.5; (This would have meant that the slippers came into contact with the guide before the wheels were loaded significantly, so that these measurements are not very meaningful) and Western Holdings No. 1 shaft skip which was the only skip with an aluminium bridle tested. (The top transom is steel, but the lighter and more flexible bridle legs and bottom transom would tend to lead to smaller wheel loads. The guide wheels in this shaft were also set just clear of the guides, giving zero preload, but possibly more slipper contact).

(vii) High preloads did not reduce the dynamic behaviour in the two tests where measurements were obtained with higher preloads. In both cases the average load increased approximately by the increased preload, and the standard deviation increased as well, as shown by the Western Deep Levels No. 2 shaft skip. The increased standard deviation is due to either increased dynamic behaviour or an increased effect of misalignment with a higher preload. The effect of this increased standard deviation is to increase the predicted long term wheel loads. It thus appears that high preloads should be avoided in order to reduce wheel loads and give longer wheel life.

(viii) An assessment of the variation of wheel load with hoisting speed in the various shafts, indicates approximately a linear increase of wheel loads with hoisting speed. Extrapolating backwards, zero load would occur at between -8 m/sec and -12 m/sec in most cases, or an average of -10 m/sec, the design wheel load at any other hoisting speed is given by:-

$$\text{WHEEL LOAD} = \frac{W}{10} \times \frac{(V+10)}{25}$$

In two cases this did not apply. The first was Hartebeestfontein No. 6 shaft, where the wheel load was due primarily to a high preload. In this case the wheel load reduced very little with reducing speed. The second case was President Steyn No. 4 shaft, where there was an exponential decrease with decreasing speed. This was thought to be due to the magnification (or resonant) condition at 15 m/sec which magnified the wheel load above a linear increase.

4.2.2 Fatigue cycle analysis

A fatigue analysis on the wheel loads was carried out by Fotopoulos[15], using a peak to trough cycle counting technique. His analysis then calculates the equivalent number of 5 kN cycles which would amount to the same level of fatigue damage. His final conclusions, in the form of an equation to derive the equivalent number of cycles for design are not yet available. His analysis, when applied to consecutive runs under the same conditions in one shaft gives very similar results, except when a run included one high impact load, in which case the results differed markedly. Further consideration is being given to this problem.

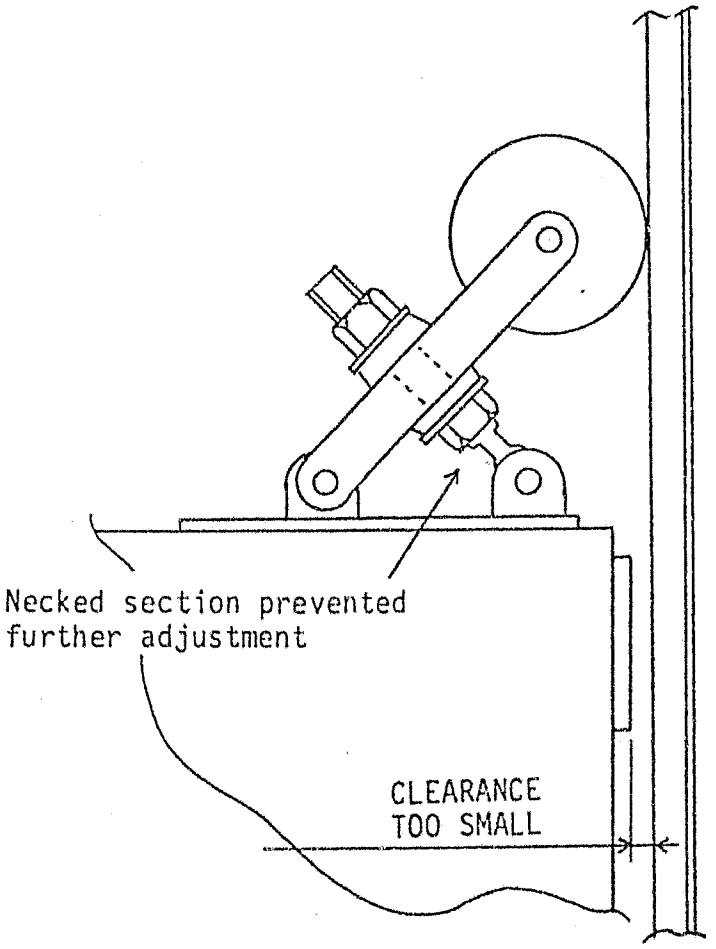


FIGURE 4.5 : Blyvooruitsig guide wheels

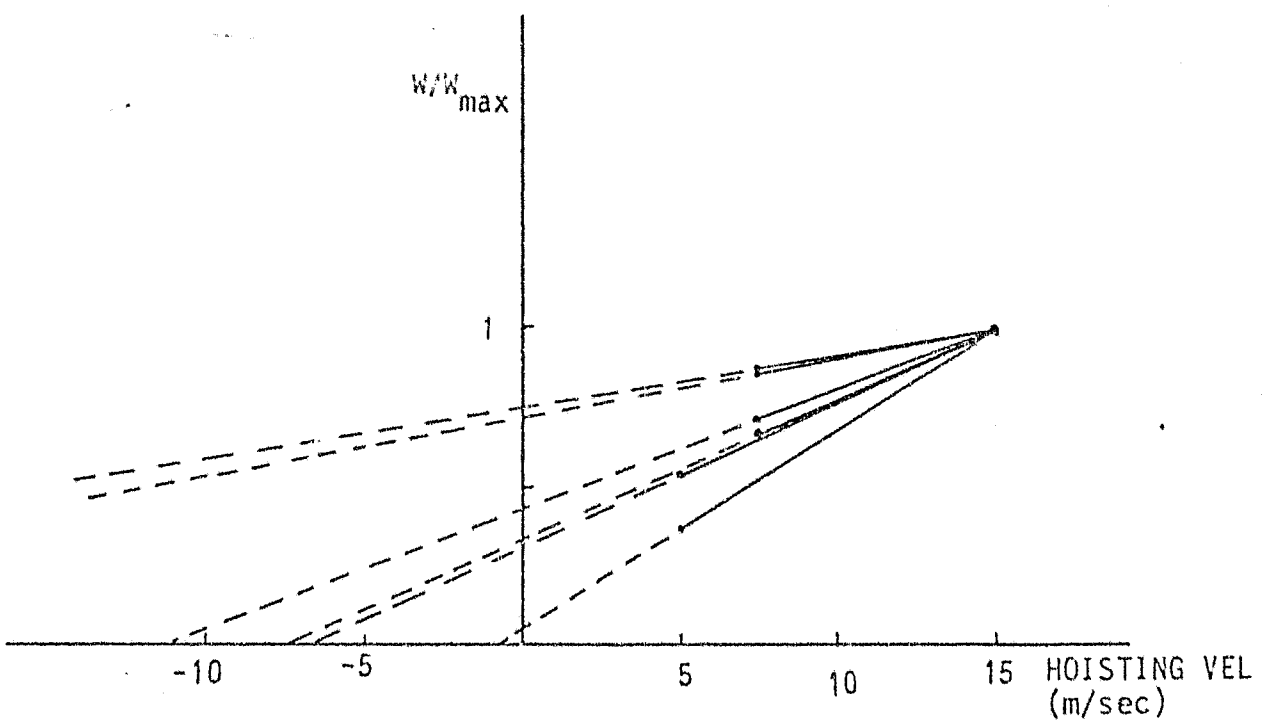


Figure 4.6 : Wheel load variation with hoisting speed

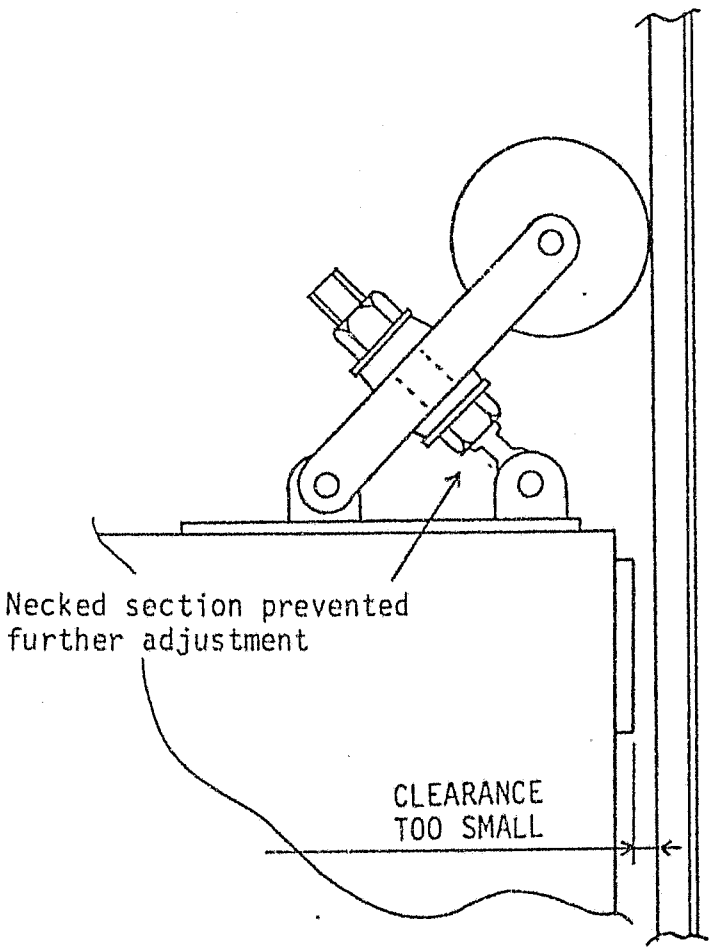


FIGURE 4.5 : Blyvooruitsig guide wheels

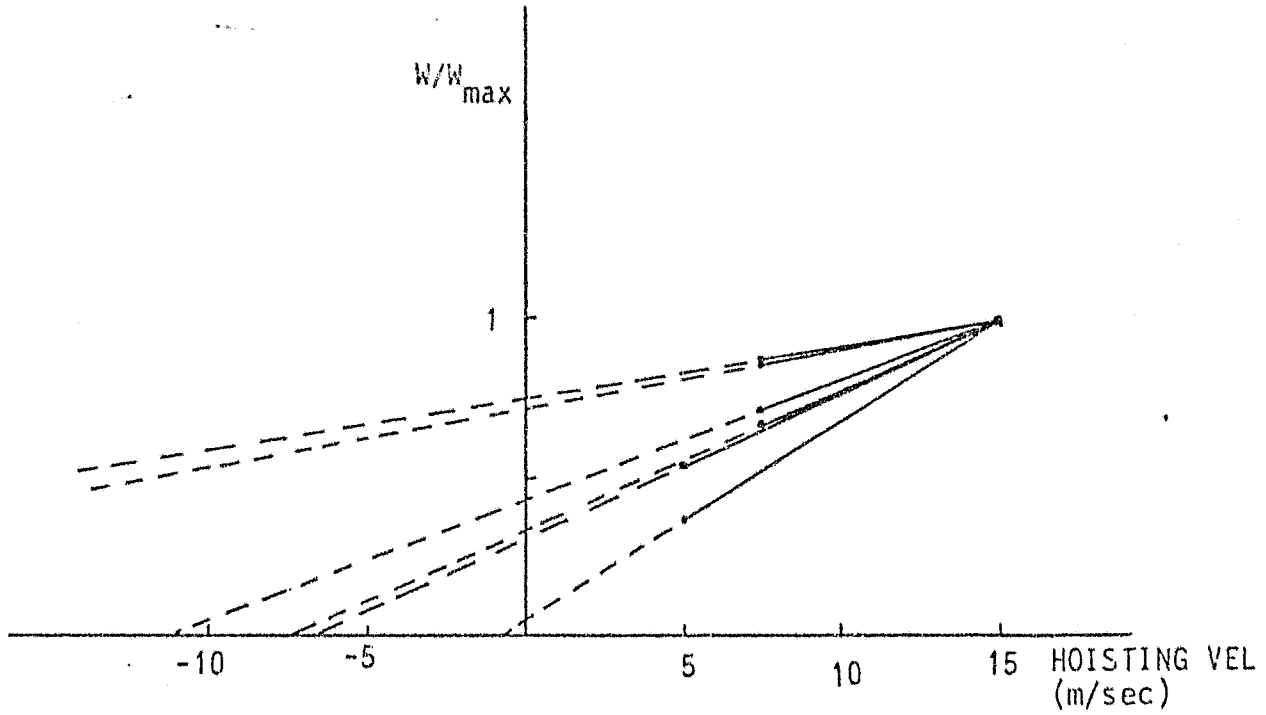


Figure 4.6 : Wheel load variation with hoisting speed

4.2.3 Expected value analysis

This analysis is here distinguished from the earlier probability analysis, in that the approach is to calculate the power spectrum of the wheel loads and accelerations, and hence the expected maximum values. Where the mean is zero, Fertis[17] gives:

$$E\{|y(t)|^2\} = \frac{1}{2\pi}\int_{-\infty}^{\infty} Syy\ (\omega)\ d\omega$$

where $E\{|y(t)|^2\}$ is the expected value of the square of the variable and Syy (ω) is the power spectrum of the variable. The FFT used by Alport[16] in deriving the power spectrum, however, calculates the value

$$Syy(\omega)/_{2\pi}$$

The power spectrum is always symmetrical about zero, so this could equally be written:

$$E\{|y(y)|^2\} = 2\int_{0}^{\infty} \frac{Syy}{2\pi}\ (\omega)\ d\omega$$

This can be approximated by:-

$$E\{y_{RMS}\} = \sqrt{2\sum_{n=o}^{N} \frac{Syy}{2\pi}\ (\omega_n)\ .\ \Delta\omega}$$

where y_{RMS} is the root-mean-square value of y(t), N is the total number of points in the half power spectrum, and $\Delta\omega$ is the frequency increment between points on the power spectrum.

$$\Delta\omega = \frac{\omega_N}{N}$$

where F_N is the frequency limit of the power spectrum. In all analyses a 512 power spectrum was used, so that N in these analyses is always 256. Thus:

$$E\{y_{RMS}\} = \sqrt{\frac{2F_N}{256} \sum_{n=o}^{N} \frac{Syy\ (\omega_n)}{2\pi}}$$

$$= 0,0884 \sqrt{F_N \sum_{n=o}^{N} \frac{Syy\ (\omega n)}{2\pi}}$$

The summation in this expression is calculated when the power spectrum is plotted, and can be abbreviated to ΣS. The summation is only to F_N, not infinity, but F_N is chosen such that there are not significant frequencies beyond it, so this curtailment does not lead to large errors.

For zero mean, which is always the case here because all data is corrected for zero mean before the power spectrum is calculated, the expected value is equivalent to the standard deviation. If a probability of non-exceedance of 0,01% is now accepted as a satisfactory measure of the maximum load and a normal distribution is assumed we have

$$(y_{RMS})_{max} = 3,8\ (E\{y_{RMS}\})$$

$$= 0,336 \sqrt{F_N . \Sigma S}$$

In order to find the maximum absolute value of y, the RMS value can be multiplied by $\sqrt{\frac{1}{2}}$ which is the conversion factor between peak and RMS values for a sine wave. Clearly the functions dealt with are not sine waves, but this should give an acceptable approximation.

Thus:

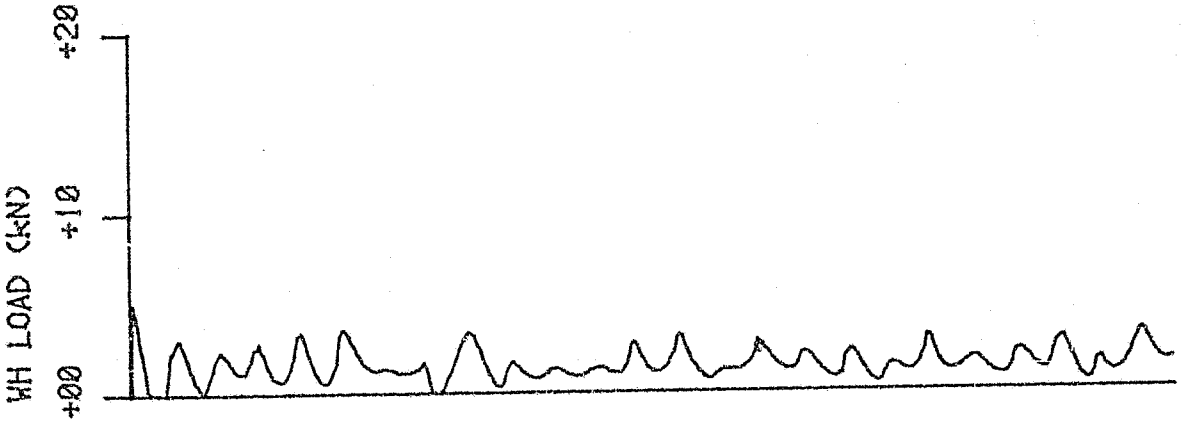
$$y_{max} = 0,48 \sqrt{F_N \cdot \Sigma S}$$

This expression can be used as it is for accelerations, but requires modification as below for wheel loads. The mean value, which will be approximately equal to the wheel preload, has been subtracted out to calculate the power spectrum, so it must be added in again.

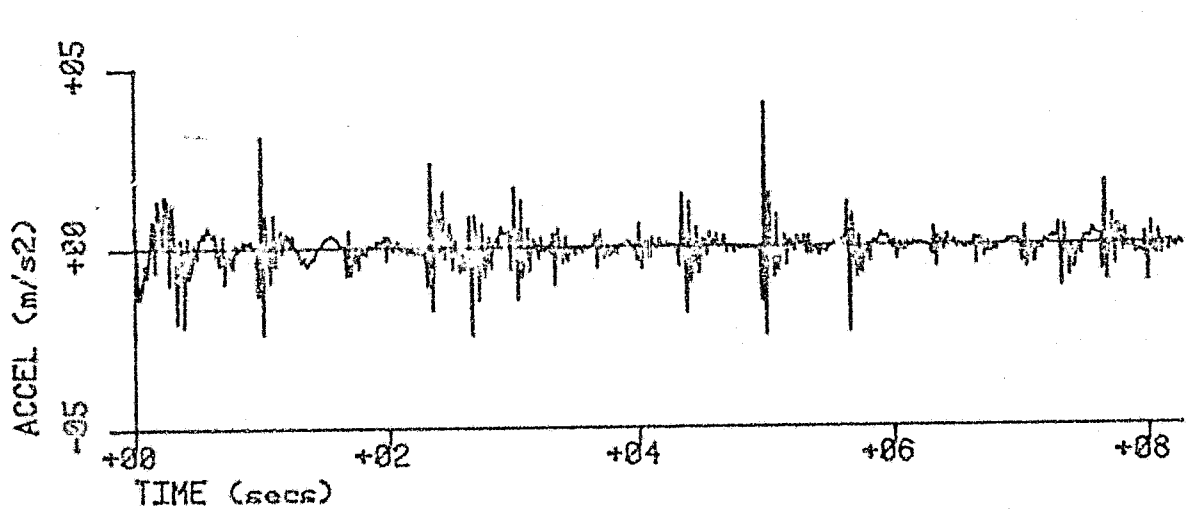
$$W_{max} = 0,48 \sqrt{F_N \Sigma S} + \text{PRELOAD}$$

This analysis assumes a constant amplitude of oscillation in the basic data, and where this is approximated the above analysis gives reasonably good values, as for example the wheel load trace in figure 4.7(a) where a maximum wheel load of 6,1 kN is predicted. Where the measurements show high peaks this analysis is not accurate severely underestimating results as for example the acceleration trace shown in figure 4.7(b) where a maximum value of 0,9 m/sec² is predicted. Using this approach, the maximum values of accelerations and wheel loads for some tests are given in Table 4.2 The equivalent values from the probability analysis and acceleration study are also listed in Table 4.2.

Clearly, because of the altering amplitudes, this analysis does not give a good result, so it is not pursued further.

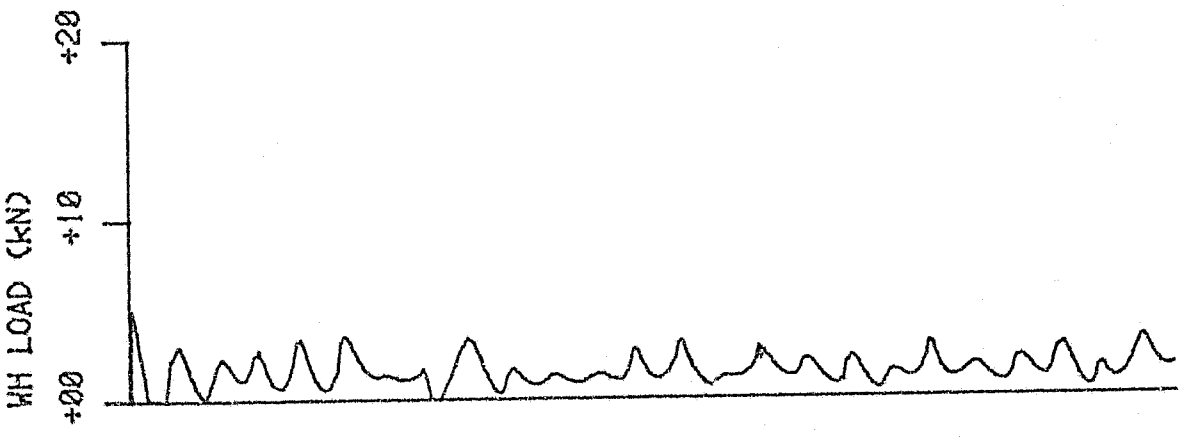


(a) Wheel load

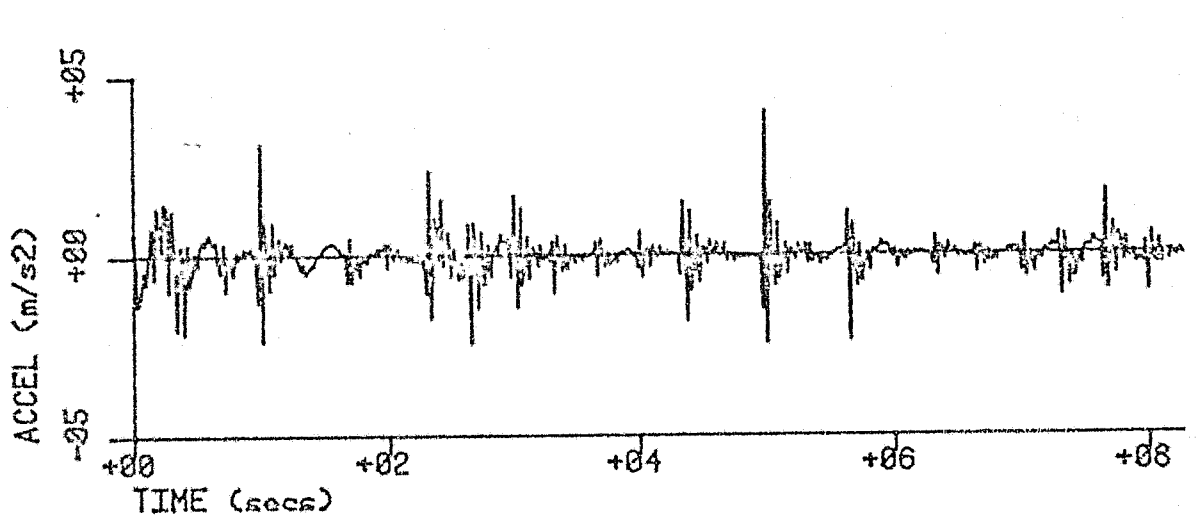


(b) Acceleration

FIGURE 4.7 : Traces subjected to expected value analysis



(a) Wheel load



(b) Acceleration

FIGURE 4.7 : Traces subjected to expected value analysis

TABLE 4.2 : EXPECTED MAXIMUM VALUES OF WHEEL LOADS AND ACCELERATION

SHAFT	Wheel Loads (kN)		Accelerations (m/sec²)	
	Expected value	Probability value	Expected value	Peak value
Hartebeestfontein 8# cage full, top wheel	4,1	6,2	2,1	3
Western Holdings 1# skip empty, top wheel	2,0	3,7	1,3	4
President Steyn 4# 10t skip full, bottom wheel	13,0	16,3	10,0	13
Deelkraal 1# 21t skip full, top wheel	6,7	9,9	2,4	7

4.2.4 Frequency analysis

As found by Reinke[8], the significant frequencies were of two types.

(i) The first type were not velocity dependent. These must thus be natural frequencies, probably of the conveyance itself, or perhaps of the shaft steelwork, although the latter are unlikely to be transmitted to any large extent into the conveyance behaviour. There were typically one or two and sometimes three velocity independent frequencies below about 5 hz, which are the natural frequencies of rotation and translation of the entire conveyance. The reason for only one frequency being apparent in some cases is probably that due to certain geometrical ratios only one natural frequency is excited. This is further discussed in section 5.4.2. These are referred to as natural frequencies below.

(ii) The second group of frequencies were proportional to the velocity. The major frequency in this group was the frequency of revolution of the guide wheels. In several cases the frequency of passing buntons was not evident at all, and in general it was only significant when a high preload was used.

In general the power spectra for accelerations and for wheel loads gave similar significant frequencies. The only important diversion from this was that the accelerations tended sometimes to emphasize the natural frequencies rather than the velocity dependent forcing frequencies. This is to be expected as the accelerations are the response of the conveyance to the wheel loads.

Comparing these two groups of frequencies produced interesting and to some extent unexpected results, described below.

(i) the frequency of passing buntons, which initially was expected to be the primary exciting frequency, was only significant at Hartebeestfontein No. 6 and 8 shafts where a high preload was applied. Even at these shafts, it was much less significant in the acceleration measurements, indicating that the preload was being transferred from side to side through the transoms without significantly affecting the dynamic behaviour.

The natural frequencies of these conveyances and the frequency of passing buntons at the test speeds are shown in Table 4.3 below.

TABLE 4.3 : HARTEBEESTFONTEIN FREQUENCIES

Conveyance	Lower natural frequencies	Bunton pass frequency 7,5 m/s	15 m/s
8# cage	0,3 3,1 4,0	1,6	3,2
6# cage	0,4 1,8 2,4 4,9	-	3,2
8# skip	4,5 8,0/9,5	1,6	3,2

From this table it is clear that none of the measured natural frequencies coincides with the bunton passing frequency at either of the test speeds so that dynamic magnification would not be expected and certainly none was recorded. The Western Deep Levels No. 2 shaft 18 tonne skip however, had natural frequencies of 1,5 hz and 3,3 hz when empty. The higher of these frequencies, i.e. the rotation mode, coincides exactly with the frequency of passing buntons at 15 m/sec, but the measurements did not show dynamic magnification. The two very bad shafts in which tests were conducted, i.e. President Steyn No. 4 shaft and Deelkraal No. 2 shaft, did not appear to have natural frequencies which coincided with the bunton passing frequency, as shown in Table 4.4 below. All the present measurements thus appear to show that the bunton passing frequency is not a problem.

TABLE 4.4 : FREQUENCY COMPARISONS

SHAFT	Natural frequencies	Bunton passing frequency at 15 m/s
Pres. Steyn 4#	1,5 (full) 2,1 (empty)	3,3 hz
Deelkraal 2#	1,2 2,3 3,3 18,5	3,8

(ii) the frequency of revolution of the wheels has been one of the most important frequencies in most of the measurements. It is felt that this is in fact the problem frequency in the two bad shafts mentioned above. At Deelkraal No. 2 shaft, there was a natural frequency at 18,5 hz which is the wheel revolution frequency at 15 m/sec. On the President Steyn No. 4 shaft skips a simple calculation shows that the natural frequency of vibration of the wheel itself about its pivot is about the same as the frequency of revolution of the wheel. This is still to be checked by measurement, but indicates possible dynamic magnification due to resonance within the wheelset itself.

(iii) in general it was difficult to clearly distinguish decreasing natural frequencies with increasing mass.

In cages this is probably to be expected, because the only loading was with men, who would not form an integral mass with the cage, but would tend to sway as the cage moves. This is borne out by the

reduction in wheel loads in loaded cages, which is due to the much higher damping within the load, as the men move against each other and relative to the cage. The only natural frequencies thus remain the natural frequencies of the empty cage.

In some cases there was a definite reduction of the two lower natural frequencies of skips, see Table 4.5. The rock load in skips would be expected to form an integral solid mass with the body of the skip, so this is as expected. In other cases this was not evident at all, a fact which could not be adequately explained.

TABLE 4.5 : NATURAL FREQUENCIES WITH VARYING LOAD CONDITIONS

SHAFT	NATURAL FREQUENCIES (hz) Empty	Half full	Full
P.S. 4# 19t skip	(1,5 to 2,1 range)		
W.D.L. 2# skip	1,5 3,3	-	1,1 3,1
W.H. 1# skip	1,5 2,5	-	1,5 2,5
R.E. 2# skip	1,5 4,3	1,4 4,0	1,3 3,7
HAST 8# skip	3,1 4,0	-	3,1 4,0
MY 4# skip	1,6	-	1,4
PSG 5# skip	1,6 3,1	-	1,6 2,7
D K 1# skip	0,9 1,8 2,9	-	0,7 1,6 2,5

Natural frequency measurements were taken in one cage, as described in section 3.2.2. In this case the natural frequencies measured by this means were fairly similar to those shown by the spectral analysis.

4.2.5 Accelerations

No detailed analysis was made of peak acceleration values but the accelerations were very seldom greater than 10 m/s^2 except for isolated peaks and a few out-of-plane values. In the best shafts measured accelerations seldom exceeded 3 m/sec^2. Shafts with accelerations up to 6 m/sec^2 or even 7 m/sec^2 do not appear to present any problems. For maintenance purposes, it would thus seem to make sense to specify repair work in areas where lateral accelerations exceed 7 m/sec^2, although it should be noted that these accelerations do not bear any direct resemblance to the wheel loads listed in Table 4.1. Table 4.6 shows the peak accelerations recorded in the various sets of measurements.

TABLE 4.6 : PEAK ACCELERATION VALUES

SHAFT	Peak accelerations (m/sec²) 5 m/sec FULL	5 m/sec EMPTY	10 m/sec FULL	10 m/sec EMPTY	15 m/sec FULL	15 m/sec EMPTY
W.D.L. 2# skip	-	-	4	4	5	5
P.S. 4# 19t skip	-	3	-	5	11	8
HART 8# cage	-	-	-	3	3	4
W.H. 1# skip	5	2	4	-	9	4
HART 8# skip	-	6	-	-	9	11
HART 6# cage	-	-	-	-	10	12
R.E. 2# skip	5	4	5	4	7	6
D.R.D. 5A# cage	-	4	-	12	-	-
BLY 4# skip	-	-	8	8	12	12
D.R.D. 5a# skip	-	-	-	-	-	12
D.K. 2# cage	-	5	-	8	-	10
P.S. 4# 10t skip	4	-	6	-	13	-
D.K. 1# 21t skip	-	-	3	4	7	8

NOTE: These values are taken from acceleration plots. Where the listed hoisting velocities are not the velocities at which measurements were taken, the above values are obtained by interpolation.

4.3 COMPARISON BETWEEN DISCS AND MEASUREMENT

Several of the shafts in which measurements were taken were modelled on DISCS. In general there were two problems to this. The first was that no mine had measured values of misalignment, and in most cases the engineers could not give any real assessment of the magnitude of misalignment. This meant that the misalignment specified in the DISCS runs was assumed,

usually at up to 8 mms incremental misalignment, 2 mms on gauge and 50 mms maximum overall. In some cases where the results were obviously too large or too small, further runs were carried out with adjusted values.

The second problem was that the model was set up before it became evident that the wheels played a primary part in dynamic behaviour. Where there was dynamic magnification at the wheel revolution frequency, it was necessary to introduce artificially large values of wheel irregularity to obtain satisfactory results from DISCS.

In setting up the model, it was anticipated that initial rough comparisons between the predictions and measurements would be necessary in order to assess and then adjust certain assumptions, to achieve satisfactory results. The wheel irregularity mentioned above was one such adjustment. In other cases the damping and/or magnitude of guide misalignment were also adjusted. The comparisons which were made, together with the assumed magnitudes of misalignment, damping, and wheel irregularity are listed below, together with comments as to adjustments which were found necessary.

(a) President Steyn No. 4 shaft 19 tonne skip.

Maximum misalignment	± 8 mm
Damping	6%
Wheel irregularity	1 mm

usually at up to 8 mms incremental misalignment, 2 mms on gauge and 50 mms maximum overall. In some cases where the results were obviously too large or too small, further runs were carried out with adjusted values.

The second problem was that the model was set up before it became evident that the wheels played a primary part in dynamic behaviour. Where there was dynamic magnification at the wheel revolution frequency, it was necessary to introduce artificially large values of wheel irregularity to obtain satisfactory results from DISCS.

In setting up the model, it was anticipated that initial rough comparisons between the predictions and measurements would be necessary in order to assess and then adjust certain assumptions, to achieve satisfactory results. The wheel irregularity mentioned above was one such adjustment. In other cases the damping and/or magnitude of guide misalignment were also adjusted. The comparisons which were made, together with the assumed magnitudes of misalignment, damping, and wheel irregularity are listed below, together with comments as to adjustments which were found necessary.

(a) President Steyn No. 4 shaft 19 tonne skip.

Maximum misalignment	8 mm
Damping	6%
Wheel irregularity	1 mm

In this case the wheel irregularity was increased in order to obtain the high amplitude, at the wheel revolution frequency, which was evident on the measurements. This is discussed in more detail in Chapter 5.

(b) Western Deep Levels No. 2 shaft 21 tonne skip.

Maximum misalignment increment	± 6 mm
Maximum misalignment	± 50 mm
Damping	10%
Wheel irregularity	0,3 mm

This is a koepe winder, and thus there are heavy tailropes suspended from the skip, which probably increases the damping. The damping used here was thus increased to give satisfactory results.

(c) Western Holdings No. 1 shaft 10 tonne skip.

Maximum misalignment increment	± 6 mm
Maximum misalignment	± 50 mm
Damping	6%
Wheel irregularity	0,5 mm

(d) Haartebeesfontein No. 8 shaft 105 man cage.

Maximum misalignment increment	± 8 mm
Maximum misalignment	± 50 mm
Damping	6%
Wheel irregularity	0,5 mm

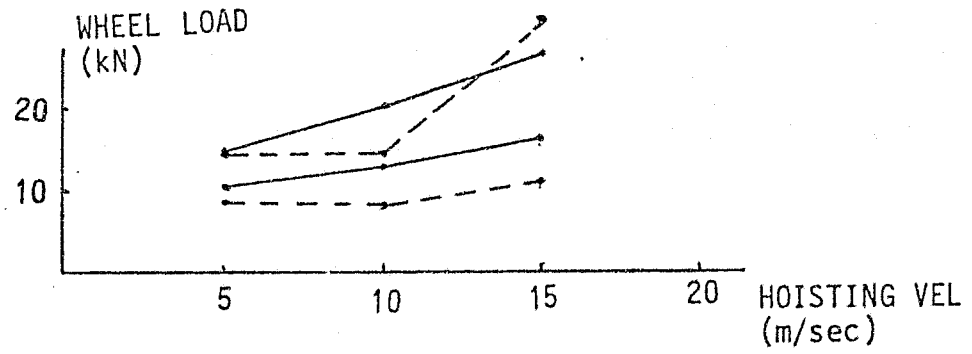
(e) Deelkraal No. 1 shaft 21 tonne skip.

Maximum misalignment increment	± 6 mm
Maximum misalignment	± 50 mm
Damping	8%
Wheel irregularity	0,3 mm

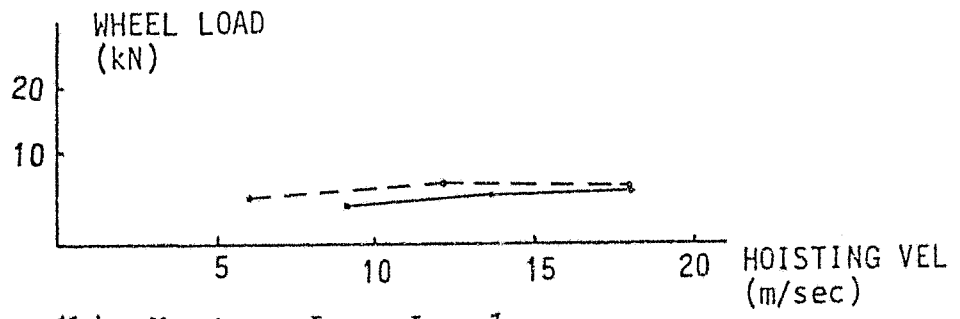
In this case it was necessary to alter the wheel irregularity, maximum misalignment increment and spring travel to achieve reasonable predictions, because of the extra sensitivity which DISCS shows to dynamic magnification.

4.3.1 Wheel loads

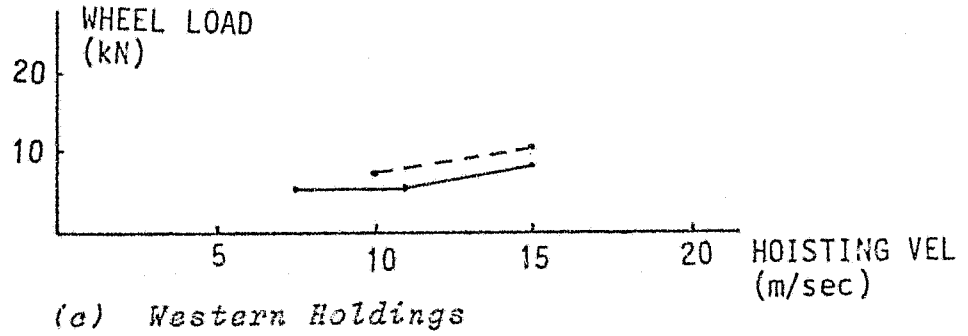
Figure 4.8 shows the results of the probability analysis of wheel loads measured at various mines and the corresponding DISCS predictions (for one million events). From these comparisons, it is clear that in general DISCS predicts wheel loads which are within 35% of the measured loads. The increase in wheel loads with increasing hoisting speed is also predicted by DISCS to be similar to what is shown by measurements. The only exception to this is the comparison for Deelkraal, where DISCS predicts a dynamic magnification peak at 12,5 hz, whereas it was measured at 10 hz, although the magnitude of this peak is similar in both cases. It should also be noted that the measurements for Deelkraal have been extrapolated to 17,8 m/s because at that speed the measurement showed one very high peak, which produced unreasonably high wheel loads at one million events. The Deelkraal comparison is also considered to be less reliable because DISCS assumes buntons of equal stiffness on both sides of the conveyance. In all the cases above except Deelkraal this is very nearly the situation. The Deelkraal skip has guides connected to buntons on the



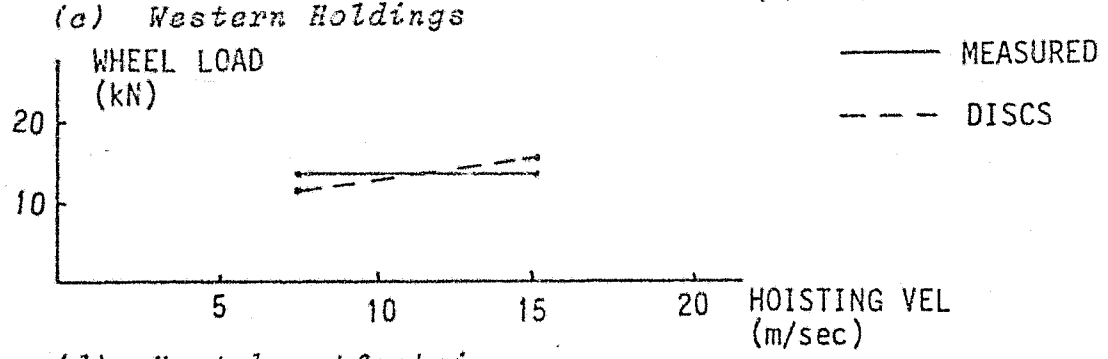
(a) President Steyn



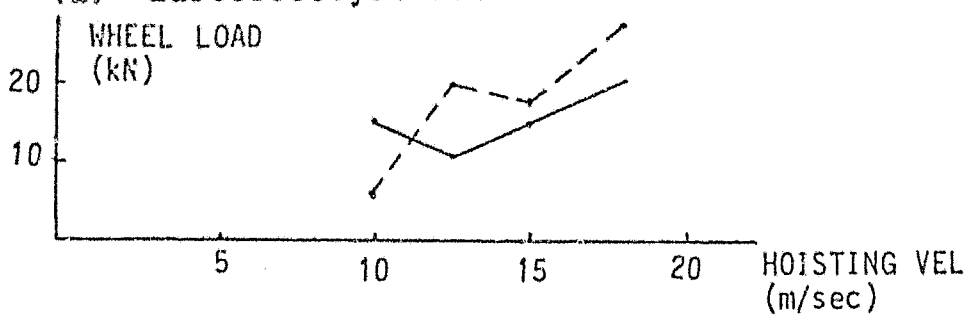
(b) Western Deep Levels



(c) Western Holdings



(d) Hartebeestfontein



(e) Deelkraal

FIGURE 4.8 : Comparison of measured and DISCS wheel loads

one side, but fixed by means of a bracket to the shaft wall on the other side, so that the stiffness at the bunton level is very different on the two sides.

Thus, at present, DISCS can be expected to predict wheel loads to within about 35% of their real value, provided that the bunton stiffnesses are similar on both sides of the conveyance.

4.3.2 Fatigue Values

Fotopoulos[15] has carried out a fatigue analysis on one set of DISCS predictions and it appears that the comparison is reasonable, although on the basis of one comparison it is not possible to draw definite conclusions. He found that where measurements gave approximately 1,6 cycles of 5 kN per bunton passed, DISCS gave an average of about 1,45 cycles of 5 kN. However, on one wheel, where high loads were measured, the analysis gave about 7,5 cycles of 5 kN per bunton passed, which was not predicted by DISCS, probably because the wheel was in a very bad condition.

4.3.3 Frequencies

At the lower frequencies, there was good correlation between DISCS predictions and the measured natural frequencies. The measurements had one extra lower natural frequency in many cases, but this was interaction with an out-of-plane natural frequency which is never present in DISCS. For the overall translation and rotation frequencies, DISCS thus gives a reliable prediction.

one side, but fixed by means of a bracket to the shaft wall on the other side, so that the stiffness at the bunton level is very different on the two sides.

Thus, at present, DISCS can be expected to predict wheel loads to within about 35% of their real value, provided that the bunton stiffnesses are similar on both sides of the conveyance.

4.3.2 Fatigue Values

Fotopoulos[15] has carried out a fatigue analysis on one set of DISCS predictions and it appears that the comparison is reasonable, although on the basis of one comparison it is not possible to draw definite conclusions. He found that where measurements gave approximately 1,6 cycles of 5 kN per bunton passed, DISCS gave an average of about 1,45 cycles of 5 kN. However, on one wheel, where high loads were measured, the analysis gave about 7,5 cycles of 5 kN per bunton passed, which was not predicted by DISCS, probably because the wheel was in a very bad condition.

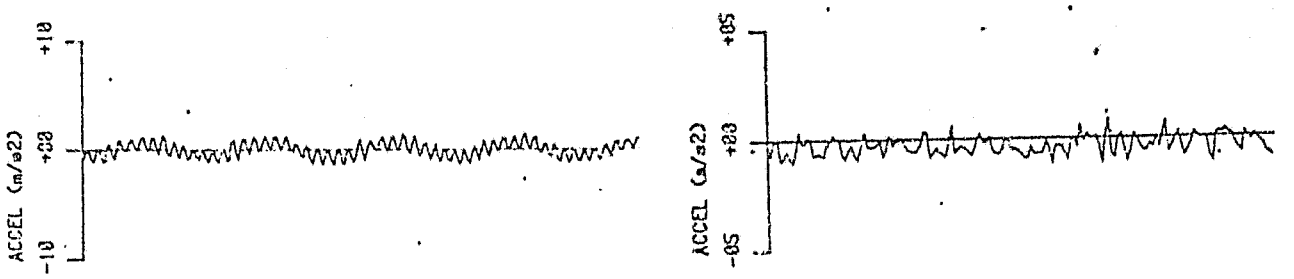
4.3.3 Frequencies

At the lower frequencies, there was good correlation between DISCS predictions and the measured natural frequencies. The measurements had one extra lower natural frequency in many cases, but this was interaction with an out-of-plane natural frequency which is never present in DISCS. For the overall translation and rotation frequencies, DISCS thus gives a reliable prediction.

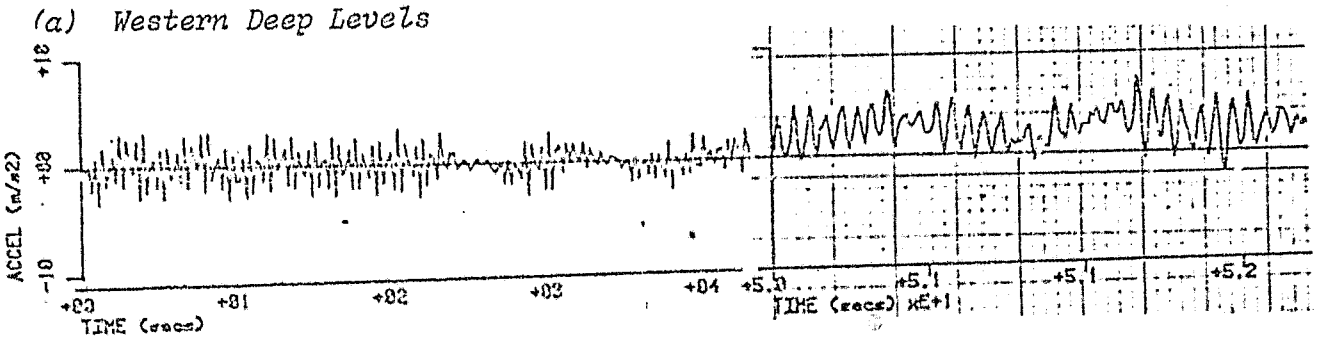
The difficulty of correctly assessing the actual stiffnesses of the bridle and other elements meant that DISCS did not predict the higher order natural frequencies very well, i.e. those relating to deformation of the conveyance. The predictions were of the right order of magnitude in some instances, as can be seen from Table 4.6, but even these differences can become very important if dynamic magnification is possible. In order to acceptably predict the higher order natural frequencies, DISCS thus needs a more accurate input, perhaps experimentally derived, rather than theoretically calculated.

TABLE 4.7 : FREQUENCY COMPARISON

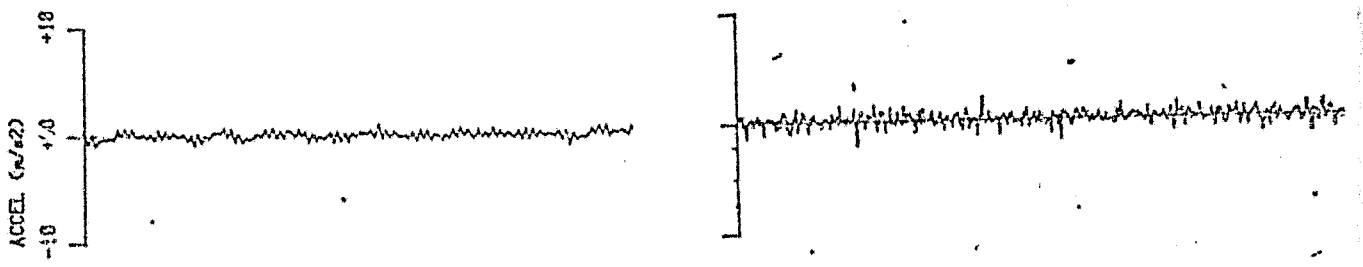
Mine	Overall frequencies			Deformation frequencies		
	1	2	3	1	2	3
President Steyn measured DISCS	(1,5 to 2,1) 1,24	- 2,31	- -	13,5 12,0	19,0 -	20,7 -
Western Deep Levels measured DISCS	1,2 1,8	3,1 3,5	- -	10 -	17,5 -	- -
Western Holdings measured DISCS	1,5 0,9	2,5 2,38	5,0 -	9,5 7,5	- -	- -
Haartebeesfontein measured DISCS	0,2 -	3,1 3,4	4,0 -	9,0 9,7	10,5 11,2	14,5 -
Deelkraal measured DISCS	0,7 -	1,6 1,1	2,5 3,8	5,[illegible] 6,0	8,7 -	12,0 -



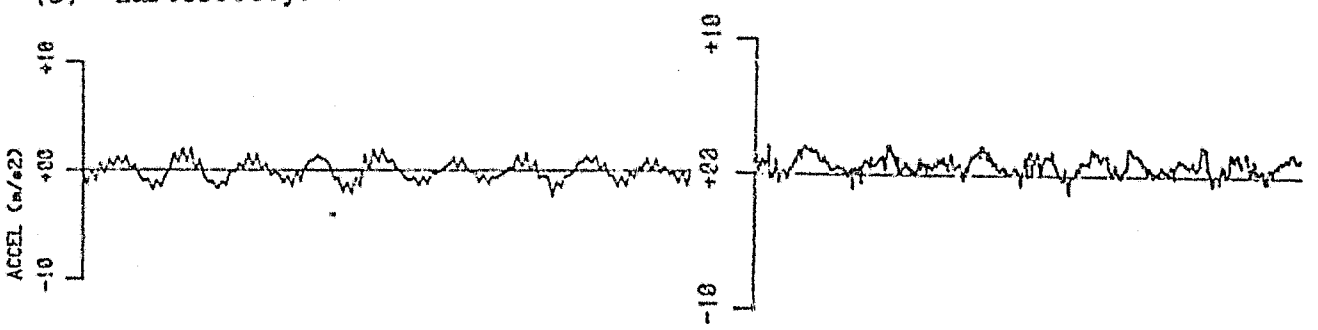
(a) Western Deep Levels



(b) President Steyn



(c) Hartebeestfontein



(d) Western Holdings

FIGURE 4.9 : Accelerations - Measured and DISCS predictions

(Time and accelerations scales are the same for DISCS and measured results, except where shown otherwise).

4.3.4 Accelerations

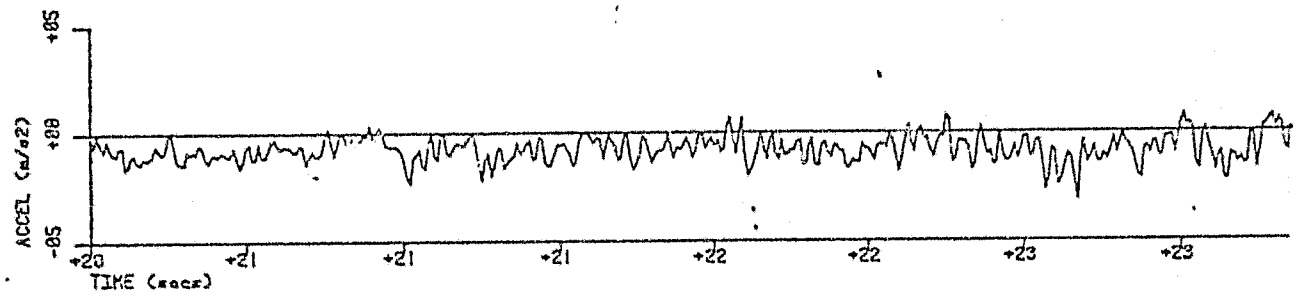
In general the accelerations predicted by DISCS compared well with the measured accelerations. Figure 4.9 shows some typical comparative values.

The accelerations predicted by DISCS were very sensitive to the state of the wheel. A change in the wheel irregularity or the phase angles of the irregularity had a more marked effect on the accelerations than on the wheel loads. This led, in some instances to badly predicted acceleration values, see Figure 4.10. This was borne out by measurements, where the tyres failed on some wheels and resulted in a greater increase in accelerations than in wheel loads.

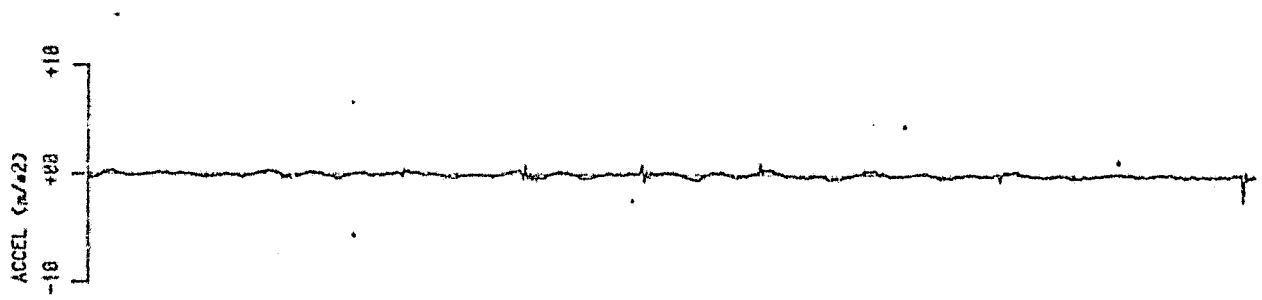
Apart from a few poor comparisons the predicted accelerations were within 40% of those measured in all five cases.

4.3.5 The practical usefullness of DISCS

With the exception of the higher order frequencies, the predictions made by DISCS thus give results which are within 40% of the measured values. The DISCS predictions are also qualitatively similar to the measurements, i.e. where an alteration to a variable increases the measured wheel loads or accelerations, the predicted wheel loads or accelerations are also increased by altering the variable in the same way. Thus, for example, where it was found at President Steyn No. 4 shaft that an increased guide stiffness reduced the dynamic behaviour, the same alteration in DISCS also predicted improved behaviour.

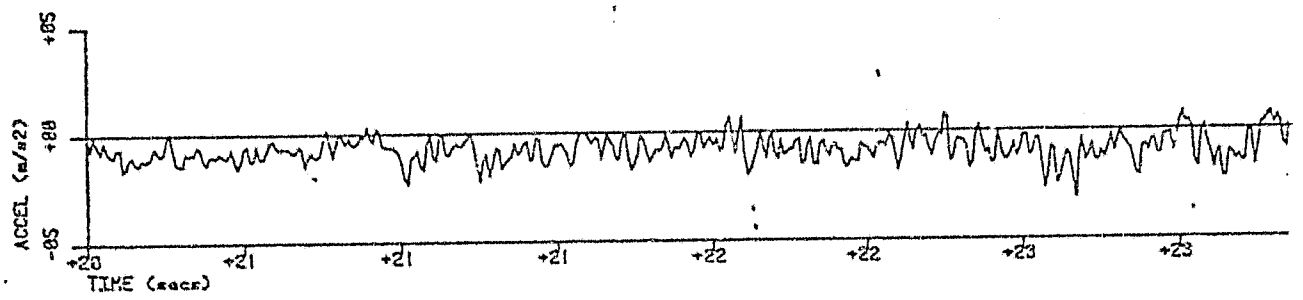


(a) measured values

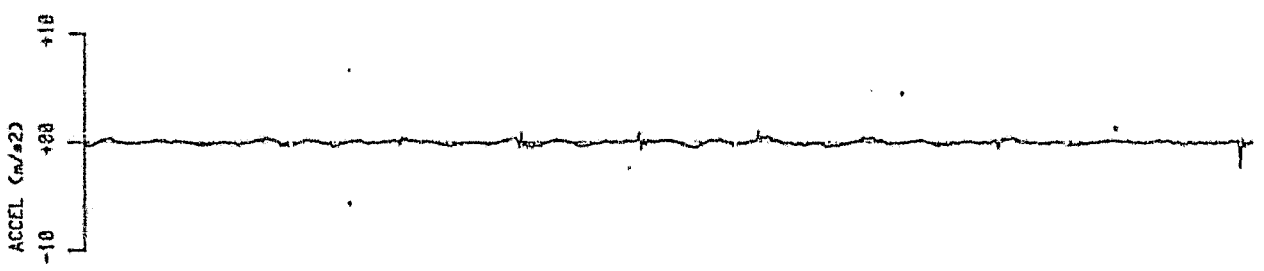


(b) DISCS values

FIGURE 4.10 : Acceleration on Western Deep Levels top wheel



(a) measured values



(b) DISCS values

FIGURE 4.10 : Acceleration on Western Deep Levels top wheel

In using DISCS as a design tool, the most important value is the predicted wheel load. DISCS can thus be used in design provided that the wheel load predicted for one million return events, dynamic magnification and the fatigue load cycles are reasonably accurately predicted. From the comparisons discussed above it has been found that:

(a) the wheel load for one million return events is predicted to within 35% of its actual value

(b) in the one case where dynamic magnification was measured, it was also predicted, at a slightly higher frequency, to have a very similar magnitude, and

(c) it appears that the equivalent number of fatigue cycles for a 5 kN load variation may be predicted reasonably accurately.

Provided the basic assumptions and limitations of DISCS are considered in establishing the input parameters and in interpreting the predictions, DISCS can thus be adjusted to give some confidence in establishing design wheel loads.

4.4 EMPIRICAL DERIVATION OF MAXIMUM WHEEL LOADS

In dealing with the effects of altering certain variables, or with the relationship between variables and wheel loads or accelerations, the measurements and, where necessary, parametric studies using DISCS are employed. The most important variables are considered below, and an empirical equation for maximum wheel loads is derived.

4.4.1 Effect of hoisting velocity

This has already been dealt with to some extent in discussing the maximum wheel load values, where it is shown that the wheel loads are proportional to:

$$\frac{V+10}{25} \quad \text{where } V = \text{velocity in m/sec}$$

Considering the measured accelerations, the expected values show a similar, usually linear increase with velocity. Here however, the expected value would be close to zero velocity, as shown in Figure 4.11.

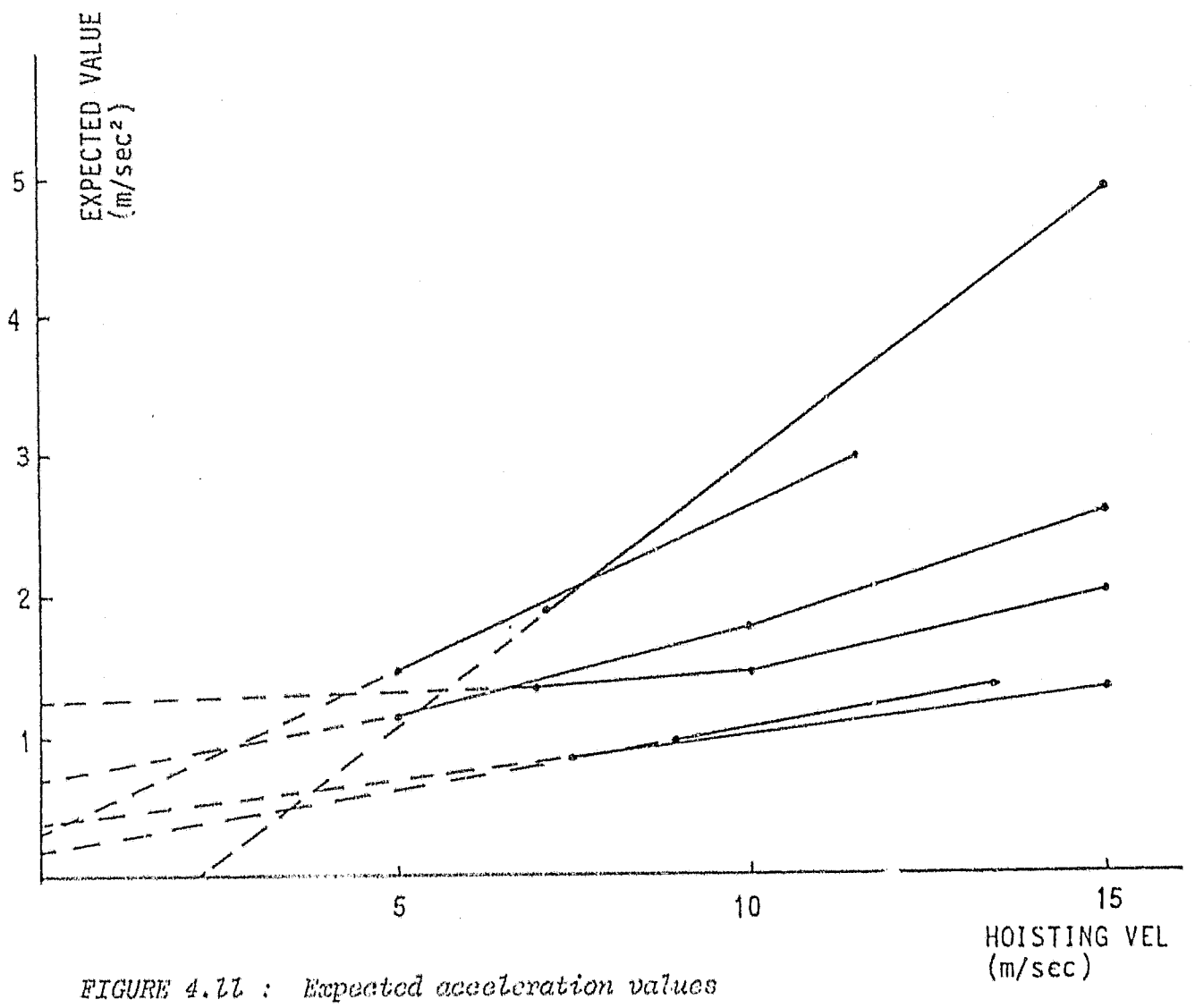


FIGURE 4.11 : Expected acceleration values

This suggests that the wheel load should also have a similar relationship to velocity. Based on this observation, the wheel load curves were reconsidered in two components, a static constant wheel load equal to the preload with the wheels at a bunton, and a dynamic wheel load which varied with velocity.

Figure 4.12 shows several typical curves resulting from subtracting the estimated preload from the wheel load values. Apart from those cases exhibiting dynamic magnification which were discussed under maximum wheel loads, the general pattern here is very similar to that shown for accelerations, i.e. a linear increase with velocity, from a zero value at zero velocity.

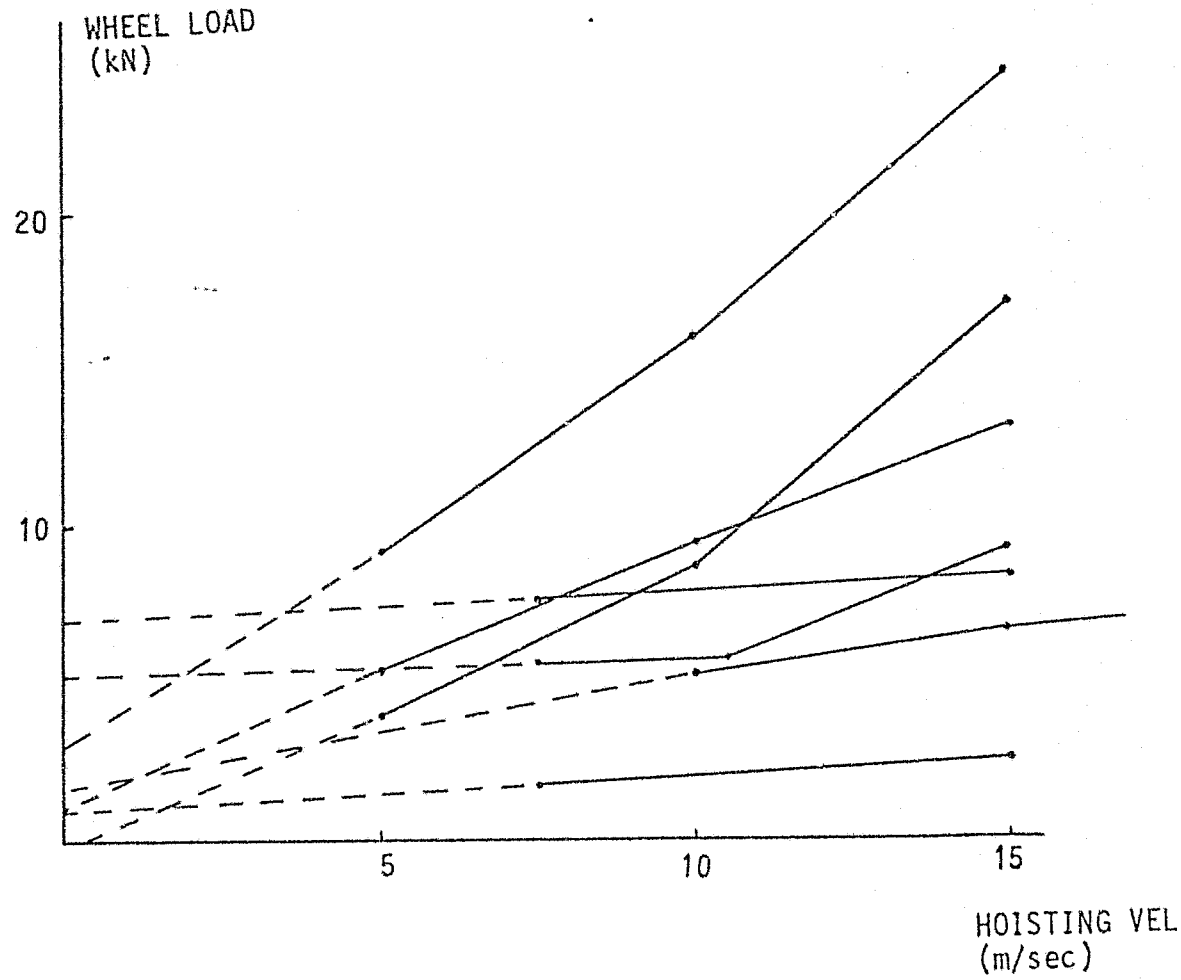


FIGURE 4.12 : Wheel loads with preload subtracted

This suggests that the wheel load should also have a similar relationship to velocity. Based on this observation, the wheel load curves were reconsidered in two components, a static constant wheel load equal to the preload with the wheels at a bunton, and a dynamic wheel load which varied with velocity.

Figure 4.12 shows several typical curves resulting from subtracting the estimated preload from the wheel load values. Apart from those cases exhibiting dynamic magnification which were discussed under maximum wheel loads, the general pattern here is very similar to that shown for accelerations, i.e. a linear increase with velocity, from a zero value at zero velocity.

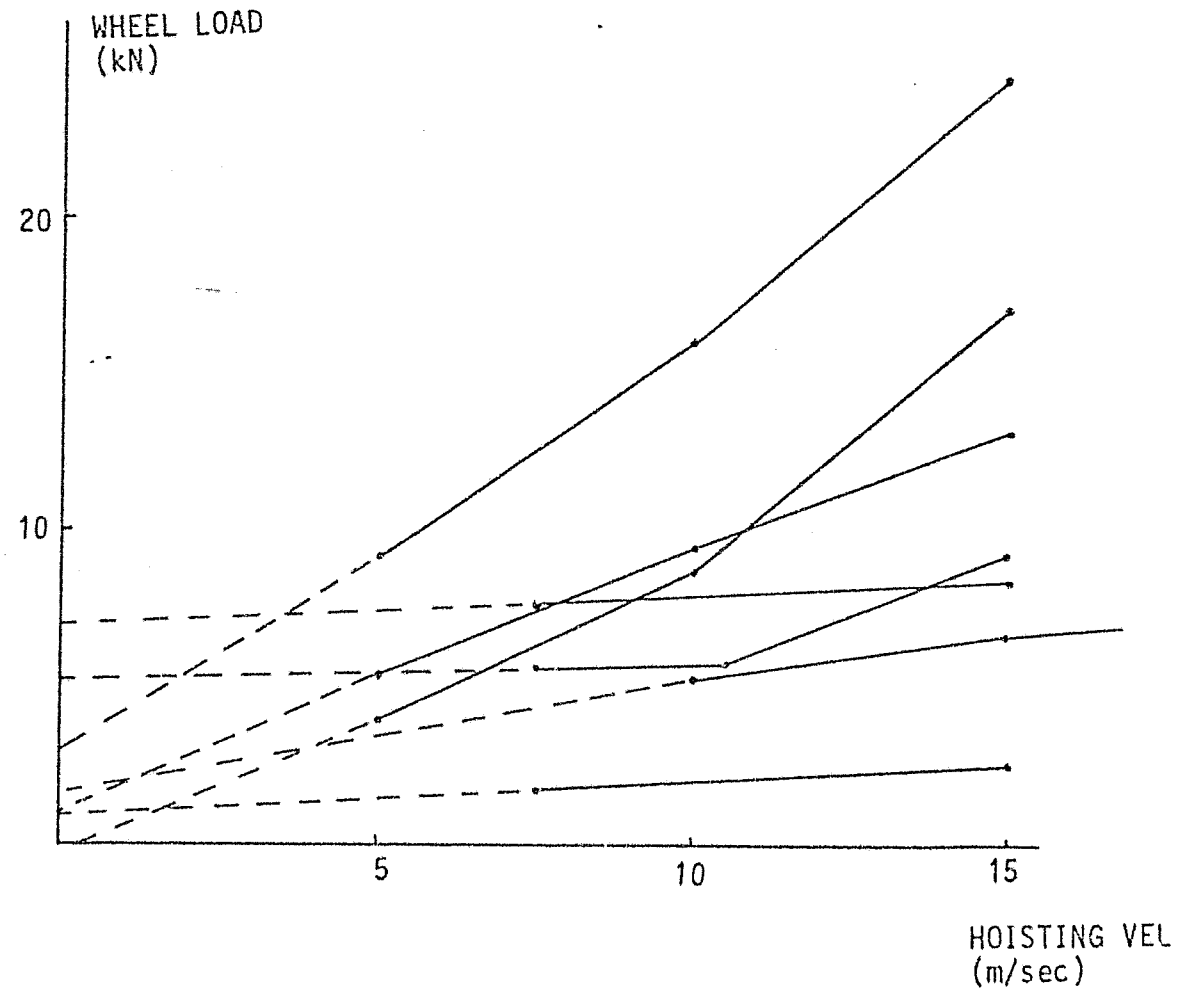


FIGURE 4.12 : Wheel loads with preload subtracted

The wheel load is thus given by:

$$W = K_w \frac{V}{15} + \text{PRELOAD} \times K_p$$

where K_w and K_p are constants discussed subsequently.

Two runs on DISCS with the Hartebeestfontein parameters showed a very similar result.

4.4.2 Effect of conveyance mass

As discussed above, for any one specific conveyance, the wheel loads are not dependent on the payload to a very great extent, and the accelerations tend to decrease with increasing payload. On the other hand there is a definite trend of increasing maximum wheel loads for increasing conveyance size. Table 4.8 summarises the ratio of maximum wheel loads (i.e. average load plus 3,8 standard deviations) minus the preload at 15 m/s to total conveyance weight plus payload, as well as the ratio of maximum wheel loads to empty conveyance weight.

4.4.3 Effect of conveyance length

The length of the conveyance is also a measure of its size so also included on Table 4.8 is the ratio of maximum wheel load to overall conveyance length, and the ratio of maximum wheel load to the product of overall length and empty conveyance weight. The wheel loads also depend on the position of the centre of gravity so the ratio of wheel load to the distance between the other wheel and the conveyance centre of gravity is also given. A study of Table 4.8 shows that for skips the

most constant ratio is that between maximum wheel load and the empty weight, showing a coefficient of variation of 33%. For cages, the most constant ratio is the same ratio, with a coefficient of variation of 33%. For an empirical design value the average ratio plus two standard deviations will be taken. For skips this gives 0,16 and for cages 0,20. It should be noted that this figure for cages is based on two similar cages only, so may well need modification when more measurements become available.

The factor K_w above should thus be:

$$K_w = 0,16\ W_E\ K_m \text{ for skips}$$

or $$K_w = 0,20\ W_E\ K_m \text{ for cages}$$

where W_E = empty conveyance weight

K_m = a constant discussed subsequently.

4.4.4 Effect of misalignment

The effects of misalignment are not easy to establish from measurements because of the difficulty of measuring the actual misalignment values. Where the engineers at the mines could give an assessment of misalignment, the misalignment increment between consecutive buntons was of the order of 6 to 8 mm for a reasonable shaft to 12 mm or more in bad areas of shafts. A parametric study using DISCS showed approximately a linear increase of wheel loads with misalignment, which should be expected because the force required to move a given mass a certain distance in a given time is directly proportional to the distance moved.

most constant ratio is that between maximum wheel load and the empty weight, showing a coefficient of variation of 33%. For cages, the most constant ratio is the same ratio, with a coefficient of variation of 33%. For an empirical design value the average ratio plus two standard deviations will be taken. For skips this gives 0,16 and for cages 0,20. It should be noted that this figure for cages is based on two similar cages only, so may well need modification when more measurements become available.

The factor K_w above should thus be:

$$K_w = 0,16\ W_E\ K_m \text{ for skips}$$

or $$K_w = 0,20\ W_E\ K_m \text{ for cages}$$

where W_E = empty conveyance weight

K_m = a constant discussed subsequently.

4.4.4 Effect of misalignment

The effects of misalignment are not easy to establish from measurements because of the difficulty of measuring the actual misalignment values. Where the engineers at the mines could give an assessment of misalignment, the misalignment increment between consecutive buntons was of the order of 6 to 8 mm for a reasonable shaft to 12 mm or more in bad areas of shafts. A parametric study using DISCS showed approximately a linear increase of wheel loads with misalignment, which should be expected because the force required to move a given mass a certain distance in a given time is directly proportional to the distance moved.

TABLE 4.8(a) MAXIMUM WHEEL LOAD RATIOS - SKIPS

Mineshaft	Ratio of maximum wheel load to: Full weight	Empty weight	Length	Empty weight X length	Dist.C G to other wheel	Empty wt X dist.
Western Deep Levels 2# (top wheel)						
Full skip	0,013	0,037	0,393	0,004	0,578	0,006
½ full skip	0,013	0,036	0,383	0,004	0,563	0,006
Empty skip	0,012	0,032	0,340	0,004	0,478	0,005
Empty skip (higher preload)	0,014	0,040	0,425	0,004	0,600	0,006
Pres. Steyn 4# 19t skip (top wheel)						
Full	0,024	0,062	0,714	0,006	1,762	0,015
Empty (bottom wheel)	0,028	0,071	0,820	0,007	2,024	0,017
Full	0,043	0,110	1,273	0,011	2,139	0,018
Empty	0,053	0,136	1,572	0,013	2,642	0,022
10t skip (top wheel)						
Full (bottom wheel)	0,062	0,153	1,374	0,021	2,710	0,040
Full	0,074	0,183	1,640	0,024	2,388	0,036
Western Holdings 1# (top wheel)						
Empty	0,027	0,097	0,607	0,016	1,850	0,049
8,0t payload	0,033	0,118	0,738	0,019	2,250	0,059
Full (bottom wheel)	0,041	0,147	0,918	0,024	2,800	0,074
Empty	0,033	0,118	0,738	0,019	1,098	0,029
8,0t payload	0,017	0,061	0,377	0,010	0,561	0,015
Full	0,024	0,084	0,525	0,014	0,781	0,021

TABLE 4.8(a) continued

MINESHAFT	Full weight	Ratio of maximum wheel load to: Empty weight	Length	Empty weight X length	Dist.C G to other Wheel	Empty wt X dist.
Hartebeestfontein 8# Skip						
Empty	0,047	0,106	1,308	0,016	2,616	0,033
Full	0,050	0,114	1,400	0,017	2,800	0,035
Deelkraal 1# Skip (Top wheel)						
Empty	0,036	0,078	0,866	0,007	2,239	0,017
Full (bottom wheel)	0,033	0,071	0,790	0,006	2,044	0,015
Empty	0,053	0,115	1,277	0,010	2,082	0,016
Full	0,039	0,085	0,941	0,007	1,534	0,012
Average	0,037	0,100	0,953	0,013	1,853	0,026
Std. deviation	0,014	0,033	0,349	0,006	0,700	0,017
Std. deviation as % of average	39	33	37	47	38	68

TABLE 4.8(b) MAXIMUM WHEEL LOAD RATIOS - CAGES

MINESHAFT	Full weight	Ratio of maximum wheel load to: Empty weight	Length	Empty wt x length	Dist C G to other wheel	Empty wt x C G dist
Hartebeestfontein 8# mancage (top wheel)						
Empty	0,039	0,086	0,776	0,013	1,553	0,025
64 men	0,046	0,100	0,912	0,015	1,821	0,030
106 men	0,028	0,061	0,553	0,009	1,105	0,018
(bottom wheels)						
Empty	0,043	0,095	0,866	0,014	1,731	0,028
64 men	0,046	0,102	0,925	0,015	1,851	0,030
106 men	0,048	0,105	0,955	0,016	1,911	0,031

TABLE 4.8(b) continued

Mineshaft	Ratio of maximum wheel load to: Full weight	Empty weight	Length	Empty wt x length	Dist C G to other wheel	Empty wt x C G dist
Hartebeestfontein 6# mancage (top wheel)						
Empty	0,065	0,141	1,284	0,021	2,567	0,042
Full	0,069	0,151	1,373	0,023	2,746	0,045
(bottom wheel)						
Empty	0,084	0,184	1,672	0,028	3,343	0,055
Full	0,079	0,172	1,567	0,026	3,134	0,052
Average	0,055	0,120	1,088	0,018	2,176	0,036
Std deviation	0,018	0,040	0,365	0,006	0,730	0,012
Std deviation as % of average	33	33	33	33	33	33

The maximum wheel loads recorded were not in good shafts, so that the factor K_m above becomes:

$$K_m = \frac{\Delta}{0,010} \; K_D$$

where Δ = maximum misalignment increment in m

K_D = a constant discussed subsequently.

Author Krige G J
Name of thesis The behaviour and design of mineshaft steelwork and conveyances 1983

PUBLISHER:
University of the Witwatersrand, Johannesburg
©2013

LEGAL NOTICES:

Copyright Notice: All materials on the University of the Witwatersrand, Johannesburg Library website are protected by South African copyright law and may not be distributed, transmitted, displayed, or otherwise published in any format, without the prior written permission of the copyright owner.

Disclaimer and Terms of Use: Provided that you maintain all copyright and other notices contained therein, you may download material (one machine readable copy and one print copy per page) for your personal and/or educational non-commercial use only.

The University of the Witwatersrand, Johannesburg, is not responsible for any errors or omissions and excludes any and all liability for any errors in or omissions from the information on the Library website.